

AFOSR 70-2391TR.

1. This document has been approved for public release and sale; its distribution is unlimited.

8071-33-F1

AD 712092

## DIGITAL SIMULATION OF SEISMIC RAYS

Supplement to Final Report

1 June 1966 Through 30 May 1970

Prepared for  
Geophysics Division  
Air Force Office of Scientific Research  
Arlington, Virginia 22209

By  
P. L. JACKSON

SEP 30 1970

August 1970



GEOPHYSICS LABORATORY

*Willow Run Laboratories*

INSTITUTE OF SCIENCE AND TECHNOLOGY

Sponsored by  
Advanced Research Projects Agency  
Nuclear Monitoring Research Office  
Project VELA UNIFORM  
ARPA Order No. 292, Amendments 32 and 37  
Contract AF 49(638)-1759

~~Distribution of this document is unlimited~~

# DISCLAIMER NOTICE

THIS DOCUMENT IS THE BEST  
QUALITY AVAILABLE.

COPY FURNISHED CONTAINED  
A SIGNIFICANT NUMBER OF  
PAGES WHICH DO NOT  
REPRODUCE LEGIBLY.

8071-33-F<sub>1</sub>

# **DIGITAL SIMULATION OF SEISMIC RAYS**

**Supplement to Final Report**

**1 June 1966 Through 30 May 1970**

**Prepared for  
Geophysics Division  
Air Force Office of Scientific Research  
Arlington, Virginia 22209**

**By  
P. L. JACKSON**

**Sponsored By  
Advanced Research Projects Agency  
Nuclear Monitoring Research Office  
Project VELA UNIFORM  
ARPA Order No. 292, Amendments 32 and 37**

**August 1970**

**Geophysics Laboratory**  
***Willow Run Laboratories***  
**THE INSTITUTE OF SCIENCE AND TECHNOLOGY**  
**THE UNIVERSITY OF MICHIGAN**  
**Ann Arbor, Michigan**

### **FOREWORD**

The research described in this report was conducted by the Geophysics Laboratory of Willow Run Laboratories, a unit of The University of Michigan's Institute of Science and Technology. The work was performed as part of Project VELA UNIFORM, sponsored by the Advanced Research Projects Agency and monitored by the Air Force Office of Scientific Research under Contract No. AF 49(638)-1759. The research period extended from 1 June 1966 through 30 May 1970; the Project Scientist is Mr. William J. Best.

The principal investigators for this project were P. Jackson, R. Turpening, and D. Willis. This report was submitted for publication in July 1970. The Willow Run Laboratories' report number is 8071-33-F<sub>1</sub>.

## PREFACE

The investigation reported in this dissertation was conducted at the Geophysics Laboratory of the Institute of Science and Technology, The University of Michigan, over a three-year period. During this period the preliminary results of this work have been described in presentations, reports, and a journal article.

On April 5, 1968, a slide presentation of computer-drawn plots was made to the Geophysical Advisory Committee of the U. S. Air Force Office of Scientific Research, Alexandria, Virginia.

On April 13, 1968, a paper concerning this work was presented to the Annual Meeting of the Seismological Society of America, in Tucson, Arizona (Jackson, 1968).

A major report, including listings and flow diagrams of computer programs was submitted in September, 1968 to the Air Force Office of Scientific Research (Willis and Jackson, 1968).

On October 5, 1969, a paper was presented to the Annual Meeting of the Eastern Section of the Seismological Society of America in Blacksburg, Virginia (Jackson, 1969).

A journal article describing the application to a spherical earth appeared in the Bulletin of the Seismological Society of America in June, 1970 (Jackson, 1970).

During this three-year period numerous progress reports on this investigation have been submitted to the Air Force Office of Scientific Research and the American Petroleum Institute.

The author would like to thank David E. Willis, James T. Wilson, Charles G. Bufo, Henry N. Pollack, Paul W. Pomeroy, Timothy C. Swanson, and Roger M. Turpening for helpful suggestions and encouragement. He also would like to thank Mrs. Clara M. Randazzo for invaluable help in preparing the manuscript.

## **ABSTRACT**

**Simulation of seismic rays for a spherical earth and a flat earth has been achieved in highly complex models. Travel times and approximate amplitudes of seismic waves can be found for both two- and three-dimensional models of portions of the earth. In seismology and other disciplines ray construction customarily has been applied to simplified geometries. It has been necessary to assume that the seismic wave velocity distribution of the earth was relatively uniform and symmetric.**

**Recently, however, the earth has been found to be more complex and non-uniform than formerly assumed. A need has thus arisen in seismology to test highly heterogeneous models of seismic velocity distribution. At the same time the development of the modern digital computer has provided a means of performing the necessary ray constructions and numerical calculations.**

**The problem of complicated seismic velocity distributions was therefore investigated in terms of the most appropriate use of the digital computer. For this investigation a velocity field was set up, and the propagation computations made for short segments of rays within this field. Total travel times are found by adding the travel times of connected ray segments. Essentially, the nature of propagation was duplicated on the computer, in that, at the location of each segment along the path of propagation, the initial condition and effect of the surroundings determine the succeeding direction of the following segment.**

**Both visual and numerical results have shown that this simulation method can be usefully applied to investigation of seismic velocity distributions of portions of the earth of any size or complexity.**

## CONTENTS

Preface .....	ii
List of Figures .....	v
Introduction .....	1
Two-Dimensional Simulation .....	9
Flat Earth .....	9
Spherical Earth .....	12
Three-Dimensional Simulation .....	14
Auxiliary Computations .....	18
Travel Time .....	18
Approximation of Amplitude .....	19
Reflection .....	20
Multiple Reflections and Refractions .....	20
Interface Location .....	22
Computer Programs .....	22
Results .....	24
Accuracy .....	24
Plane Waves .....	26
Spherical Earth .....	27
Three-Dimensional .....	27
Potential Application to Seafloor Spreading Problem .....	29
Conclusions .....	33
Appendix: Listings of Computer Programs .....	57



## FIGURES

1. Reference Frame for Incrementing Rays.	37
2. Computer Output Using Direct Ray Simulation for Five P-Rays.	38
3. Propagation of P Through Hypothetical Crust and Upper Mantle Structure.	39
4. Propagation of PcP Through Hypothetical Crust and Upper Mantle Structure Shown in Figure 3.	40
5. Plots of P, PcP, PKP, PKIKP, PKKP, and PKIKKIKP Rays Generated with a Spherical Earth Program.	41
6. Multiple Reflection. PcP and PKP Rays up to PKKKKKP.	42
7. Uniformity of Plotting and Travel Times Symmetrically Plotted from 700 km Depth.	43
8. Three-Dimensional Ray Tracing in a Region Defined by 30 x 30 x 30 Velocity Samples.	44
9. Line Source at Depth for Three-Dimensional Representation as Shown in Figure 8.	45
10. Three-Dimensional Ray Tracing with Velocity Distribution Defined by Continuous Mathematical Function.	46
11. Three-Dimensional Ray Tracing with Velocity Functions Specified for Different Regions.	47
12. Ray Paths From Earthquake Above Underthrusting Lithosphere at Continental Plate Boundary. Depth of Focus: 50 km.	48
13. Ray Paths From Earthquake Above Underthrusting Lithosphere at Continental Plate Boundary. Depth of Focus: 100 km.	49
14. Ray Paths From Earthquake Within Underthrusting Lithosphere at Continental Plate Boundary. Depth of Focus: 60 km.	50
15. Ray Paths From Earthquake Within Underthrusting Lithosphere at Continental Plate Boundary. Depth of Focus: 110 km.	51
16. Earthquake Above Underthrusting Lithosphere at Continental Plate Boundary. Depth of Focus: 50 km.	52

17. Earthquake Above Underthrusting Lithosphere at Continental Plate Boundary. Depth of Focus: 100 km.	53
18. Earthquake Within Underthrusting Lithosphere at Continental Plate Boundary. Depth of Focus: 60 km.	54
19. Earthquake Within Underthrusting Lithosphere at Continental Plate Boundary. Depth of Focus: 110 km.	55

## Introduction

Possibly no artificial construction has been more useful to science than the ancient concept of the ray. Not only in seismology, but in all scientific fields concerned with the transfer of energy, reasoning with and construction of rays have resulted in fundamental advances.

The firm basis of rays in science is most dramatically shown in optics. From ancient times to the present, light rays have been used for intuitive visualization and have resulted in advances in optics and related fields. Archimedes, Aristotle, Roger Bacon, Kepler, Newton, Young, Fresnel, Rutherford, and Compton all used the ray concept. Newton's *Optiks* (1730; 1952) is probably the most lucid example of rays as both a rationale and a means of intuitive understanding and imaginative discovery; almost every figure in Newton's book is a ray tracing.

In seismology, with which this thesis is concerned, the use of rays aided Mohovoričić (1910) in discovering the discontinuity between the mantle and the crust; Gutenberg (1914) inferred the existence and estimated the size of the earth's core with the aid of rays; and, in theoretical analysis, Zoeppritz (1919) employed the ray concept to derive the relationships of reflected and refracted dilatational and distortional waves at an interface.

Current seismological contributions to the knowledge of the earth continue to rely on the concept of rays. Current issues of scientific journals in seismology usually contain several articles which are illustrated by and rely on seismic rays.

In seismics most ray tracing has been based on Herglotz-Wiechert formulation as extended by Bullen (1963). Helbig (1965) used this geometrical construction for a graphical method for spherical shells. Spherically symmetric ray tracing has also been described by Julian and Anderson (1968) and shown by Lewis and Meyer (1968). Engdahl, et al. (1968) employed the formulation for the 1968 P-Phase Tables (Taggart, et al., 1968).

Iyer and Punton (1963) broke away from rigid geometrical limitations in constructing successive wavefronts by applying Huygens' principle involving complicated logic. Yacoub, et al. (1968) also departed from rigid geometry by considering regions of constant velocity in which the interfaces can be oriented in any direction. He also computed the amplitudes by Zoeppritz's equations for rays crossing an interface.

The ray simulation described in this dissertation is based upon a new concept leading to the treatment of heterogeneous structures and the travel-time solutions for any discretely specified and/or analytically represented velocity distributions.

An advance in the art of tracing rays is thus a significant contribution to the science of seismology; and, by extension, to other sciences. Currently two aspects of recent scientific and technological development provide, first, a new requirement and, second, a practical means of satisfying this requirement.

The requirement to investigate non-simplified, heterogeneous velocity distributions, has arisen from the discovery that the earth is less symmetric and more heterogeneous than previously supposed. More accurate

and extensive seismic measurements are currently being made. The need for greater understanding has made simplifying assumptions of the velocity distribution of the earth less useful. Tracing rays through heterogeneous velocity structures and determining their travel times would be useful in gaining detailed understanding of the earth.

The practical means to achieve the tracing of rays and determination of travel times through complex velocity distributions is the employment of the modern digital computer. Complicated velocity distributions imply unpredictable velocity gradients. In large regions a ray must be constructed with many different computations because of changes within relatively small regions. With a digital computer one can carry out successive computations, which enables one to treat the complicated velocity distributions indicated by modern seismology.

With these two aspects in mind—the requirement and the apparent means of fulfilling the requirement—a preliminary trial was made to develop a new method of ray tracing. The point of departure was to somehow propagate rays through some type of mathematical or representational cross-section of a velocity distribution. The approach was to use a sampled structure into which a short segment of a ray could be introduced at a given location and with which the directions and positions of successively added segments could be found as functions of the velocity distribution represented by the structure.

A rectangular two-dimensional grid of equally-spaced points was considered. The grid points represented positions on a vertical cross-section of the earth, each point corresponding to a given horizontal and

vertical distance from a reference point. A "sampled" velocity and slope would correspond to each point of the grid. A means was then required of using the velocities and slopes, and the relationships between neighboring samples of their values, to "propagate" short successive segments of the rays through the sampled velocity distribution. This means was found. An introductory description follows.

The aforementioned grid was considered as a matrix in which the rows represented discrete horizontal distances along the cross-section, while the columns represented discrete vertical distances, as shown in Figure 1. Such a matrix can be represented as a vector with two indices. Call the vector  $V_{ij}$ , in which  $i$  represents the row, and  $j$  the column of the matrix. For each set of indices  $(i,j)$  a position on the cross-section can be identified. For example, let the interval between the samples be 10 km. Then the indices  $(i = 1, j = 1)$  could represent the reference point  $(0,0)$  at the surface of the earth and on the cross-section; the indices  $(i = 10, j = 1)$  represent a distance 90 km from the reference point on the surface; the indices  $(i = 5, j = 3)$  a horizontal distance 40 km from the reference point at a depth of 20 km. The indices must be integers greater than zero to represent the matrix in the computer. For this reason the smallest pair of indices  $(1,1)$  are taken to represent an origin  $(0,0)$ . This bias is easily handled, as the source can be anywhere within the bounds of the matrix, provision for measuring from the source location must be made.

At each location defined by two indices there corresponds a velocity  $V_{ij}$  and a slope  $S_{ij}$ . These values at discrete points can be referenced

from locations closest to them. A ray, however, is a succession of short segments of possibly differing directions. These segments may be joined together at non-discrete locations, say the coordinates  $(h,d)$ , where  $h$  is horizontal distance and  $d$  is depth in a cross-section of the earth. At each matrix location  $(h,d)$  a computation must be made to determine the direction and hence end position of a succeeding segment. The ray segment midpoints could then be referred to the nearest discrete  $(i,j)$  location to determine the velocity  $V$  and slope  $S$ . For example, consider the scale, or sampling interval as shown in Figure 1 was 10 km, and the ray segment midpoint was located with respect to the matrix at  $h = 4.75$ ,  $d = 3.25$  corresponding to  $H = 37.5$  km and  $D = 22.5$  km on the referenced cross-section of the earth. The velocity  $V$  and slope  $S$  would be found at the location indicated by the indices  $(i = 5, j = 3)$ , and could be easily referenced; if desired, one could interpolate the values between those found at  $(i = 5, j = 3)$  and  $(i = 4, j = 4)$ .

At the midpoint of every ray segment a value for velocity and slope is found. For geometrical ray tracing, Snell's law requires the knowledge of an incident direction with respect to an interface and the velocity of the medium on either side of the interface. The representational structure described above supplies this information. The direction of the incident ray segment and the slope of the interface are known, therefore the incident angle for Snell's law can be found. The velocity  $V_1$  of the medium on the incident side of the interface is found as described in the last paragraph. The velocity  $V_2$  on the emerging side can be found by extending the ray segment in the same direction as the incident ray for

the segment, again using the technique described in the last paragraph.

For a fixed rectangular Cartesian coordinate system, a horizontal distance can be represented as  $L \sin \theta$  and a vertical distance as  $L \cos \theta$ , where  $L$  is a length of a ray segment and  $\theta$  is the angle from the upward vertical.  $\theta$  is positive in the counterclockwise direction. Now consider that the head of an incident ray segment of angle  $\theta_k$  located at  $(h_k, d_k)$ , and, by invoking Snell's law the emerging angle is found to be  $\theta_m$ , as shown in Figure 1. The location of the tail end of the emerging ray segment is found to be  $h_e = h_k + 0.5 L \sin \theta$ ,  $d_e = d_k + 0.5 L \cos \theta$ . As the direction and location of the emerging ray segment as well as the velocities and slopes of the immediate surrounding regions are known whenever they may be within the defined matrix, the emerging ray segment can be redefined as the new incident ray segment, and succeeding segments generated and joined end-to-end until a complete ray is formed.

Travel times of the radiation of seismic waves from the disturbance to the seismometer are of fundamental importance in seismology. The information to determine travel times is available with this ray tracing method. Each segment of the ray is located in a region in which the velocity is known. The travel time for each segment can be found by dividing the length of the segment by the average velocity along its length. The travel time for the ray is then the sum of the travel times of the segments. The distance of travel is found by summing the lengths of the segments. This distance is useful for computing spherical spreading and logarithmic attenuation.



The approach described above was tested with a computer program. The initial results were promising, and the ideas seemed to be valid. A seismic ray could be simulated through a matrix representing a sampled velocity distribution in a vertical cross-section of the earth. The investigation to produce a useful, accurate, and versatile seismic ray simulation was then commenced. The ensuing investigation was mainly devoted to attacking the following problems:

1. Accommodating ray angles through the entire range of  $360^\circ$ , and of using any defined slope in association with any given ray angle,
2. Reflection from an interface,
3. Both critical and non-critical multiple reflections,
4. Precisely locating an interface between matrix-designated discrete locations and extending the ray to this interface,
5. Developing and testing a method to obtain high accuracy, of determining travel times and approximate amplitude in a multiply-reflecting model,
6. Adding the capability of specifying regions of velocity characteristics defined by an analytical mathematical function,
7. Treating both curved and flat earth,
8. Applying the concept to a three-dimensional model, and
9. Making the method general so that one program can be used for many different regions of the earth.

A versatile tool has been developed for the scientific investigation of velocity distribution in the earth. Any conceivable velocity distribution can be simulated and compared to actual travel times in

investigations where geometrical ray approximations are valid. In addition, the method is expandable, and can be used as a base for mode conversion, the addition of Zoeppritz's equations for amplitude, extension to the atmosphere where winds provide a moving medium, and, possibly, for geometric diffraction.

The simulation of seismic rays can be performed with either two- or three-dimensional models. Flat earth models naturally accommodate themselves to a rectangular Cartesian coordinate system. Curved earth models, which at first glance would appear to be better treated in polar coordinates, are also treated in a rectangular Cartesian system because the velocities and slopes for a spherical earth are easily referenced. Also the compatibility of coordinate systems between flat and spherical earth enables one to insert sampled values for anomalous regions within a spherical earth model.

As first conceived, it was thought that the two-dimensional technique of ray tracing could be incorporated into the three-dimensional technique, and two-dimensional tracing performed when holding the values along one of the axes of the three dimensions constant. However, the use of three-dimensional models required a sufficiently different technique that the two types are better explained separately. The description of the use of the three-dimensional model is not self-contained. To avoid repetition of identical material, pertinent matter presented in the two-dimensional section will be referred to when describing its use in three dimensions.

## Two-Dimensional Simulation

### Flat Earth

Both discrete values assigned to a matrix and continuous mathematical functions may be employed to reference velocity. To aid in visualization, the following exposition is based on the discrete case.

Construct a two-dimensional scalar field representing the seismic velocity characteristics and slopes along a plane in a medium, such that

$$V = f(x,z) \quad (1)$$

$$S = g(x,z) = h(V) \quad (2)$$

where  $V$  is the velocity (actually the speed with which seismic P-waves propagate, but to be referred to henceforth as velocity, in keeping with common practice in seismology),  $f$ ,  $g$ , and  $h$  are functions, and  $x,z$  represent distances parallel to the axes of a rectangular Cartesian coordinate system. The functions  $f$  and  $g$  may be defined differently for specified regions of the field, and can include both continuous mathematical functions and references to tables of arbitrary and discretely changing values. The function  $g$  may be derived directly from  $f$  as the normal to the gradient, or specified separately. One might term  $S$  a vector, as it corresponds to a direction and is based on the gradient. However, it is defined as an angle and is used as a scalar quantity in the computation.

Consider a matrix of discrete values, the rows of which represent equally spaced horizontal positions within the scalar field. For each element of the matrix a velocity and slope is assigned which corresponds to the location represented in the scalar field. Values for velocities and slopes can be found in the scalar field at any point not corresponding

to the discrete locations represented by the matrix elements. These values are found by either using those of the matrix elements to which the location is closest or interpolating between the nearest horizontal and vertical elements of the matrix. Thus for any position in the scalar field, the value for the velocity and slope can be found by reference to the nearest element of the matrix.

As arbitrary values can be stored in the matrix, any type of velocity distribution can be referenced to the scalar field. Through such a reference system a completely heterogeneous velocity distribution can be used for ray tracing; the limits of heterogeneity are limited only by the detail with which the matrix elements represent the scalar field. That is, by the distance represented by two adjacent elements of the matrix. The matrix with the velocities and slopes represented as its elements is necessary to arbitrarily represent velocity distributions, but not to perform ray tracing through the scalar field.

Select a position  $x_k, z_k$  for the head end of an incident ray segment of length  $L$  and an angle  $\theta_k$  ( $0^\circ < \theta < 360^\circ$ ). The midpoint of this segment is the location which is used to determine the incident velocity  $V_k$  in the manner described above. Reference  $\theta_k$  to the negative  $z$ -axis, counterclockwise positive. The  $z$ -axis, which represents depth in the earth cross-section, is positive downward. Extend the ray segment a distance  $L$  in the direction  $\theta_k$ .

The initial emerging location  $P_1$  is found by extending the ray segment at the incident angle  $\theta_k$ , shown in Figure 1, using the two following equations:

$$x_p = x_k + L \sin \theta_k \quad (3a)$$

$$z_p = z_k + L \cos \theta_k \quad (3b)$$

The midpoint of this extended ray segment is the location which is used to determine the initial emerging velocity  $V_m$ .

Sufficient information (position and angle of the ray, and the velocities and slopes surrounding the region of the ray) is available to construct the ray continuation by Snell's law. The equation used for this purpose is

$$\theta_m = \text{ARCSIN}[(V_m/V_k) \sin (\theta_k - S_k)] + S_k \quad (4)$$

where  $\theta_m$  is the angle of emergence,  $V_m$  is the emerging velocity,  $V_k$  is the incident velocity, and  $S_k (-90^\circ < S \leq 90^\circ)$  is the slope of the interface referenced counterclockwise positive from the x-axis. In case of continuous velocity functions  $S_k$  is the normal to the direction of the velocity gradient. The extension of this segment is termed "probing" in the sense that one must repetitively probe for the proper emerging angle  $\theta_m$ . For the first repetition  $\theta_m$  replaces  $\theta_k$  in Equation (3) and  $P_x$ ,  $P_y$  are recomputed. A new  $\theta_m$  is determined using the newly-found  $V_m$  in Equation (4). Equations (3) and (4) are repeated in succession, each time using the previously determined value of  $\theta_m$  for  $\theta_k$  in Equation (3). The repetition is terminated when successive values of  $\theta_m$  are sufficiently close in value ( $|\theta_m - \theta_{m-1}| < \epsilon$ , where  $\epsilon$  is a predefined small value).

This repetition is necessary because the location of the extension computed with the incident angle is in general different from the location computed with the emerging angle. If the ray is penetrating into

a region of increasing velocity the emerging angle between the ray segment and the normal to the interface will be too large. If penetrating into a region of decreasing velocity this angle will be too small. These improperly evaluated angles are found because the tentative ratio  $V_m/V_k$  may be a different value from the ratio as found when extending the ray with the correct emerging angle. One can asymptotically converge to the correct emerging angle by repeating these computations. These repetitions are performed to improve accuracy for computations using any given ray segment length  $L$ . Linearity of the velocity function is assumed within the distance  $L$ . Also, to improve accuracy one might reduce the segment length  $L$ , as the accuracy is an inverse function of  $L$ , and  $L$  is not required to be equal length for all ray segments. However, it still must hold that the difference between two successively-determined emerging angles  $\theta_m$  would have to be a small value.

When the sufficiently accurate  $\theta_m$  is found by repeatedly applying Equations (3) and (4), the emerging ray segment and angle is determined. This emerging segment and angle is then treated as the incident segment with a new location and angle. Segments are repeatedly computed, the tail of the "emerging" segment joined to the head of the "incident" segment repeatedly until the ray, which is the summation of all the segments, penetrates to the surface or the boundary of the defined cross-section of the earth.

### Spherical Earth

Consider a velocity distribution with depth for a symmetric earth.

One can compute the velocity and slope for any position  $(x,y)$  within a circle representing the cross-section of the entire earth. The velocity is found as follows:

$$V_k = f(R) = f[(x_k^2 + y_k^2)^{1/2}] \quad (5)$$

where  $f$  is a function of the radius  $R$ ;  $V_k$  is found for any location defined by  $(x_k, y_k)$  from either a table and interpolating, or by computing some mathematical function of the radius  $R = (x^2 + y^2)^{1/2}$ .

For each location defined by  $(x_k, y_k)$  a slope  $S_k$  can be found,

$$S_k = \text{ARCTAN } (y_k/x_k) \pm \pi/2 \quad (6)$$

where  $y$  and  $x$  are the coordinates of a given location,  $y=0$ ,  $x=0$  are the coordinates of the center of the earth, and the sign of  $\pi/2$  depends upon the quadrant in which  $y$  and  $x$  are found.

The angular distance at which a ray emerges is found by

$$\Delta = \text{ARCTAN } (y_k/x_k) \quad (7)$$

where the proper quadrant is determined from the relationships of the signs of  $x$  and  $y$ , and where  $x$  and  $y$  are located within a small predefined distance from the surface of the earth.

The depth of penetration, or, correspondingly, the minimum radius of the ray upon reflection is found by computing the minimum radius along a given ray, and retaining that radius to correspond with the other previously described data of the emerging ray.

Any region which is defined by minimum and maximum values or functions of  $x$ ,  $y$ , or  $R$  can be postulated so that a different function can be invoked. For example, one might wish to investigate the travel times of rays which penetrate an anomalous region in an otherwise symmetric

region of the earth. Within the limits defined, any sampled value can be inserted for the positions defined by  $x$  and  $y$ , as in the flat earth case.

### Three-Dimensional Simulation

Construct a three-dimensional scalar field representing the seismic velocity characteristics of a medium, such that

$$V = f(x, y, z) \quad (8)$$

$$S_1 = g(x, y, z) \quad (9)$$

$$S_2 = h(x, y, z) \quad (10)$$

where, as in the two-dimensional fields  $V$  is the velocity,  $S_1$  represents the slope with respect to the  $z$ -axis,  $S_2$  the slope along planes parallel to the  $x, y$  plane, and  $f$ ,  $g$ , and  $h$  are functions. Positions within the field are referenced in a three-dimensional orthogonal Cartesian coordinate system. Directions within the field are referenced in a spherical coordinate system, in which the angle from the positive  $z$ -axis is  $\phi (0 < \phi < \pi)$  and the direction from the  $z$ -axis in a plane parallel to the  $x, y$  plane is the angle  $\theta (0 < \theta < 2\pi)$ , the same as that described for two dimensions. A segment  $L$  oriented in a direction defined by  $\phi$  and  $\theta$  projects a distance  $P_z$  on the  $z$ -axis

$$P_z = L \cos \phi \quad (11)$$

and on the  $x$ -axis as

$$P_x = L \sin \phi \sin \theta, \quad (12)$$

and on the  $y$ -axis as

$$P_y = L \sin \phi \cos \theta. \quad (13)$$



To visualize the role of the two slopes  $S_1$  ( $-\pi/2 < S_1 < \pi/2$ ) and  $S_2$  ( $0 < S_2 < 2\pi$ ) more clearly, consider an interface or a plane normal to the gradient which lies obliquely to all of the axes. Then the slope  $S_1$  is the dihedral angle between the z-axis and the plane of the interface (when interface is mentioned it also refers to the normal plane to the gradient). The slope  $S_2$  is found by the angle of the line which defines the intersection between the x,y plane and the plane of the interface, and is referenced as in the two-dimensional case.

The coordinate system is a right-handed system in which the z-axis is downward. Thus when a region of the earth is represented positive z values correspond to depth from the surface of the earth, or from an arbitrary horizontal boundary. Although an orthogonal Cartesian coordinate system is employed for position, a new position can be determined by employing a length L, and the angles  $\phi$  and  $\theta$ . The two coordinate systems are complementary.

We see from the foregoing definitions that, as in the case of the two-dimensional system, we have sufficient information to compute Snell's law in the three-dimensional system: L,  $\phi$ ,  $\theta$ , x, y, z, V,  $S_1$ , and  $S_2$ . However, in the three-dimensional system the algebraic and trigonometric processes become much more involved.

Consider a velocity distribution in which the gradient is everywhere parallel to the z-axis as defined above. Such a distribution would correspond to a region of the earth in which all interfaces were parallel to the surface of the earth. Therefore, no velocity change would occur along a horizontal direction. With such a velocity distribution, the

original angle  $\theta_k$  of a ray would never change, although its sign might. This is because  $V_m = V_k$  and, therefore  $\theta_m = \theta_k$ , as seen by reference to Equation (4). The straightness of the ray is illustrated in the orthographic projection in the x,y plane of Figure 8. The total change in direction will be in the angle  $\phi$ , which can be computed as

$$\phi_m = \text{ARCSIN}[(V_m/V_k) \sin(\phi_k - S_{1k})] + S_{1k} \quad (14)$$

where the subscripts m and k refer to emergence and incidence as in the two-dimensional case.

We now consider a scalar field in which the interfaces may be any orientation in three-dimensional space; the condition described in the last paragraph would not hold for this case. If the coordinates were oriented in such a manner that the z-axis was perpendicular to the interface, then the condition holds where  $\theta$  does not need to be recomputed and a simple expression for  $\phi$ , Equation (14), can be employed. At any given location within the field the angles  $\theta_k$  and  $\phi_k$  are known, as well as the slopes  $S_{1k}$  and  $S_{2k}$ . If a coordinate system can be found in which the z-axis is perpendicular to the interface defined by  $S_{1k}$  and  $S_{2k}$ , then the calculation of Snell's law for  $\phi_m$  in Equation (14) needs only to be used.

Such a coordinate system can be found by rotating the axes as a function of  $S_{1k}$  and  $S_{2k}$ . After rotation the positions x,y,z are referenced by x',y',z' and the angles  $\phi$  and  $\theta$  by  $\phi'$  and  $\theta'$  to the new orientations of the coordinate system axes. Snell's law can then be invoked with parameters referenced to the new coordinate system. The new position is found as follows.

Let  $S_2'$  be the angle by which the x- and y-axes are rotated around the z-axis, and  $S_1'$  the angle by which the x'-axis is rotated about the y'-axis (or, viewed differently, the angle with which the z-axis is tilted to become normal to the interface.) For a continuous mathematical function angle  $S_2'$  is

$$S_2' = (\pi/2) - \arctan(\Delta X/\Delta Y) \quad (15)$$

where  $\Delta X$  and  $\Delta Y$  are directional derivatives along the x-axis and y-axis respectively.  $S_1'$  is found similarly as

$$S_1' = (\pi/2) - \arccos(\Delta Z/\Delta X^2 + \Delta Y^2 + \Delta Z^2)^{1/2} \quad (16)$$

where  $\Delta Z$  is the directional derivative along the z-axis. For sampled functions  $S_1'$  and  $S_2'$  are

$$S_1' = (\pi/2) - S_1(i,j,k) \quad (17)$$

and

$$S_2' = S_2(i,j,k) \quad (18)$$

respectively.

The coordinate axes can then be rotated, and corresponding locations in the new coordinate system found by rotating first around the z-axis and next around the y'-axis:

$$X'' = X \cos (S_2') + Y \sin (S_2') \quad (19)$$

$$Y' = Y \cos (S_2') - X \sin (S_2') \quad (20)$$

$$X' = X'' \cos (S_1') - Z \sin (S_1') \quad (21)$$

$$Z' = Z \cos (S_1') + X'' \sin (S_1') \quad (22)$$

The angles  $\theta'$  and  $\phi'$  are found in a similar manner by computing a position with trigonometric functions, rotating the coordinate axes, and taking inverse trigonometric functions of the angles of a directed vector from the origin to the position in the new coordinate system.

When each segment of the ray is computed, the new position can be found by rotating the coordinates back into the originally specified coordinate system. From this position in the given coordinate system the incident velocity  $V_k$  is known, and by repeated computation in the manner described in the section on two-dimensional tracing the proper emerging angles  $\phi_m$  and  $\phi_m'$  can be asymptotically approached to within a predetermined small value.

In returning the rotated coordinate system, the values  $V_k'$  and  $V_m'$  required to compute Snell's law to determine the emerging angle  $\phi_m'$ , are

$$V_k' = V_k \quad (23)$$

$$V_m' = V_k + (V_m - V_k) \cos(\phi_m') \quad (24)$$

where, again, the prime refers to values in the new coordinate system, and  $\phi_m'$  refers to the repetitively probed value to correctly determine  $V_m$ .

In the rotated coordinate system we are concerned with only one direction of reflection, so this can be handled in the same manner as in Equation (30) of the next section. The only angle affected is  $\phi'$ , as  $\theta'$  will be unaffected. However, in the originally given coordinate system, the direction of the ray may reverse itself in its projection on the x,y plane.

### Auxiliary Computations

#### Travel Times

As each segment of the ray is found and added on to the preceding segments, the travel time can be determined. The time of travel for each segment is simply the length of the individual segment  $L_s$  divided

by the average velocity  $V_a$  at which it is propagating, so that the total travel time TT of a ray is

$$TT = \sum_{a=1}^n L_a / V_a \quad (25)$$

where n is the total number of segments from the ray's origin to its emergence on the surface.

#### Approximation of Amplitude

The total distance D a ray has travelled is

$$D = \sum_{a=1}^n L_a \quad (26)$$

Knowing this distance, one can compute the amplitude dimension due to spherical spreading and the exponential attenuation to energy dissipation as

$$A_r = A_s (1/D) \exp(-cD) \quad (27)$$

where  $A_r$  is the amplitude at the receiver,  $A_s$  is the amplitude at the source, and c is the attenuation coefficient.

In case of non-critically reflected rays and the ensuing refracted rays, the partition of energy is rigorously computed by Zoeppritz's equations. The approximate approach used here is that of Fresnel's reflection coefficient at normal incidence. At a reflective interface where non-critical reflection occurs the approximate reflected amplitude  $A_r$  is

$$A_r = A_k (v_k - v_{k+1}) / (v_k + v_{k+1}) \quad (28)$$

and the subsequently refracted amplitude is

$$A_{k+1} = A_k - A_r \quad (29)$$

### Reflection

Reflection is required whenever an interface of sufficient velocity difference is encountered by the ray, or whenever the critical angle is exceeded. At such a boundary the reflected angle  $\theta_R$  is

$$\theta_R = \pi - \theta_i + 2S_i \pm 2n\pi \quad (30)$$

where  $n$  is  $-1$ ,  $0$ , or  $1$ , so that the condition  $0 \leq \theta < 2\pi$  is fulfilled.

### Multiple Reflections and Refractions

When the ray is both reflected and refracted at an interface, it splits into two separate rays. To accommodate this fact, and to trace out both ray branches, the information of the angle, position, total travel time and distance to the interface, and approximate amplitudes computed by Fresnel's reflection coefficient at normal incidence must be stored for one ray branch while the information for the other is employed for further ray tracing. This is accomplished by continuing with the reflected ray until it emerges or strikes another interface. In emerging at the surface all the required data, such as distance, total travel time, approximate amplitude, and the depth of penetration of the ray is available. The depth of penetration is found by comparing the depth at all segments of the ray, and retaining the position most distant from the surface. One then returns to the previous interface from which non-critical reflection occurred, and, using the information listed in the last paragraph which has been retained, continues with the refracted ray. An ensemble of information can be retained from pre-

vious reflections, one is able to accommodate as many multiple reflections as desired.

The multiple reflections may be accommodated in the following manner. Consider arrays of any arbitrary number of elements for each parameter needed to construct a ray, say

$$H(i), V(i), \theta(i), TT(i), TL(i), \text{ and } A(i), \quad (31)$$

where  $H$  is horizontal position,  $V$  is vertical position,  $\theta$  is angle of the first refracted segment,  $TT$  is travel time to the interface under consideration,  $TL$  is total path length to the interface, and  $A$  is amplitude; the index  $i$  in each value in (31) represents the reflection number. One starts at the inception of a ray with  $i=1$ . At the first non-critical reflection, the refracted values are stored under the index  $i=1$ , and the reflected under the index  $i=2$ ; similarly, if another interface with non-critical reflection is encountered, the refracted ray is given the index  $i=2$ , while the reflected ray is given the index  $i=3$ , and so on. For each non-critical reflected ray the index is incremented by 1, while the corresponding refracted ray is referred to by the previous index. It is seen that any arbitrary number of reflected rays can be accommodated and traced by incrementing indices in this manner. After any given reflected ray has reached its destination the index  $i$  is reduced by 1, and the previously refracted ray is then continued by using the initial conditions of the parameters listed in (31) with the next lower index number. It can be seen that all refracted rays will be traced out until the index reverts to  $i=1$ , which is the index number of the incident ray. Also, because previously refracted rays may subsequently

encounter a new set of multiple reflections, all multiple reflections of the originally reflected or refracted rays will be accommodated.

#### Interface locations

Because interface locations are so critical in affecting the location of the emergence of a ray, a means was developed of precisely locating the interface and extending or retracting the ray to terminate precisely on the interface. This is accomplished in the following manner. The location of a point is found in the square defined by four matrix elements and located on the interface. The horizontal and vertical distance from the ray segment head end to this point is determined. Knowing the slope of the interface, the angle of the ray, and the horizontal and vertical distances to the defined point, a series of computations in which the law of sines is invoked is then made. Many different angular conditions are involved as a result of combinations of ray angle, slope, and positive or negative horizontal distances. For details, one can consult the subroutine GINMAD in the Appendix, where the computations are given in Fortran.

#### Computer Programs

Three main programs have been developed. The first is for two-dimensional flat earth, the second for two-dimensional spherical earth, and the third for three dimensions. All have been written in the most general computer language, Fortran. The version is Fortran IV-G, each program of which has been compiled and run on the IBM 360/67 computer



of The University of Michigan. The programs include plotting instructions which have been used for the illustrations.

Subroutines have been developed to precisely reflect at an interface, to extend the ray precisely to the surface, to compute Snell's law for any incident angle across an interface of any slope, to increment initial horizontal and vertical positions and angles, and to compute reference travel times for each ray making up an onsetting plane wave.

The indexing for the spherically symmetric case has been made compatible with that for velocity distributions with a rectangular reference system, in such a manner that the data for horizontal layering structures can be read in by a Fortran Namelist. In this way anomalous regions which are very heterogeneous can be included.

The programs have been made general, so that a different number of samples and size of sampling interval, number of multiple reflections, incremented or changed output, number of initializations, etc., can be entered without recompiling the programs. Thirty to forty values are read from Fortran Namelists; the values can be changed individually.

Each ray increment involves calling trigonometric functions approximately 7 to 25 times (usually about 15 times). For an indication of the time required, see Figure 7. The computation for Figure 7, including loading, 20 travel-time printouts, and plotting instructions, required 10 seconds of IBM 360/67 computer time. It is felt that this is reasonable and economical time for such ray tracing.

The three main programs and their subroutines are listed in the Appendix.

## Results

### Accuracy

The method of ray simulation was developed primarily with synthetic data. First very simple data were used for testing and developmental purposes. As the work progressed, it was felt that a test was necessary to determine its accuracy.

For this reason the method for tracing rays in spherically symmetric earth was attempted. For at least 60 years the earth has been investigated as a spherically symmetric structure in which the velocity gradient everywhere points directly at the center of the earth. Much of seismology has been concerned with this model. Because of the continued investigation of this model over most of the world for such a long period of time, many travel times from individual disturbances at many distances have been recorded.

From these travel times a velocity-depth distribution of the earth has been inferred. This distribution is one of the fundamental problems of seismology, and most seismologists have been concerned with it.

Recently Herrin, et al. (1968) published the 1968 Seismological Tables for P Phases in a special issue of the Bulletin of the Seismological Society of America (BSSA). These tables represented the latest refinements of the contributions of the science of seismology. In this special issue a velocity vs. depth distribution of the mantle was given. As both the velocity distribution and travel times were given in this special issue of BSSA, a model was available to test this method of ray tracing.

As one might expect, the ray tracing method was initially shown to be inaccurate in the first tests. Two improvements were made in the technique as it then existed. The first was to take the incident velocity at the midpoint of the incident ray segment and the emergent velocity at the midpoint of the emergent ray segment. The second change was to repeat the computation of Snell's law, as explained in the two-dimensional modelling section, until the proper emerging velocity was found. It was found with a testing program that the proper value of emerging velocity was approached in a damped, oscillating fashion. It was then a simple expedient to compare successive values until the difference between them was less than an arbitrary value.

This latter change, for which the need was not formerly apprehended, was the key to achieving as much accuracy as desired, without reducing the length of the ray segments to require an uneconomically large amount of computation. As Snell's law is the basis of both this method and that used for the 1968 P-Phase Tables (Engdahl, et al. 1968) the two methods should result in identical relationships between velocity distribution and travel times. Differences should be due only to the size of the sampling intervals, length of the incremented segments, and method of interpolation.

The equivalence between the two methods has been found. As the sampling interval and segment length were reduced, the travel times shown in the 1968 P-Phase Tables have been approached more and more closely when using the same velocity distribution.

The accuracy is illustrated in Figure 2, where the velocity distribution used for the 1968 P-Phase Tables was approximated with samples taken at 15 km intervals with 9 km segments. Figure 2 is a reproduction of a computer output using this ray tracing method and also shows corresponding distances and travel times from the 1968 P-Phase Tables. The average difference between the two methods in travel times for the five P-rays shown in Figure 1 is .252 seconds, or an average difference in travel times between methods of 1/100 of 1%. As the standard deviation of the P-Phase Tables is 1 second, .252 seconds is considered satisfactory. Every indication is that the travel time vs. velocity distribution values could be made closer by further reduction of the sampling interval and segment length.

#### Plane Waves

Figures 3 and 4 were drawn to investigate the simulation of a plane wave. The velocity structure is based upon a hypothetical velocity distribution within a cross section from the Pacific Ocean across the Coast Ranges, Central Valley of California, the Sierras, and part of Nevada. Figure 3 represents a PcP wave from  $\Delta = 30^\circ$  and Figure 4 a P wave from the same distance. The simple subroutine Planit was used as a reference for travel time across the wavefront. These figures were obtained in May 1969 as an aid in Charles G. Bufe's investigation of PcP waves (1969). Bufe was able to estimate PcP-P travel-time differences, and anticipate arrival anomalies.

### Spherical Earth

Figures 5 through 8 illustrate two-dimensional seismic ray tracings of an entire cross-section through the earth. In Figure 5 only a single reflection was allowed, enabling one to obtain PcP, PKKP, PKIKIKP, and P rays. Had no reflection been allowed below the critical angle of incidence, only the PKP, PKIKP, and P would have been drawn in Figure 5. With four reflections allowed one can generate PKP type waves up to PPKKKP, as shown in Figure 6.

In Figure 7 a source at 700 km depth was simulated. Rays were traced from this source at  $18^\circ$  intervals, and each ray traced independently of the others. Note that the second K leg of the initial  $18^\circ$  ray is overtraced by the second K leg of its symmetric counterpart the  $360^\circ - 18^\circ$ , or  $342^\circ$ , ray. This overtrace indicates high positional accuracy, in that  $\Delta$  and travel times differ by less than .01% between symmetric rays.

### Three Dimensional

Illustrations of computer plots in three dimensions are shown in Figures 8 through 11. To clearly show the paths of the rays in three dimensions a computer program was devised to show a perspective and three orthogonal projections. Figures 8 through 11 show a single-point perspective in the upper left portion of the figures, and three orthogonal projections along the principle planes in the remaining portions of the figures. Consider that the (x,y) plane represents the surface of the earth, and the positive z-axis corresponds to depth in the earth.

In Figure 8 and Figure 9 a velocity distribution increasing with depth and having zero slope everywhere with respect to the surface is shown. In Figure 8 cones of rays from a point source at the surface are shown; rays of a sufficiently large initial angle undergo critical reflection and return to the surface (x,y plane). In Figure 9 a line source at depth is shown. Points are chosen along the line, and fans of rays are propagated toward the surface. It should be pointed out here that any type of initializing rays may be chosen. For example, in Figure 9 the points of origin along the line could have been made much closer together, and the angular extent of the fan decreased, with any choice of angles between individual rays chosen. As described in the section on the computer programs, the values for the increments of these points and angles can be entered in the Namelist.

Figures 10 and 11 illustrate an oblique gradient with respect to the z-axis. The mathematical distribution of the velocities in Figure 10 is

$$V = 6.0 + X + 2Y + 3Z \quad (32)$$

These illustrative figures make use of velocity values which exceed normal earth velocities. These velocities were used for the purposes of demonstrating the capability of tracing such a distribution. In Figure 11 a sampled layer extending from a level corresponding to 40 km depth to 190 km depth is placed within the field described for Figure 9. The gradient is parallel to the z-axis within this slab, and from 140 km to 190 km depth the velocities are constant. As shown in Figure 10, one can define regions in three-dimensional space which can be either analytical mathematical functions or sampled data. The number, sizes, or shapes of the regions are not restricted.

### Potential Application to the Seafloor Spreading Problem

In the theory of seafloor spreading, the earthquake zones are associated with upward welling zones, such as the Mid-Atlantic Ridge, where surface material is being produced, and the boundary between large lithospheric plates as in the Circum-Pacific zone.

The problem of these boundaries, one of which is impinging on the other, is treated by Isacks, Oliver, and Sykes (1968). They postulate that one plate underthrusts the other, particularly in island arc regions. At this boundary the lithosphere (the upper 100 km of the earth's surface) of the oceanic plate is bent downward into the underlying asthenosphere of the continental plate. The precise geometry in which the two plates join is not known, and differs between regions. Isacks, Oliver and Sykes (1968) postulated several configurations as a function of local conditions and rate of underthrusting. Mitronovas, Isacks, and Seeber (1969) have investigated this problem in the Tonga Islands arc. Murdock (1969) has discussed velocity distribution under the Aleutian Region. Carder, et al. (1967) have documented travel-time anomalies from the LONGSHOT explosion.

Figures 12 through 15 were drawn with an arbitrarily-chosen geometry based on the models postulated. In the geometry chosen the 6.75 km/sec layer is taken as the topmost layer which bends downward and the surficial 6.00 km/sec layer is unaffected by bending. These figures show different earthquake locations and the directions of seismic waves propagating from them. Two of the earthquakes are directly above and two directly beneath the upper boundary of the underthrusting lithosphere. The two earthquakes

above the boundary are located in regions where volcanic activity and minor seismic activity is indicated (Mitronovas, Isacks, and Seeber, 1969). The two earthquakes beneath the boundary are located where most seismic stress and the highest probability of earthquakes are thought to occur. The rays for these plots were generated at 4° radial increments from a point source.

Although the frequency of earthquakes with sources above is less than the frequency of those within the underthrusting lithosphere, both source regions have been shown for contrast. This contrast arises from trapped waves within the low velocity layer when the source is within the layer. Rays from within the layer critically reflect at the interface at angles greater than 55° from the normal, to the interface. Rays from sources outside the low velocity layer can be critically reflected only when the inclination of the interface through which the rays have entered is oriented differently from the interface through which they would have otherwise emerged. Parallel interfaces bounding a low velocity layer cannot trap rays which enter from outside the layer. In the model used for Figures 12 through 15 critical reflection from externally generated rays can only occur where the interface of the low-velocity layer is curved, as shown by the one critically reflected ray in Figure 12.

The effects of the low-velocity layer are clearly seen in Figures 12 through 15. Shadow zones are found at the surface when the source is above the layer. These occur because the rays penetrating the layer are bent toward the normal of the interface. These rays are displaced from the paths they would have taken in the absence of the low-velocity layer,



and they emerge at a greater distance from the source than would otherwise be the case. From sources within the low-velocity zone, the influence of critical reflections is shown in Figures 14 and 15. Three separate groups of rays can be seen propagating up the low-velocity layer: those initially reflecting from the upper interface, those which do not touch either the upper or lower interface, and those initially reflecting from the lower interface.

Travel times from each of the four sources are shown in Figures 16 through 19. In Figures 16 and 17, the focal depths are 50 km and 100 km respectively, with sources above the layer. The shadow zones caused by the ray displacements are evident. Travel-time anomalies above 2 seconds occur near the limit of the shadow zones nearest the source.

Travel times for sources within the downward bending layer are shown in Figures 18 and 19, where the focal depths are 60 and 110 km respectively. Critical reflections occur with a large angular extent from the source. The three separate arrival sequences are produced by the three groups of rays described above. The three separate legs of the travel-time curves occur at distances approximately the same as those where the shadow zones are produced for the sources above the layer as shown in Figures 17 and 18.

These results indicate that large effects upon travel times are found within 50 km of the point where the underthrusting lithosphere starts to bend downward from the unperturbed oceanic plate. A pertinent investigation of seismic propagation in the Tonga Islands arc (Mixonovas, et al. 1969) was conducted with five seismometer locations

spaced at distances of 125 km to 200 km from this point toward the underthrusting lithosphere. The nearest seismometer location toward the oceanic plate was approximately 220 km distant on Rarotonga in the Cook Islands. Unfortunately, the location of the seismometers were dictated by the positions of the available islands, and were not within the region in which ray tracing shows shadow zones and multiple arrivals.

To investigate the travel times beyond the region shown in Figures 12 through 15, the spherical earth program was attached as a subroutine to the flat earth program. Many rays exceeded the boundaries shown in Figures 12 through 15 without reaching the surface. These rays were used as sources for the spherical earth program. This was accomplished by saving the location, angle, travel time, and distance travelled as an input to the spherical earth subroutine. Travel times out to approximately  $60^\circ$  were found. These closely paralleled the 1968 P-Phase Tables for corresponding depths of focus. The anomalies found were a maximum of .9 seconds, and were at the maximum in the region near  $25^\circ$ . No conclusions were drawn from these results.

Figures 12 through 19 illustrate the diagnostic capability of the method presented in this study. The travel times are particularly revealing at distances within 50 km of the point at which the lithosphere starts to bend downward. They depend upon the location of the source, vary with direction, and produce distinctive features in the ray diagrams and travel-time curves. Given a set of seismograms at suitable distances from the earthquake in a continental plate boundary area, an investigation of the velocity distribution and source depth can be aided

with this method. A more detailed investigation would also include azimuthal effects, which could be found by projecting the given model on cross-sections at various angles with the cross-section shown.

It is not the purpose of this study to investigate a portion of the earth in detail, but rather to present a method to aid in such investigations. For example the travel times and anomalies found with curved earth out to  $60^\circ$  were not pursued as to their meaning, but rather a method to obtain them using a spherical earth subroutine was demonstrated. Also, the model chosen for the underthrusting lithosphere did not include the 6.00 km/sec layer. Many variations of the model would be made during a detailed investigation--variations such as thicknesses of the layers, effects of depth, and, therefore, heat, on the velocity of the layers, angle of downward bending, extent of the downward thrusting layer, effects upon the overlying layers, departures from horizontal layering, and many other variations. It is apparent that such changes can be accommodated by this ray simulation method. The results of these changes are given both visually and numerically.

### Conclusions

This study has resulted in an economical and versatile method to aid in seismic analysis. Geometric ray tracing can be performed with models representing any conceivable velocity distribution within the earth. Refractive as well as reflective computations can be performed, including multiple reflections. Travel times and approximate amplitudes can be determined for these velocity distributions.

One of the primary goals of seismology is to model the velocity distributions within the earth. Hypotheses of velocity distributions are continuously being produced by seismologists. An important test for the validity of these models has been developed.

Computer drawn plots and numerical output of travel times have been used to illustrate the capabilities of this simulation method. The travel times can be made arbitrarily close to those published by the Seismological Society of America. This method of geometrical ray tracing performs as accurately and with more versatility than previously published ray tracing techniques.

It is hoped and expected that this technique will be used by the seismological profession and that it will be extended and improved, as any useful, new contribution should.

## References

- Bufe, C. G. (1969), "An estimate of the configuration of the surface of the earth's core from the consideration of surface focus PcP travel times", PhD. Dissertation, The University of Michigan.
- Carder, D. S., D. Tocher, C. G. Bufe, S. W. Steward, J. Eisler, and E. Berg (1967), "Seismic wave arrivals from LONGSHOT, 0° to 27°," Bulletin of the Seismological Society of America, Vol. 57, No. 4, pp. 573-590.
- Bullen, K. E. (1963), An introduction to the theory of seismology, Third Edition, Cambridge University Press.
- Engdahl, E. R., J. N. Taggart, J. L. Lobdell, E. P. Arnold, and G. E. Clawson (1968), "Computational methods," Bulletin of the Seismological Society of America, Vol. 58, pp. 1339-1344.
- Gutenberg, B. (1914), "Über Erdbebenwellen, VIIA. Beobachtungen an Registrierungen von Fernbeben in Göttingen und Folgerungen über die Konstitution des Erdkörper," Göttinger Nachrichten, pp. 1-52.
- Helbig, K. (1965), "A graphical method for the construction of rays and travel times in spherically layered media," Part I: Isotropic Case, Bulletin of the Seismological Society of America, Vol. 55, 641-651.
- Herrin, E., E. P. Arnold, B. A. Bolt, G. E. Clawson, E. R. Engdahl, H. W. Freedman, D. W. Gordon, A. C. Hales, J. L. Lobdell, O. Nuttli, C. F. Romney, J. N. Taggart, and W. C. Tucker (1968), "1968 Seismological tables for P-phases," Bulletin of the Seismological Society of America, Vol. 58, pp. 1193-1241.
- Isacks, B., J. Oliver, and L. R. Sykes (1968), "Seismology and the new global tectonics," Journal of Geophysical Research, Vol. 73, No. 18, pp. 5855-5899.
- Iyer, H. M. and V. W. Punton (1963), "A Computer program for plotting wavefronts and rays from a point source in dispersive mediums," Journal of Geophysical Research, Vol. 68, No. 11.
- Jackson, P. L. (1968), "Two- and Three-dimensional ray tracing through inhomogeneous media," Paper presented to the Annual Meeting of the Seismological Society of America, Tucson, Arizona, April.
- Jackson, P. L. (1969), "Seismic ray simulation," Paper presented to the Eastern Section, Seismological Society of America, Blacksburg, Va., October.
- Jackson, P. L. (1970), "Seismic ray simulation in a spherical earth," Bulletin of the Seismological Society of America, Vol. 60, No. 3, pp. 1021-1025.
- Jacob, K. H. (1970), "P-residuals and global tectonic structures investigated by three-dimensional seismic ray tracing with emphasis on LONGSHOT data," Paper presented to the Annual Meeting of the American Geophysical Union, Washington, D. C., April.

- Jeffreys, H. and K. E. Bullen (1948), Seismological tables, British Association for the Advancement of Science, London.
- Julian, B. R. and D. L. Anderson (1968), "Travel times, apparent velocities and amplitudes of body waves," Bulletin of the Seismological Society of America, Vol. 58, pp. 339-366.
- Lewis, B. T. R. and R. P. Meyer (1968), "A Seismic investigation of the upper mantle to the west of Lake Superior," Bulletin of the Seismological Society of America, Vol. 58, pp. 565-569.
- Mitronovas, W., B. Isacks, and L. Seeber (1969), "Earthquake locations and seismic wave propagation in the upper 250 km of the Tonga Island arc," Bulletin of the Seismological Society of America, Vol. 59, pp. 1115-1135.
- Mohorovičić, A. (1910), "Jahrbuch des meteorologischen," Observatoriums in Zagreb (Agram) für das Jahr 1909, Vol. 9, pt. 4, pp. 1-63.
- Murdock, J. M. (1969), "Crust-mantle system in the Central Aleutian region--A hypothesis," Bulletin of the Seismological Society of America, 59, 1543-1558.
- Newton, I. (1730; 1952), Optiks, or a treatise of the reflections, refractions, inflections, and colours of light, Reprint, based on the Fourth Edition, London, Dover Publication, Inc., New York
- Willis, D. E. and P. L. Jackson (1968), Collection and Analysis of Seismic wave propagation data, University of Michigan, Willow Run Laboratories, Geophysics Laboratory, Annual Report Number 8071-15-P.
- Yacoub, N. K., J. H. Scott, and F. A. McKeown (1968), Computer technique for tracing seismic rays in two-dimensional geological models, Geological Survey, Open-File Report, U. S. Department of the Interior.
- Zoeppritz, K. (1919), "Über Erdbebenwellen VIIb," Goettinger Nachrichten, pp. 66-84.

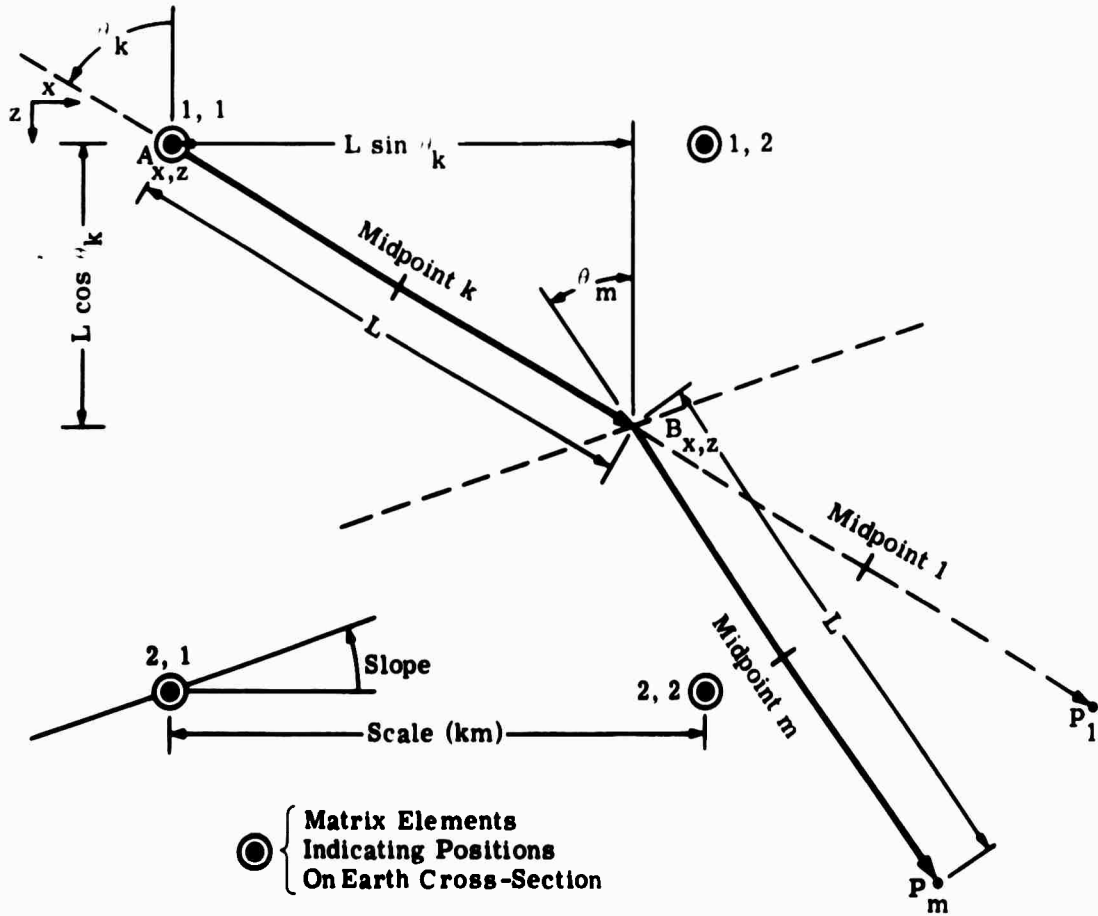


**FIGURE 1. REFERENCE FRAME FOR INCREMENTING RAYS.** Seismic velocity and slope are associated with each matrix element. Referencing for the slope is shown at element (2, 1). An interface between two velocity layers can be positioned between matrix elements as shown by the dotted line through B. The scale, or sampling interval, is the distance between matrix elements as represented in kilometers. An incident ray segment of length  $L$  and initial angle  $\theta_k$  extends from A to B. Coordinates of B are found by extension from A:  $B_x = A_x + L \sin \theta_k$ ,  $B_z = A_z + L \cos \theta_k$ . The segment  $BP_1$  is the first "probing" segment to obtain initial values of seismic velocity at midpoint 1. The angle  $\theta_m$  is computed with Snell's law, using emerging velocity at midpoint 1, incident velocity at midpoint k, and incident angle  $\theta_k$ . "Probing" segments are recomputed using successive values of  $\theta_m$  until the absolute value of  $(\theta_m - \theta_{m-1})$  is less than a predetermined small value. The velocity and slope associated with the segment  $BP_m$  and the last computed value of  $\theta_m$  are then used as the incident ray parameters, and a subsequent emerging angle computed for the ray segment proceeding from point  $P_m$ .

COMPUTER OUTPUT										CORRESPONDING TRAVEL TIMES FROM 1968 P TABLES	
> INITIAL ANGLE, > DELTA		ANGLE KM	DEPTH, & DISTANCE		TOTSEC	RADIUS	DEPTH	AMPL	MIN	SEC	
>> 17.00	0.0	0.0	MIN	SEC							
>> 52.07	9148.83	12.37	21.99	741.99	3970.18	2400.82	0.90		12	21.66	
>> 20.00	0.0	0.0									
>> 71.43	7962.47	11.36	21.62	651.63	4446.43	1922.57	1.04		11	21.49	
>> 23.00	0.0	0.0									
>> 58.41	6310.93	9.94	56.32	396.32	4880.27	1490.73	1.28		9	56.42	
>> 26.00	0.0	0.0									
>> 46.62	5196.48	8.48	29.08	309.08	5243.15	1127.85	1.62		8	29.15	
>> 29.00	0.0	0.0									
>> 33.49	3732.67	6.66	39.86	399.86	5346.36	824.64	2.27		6	40.49	

FIGURE 2. COMPUTER OUTPUT USING DIRECT RAY SIMULATING FOR 5 P RAYS. 15 km sampling interval and 9 km incrementing distance per iteration. Travel times from 1968 P-phase tables shown for comparison. Travel times are shown in integer and fraction notation in minutes, seconds corresponding to fraction of the minute, and in total seconds. For example, in the entry for = 82.070, 21.99 sec = 0.37 min, and travel time = 12 min 21.99 sec.





FIGURE 3. PROPAGATION OF P THROUGH HYPOTHETICAL CRUST AND UPPER MANTLE STRUCTURE. Cross-section from Pacific Ocean across central California to Nevada. Plane wave simulation of P-wave from source  $30^\circ$ , or 3,333 km, distance. Emerging rays indicate focussing, shadow zones, and travel time anomalies. From Bufe (1969).

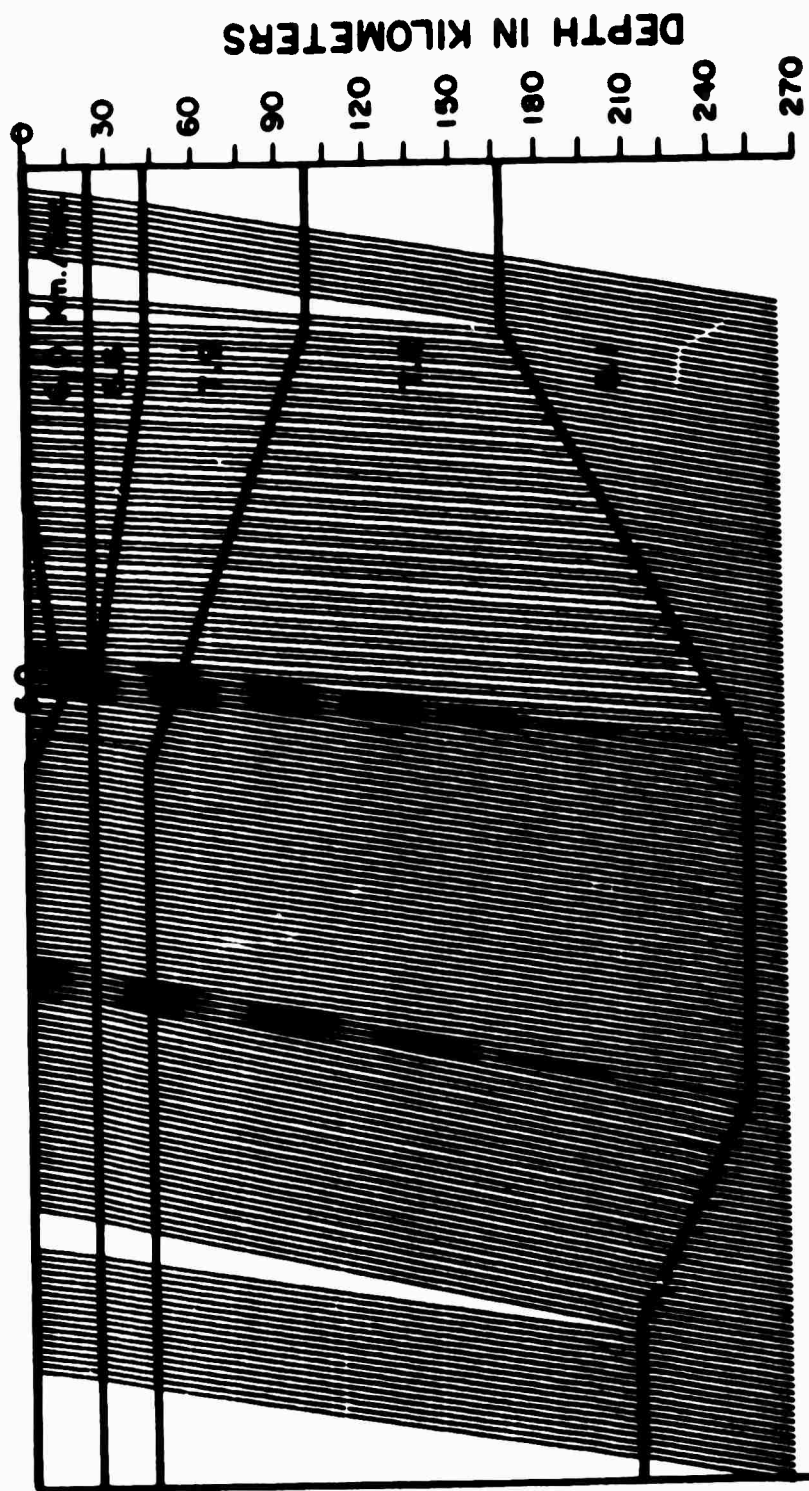
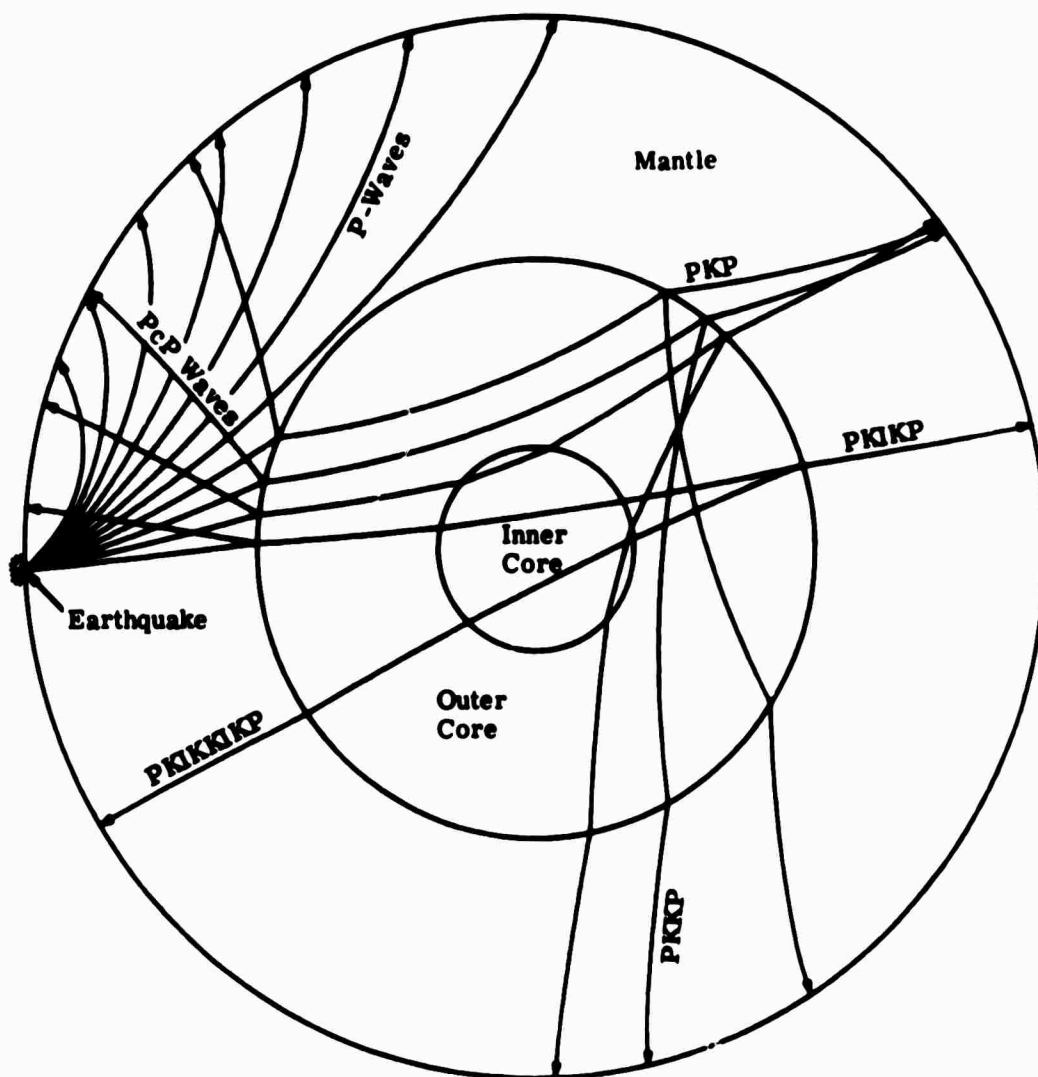
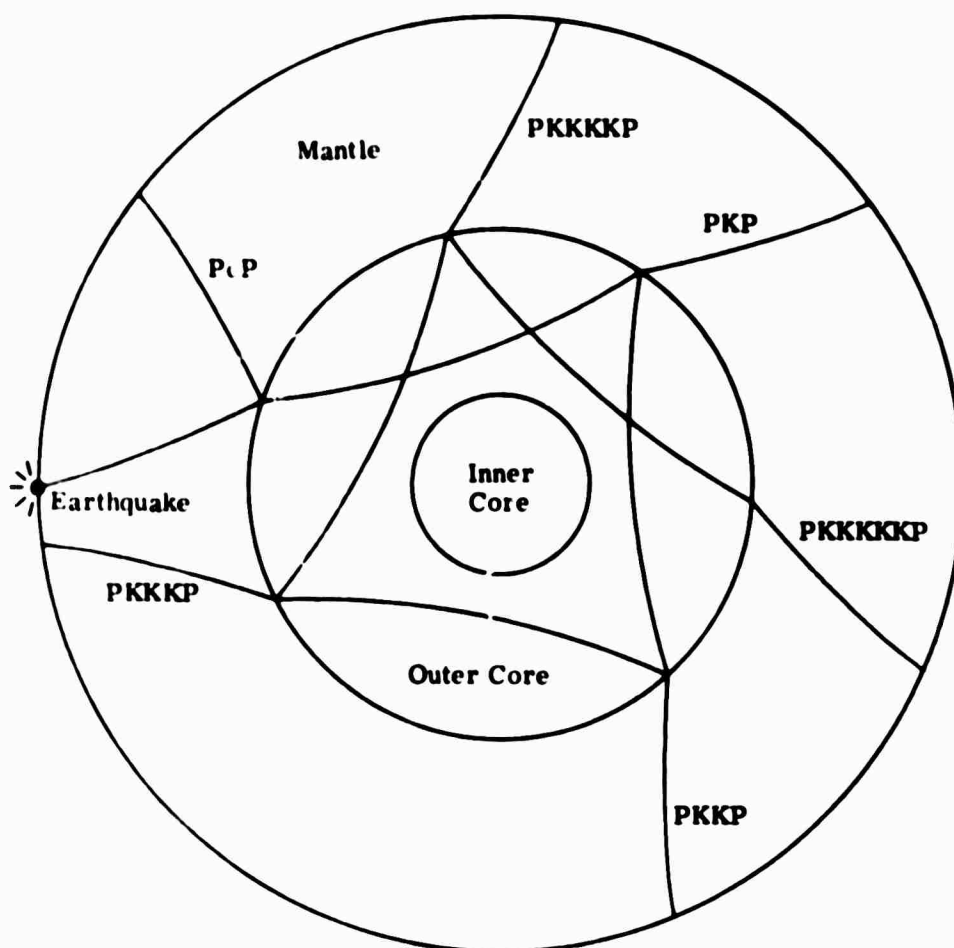


FIGURE 4. PROPAGATION OF PcP THROUGH HYPOTHETICAL CRUST AND UPPER MANTLE STRUCTURE SHOWN IN FIGURE 3. Note significantly different distribution of emerging rays from those in Figure 3. From Bufe (1969).



**FIGURE 5. PLOTS OF P, PcP, PKP, PKIKP, PKKP, AND PKIKPK RAYS GENERATED WITH A SPHERICAL EARTH PROGRAM. Jeffreys-Bullen core and 1968 P-phase mantle velocity distributions. Radial velocity distribution sampled at 70 km intervals. Rays segment lengths 70 km.**



**FIGURE 6. MULTIPLE REFLECTIONS. PcP and PKP rays up to PKKKKKP. Four multiple reflections preset into computer program. Any number of multiple reflections can be preset into program.**

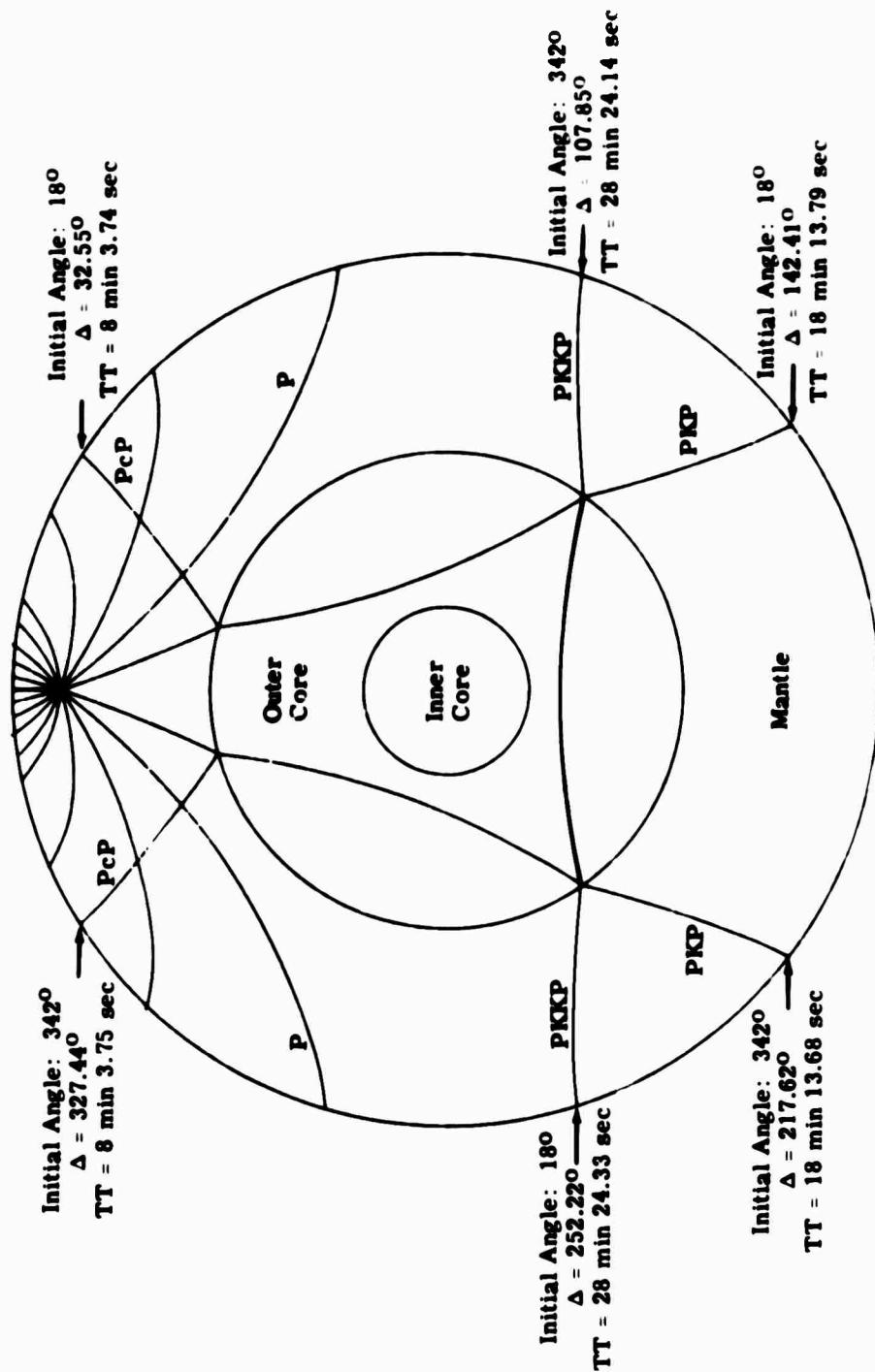


FIGURE 7. UNIFORMITY OF PLOTTING AND TRAVEL TIMES SYMMETRICALLY PLOTTED FROM 700 km DEPTH. Initial angles from source are in increments of 180 from vertical. Computer results for and travel times of emerging rays shown for 180 and 342° rays. Maximum difference in travel time between symmetric rays is 0.11 seconds in PKP rays.

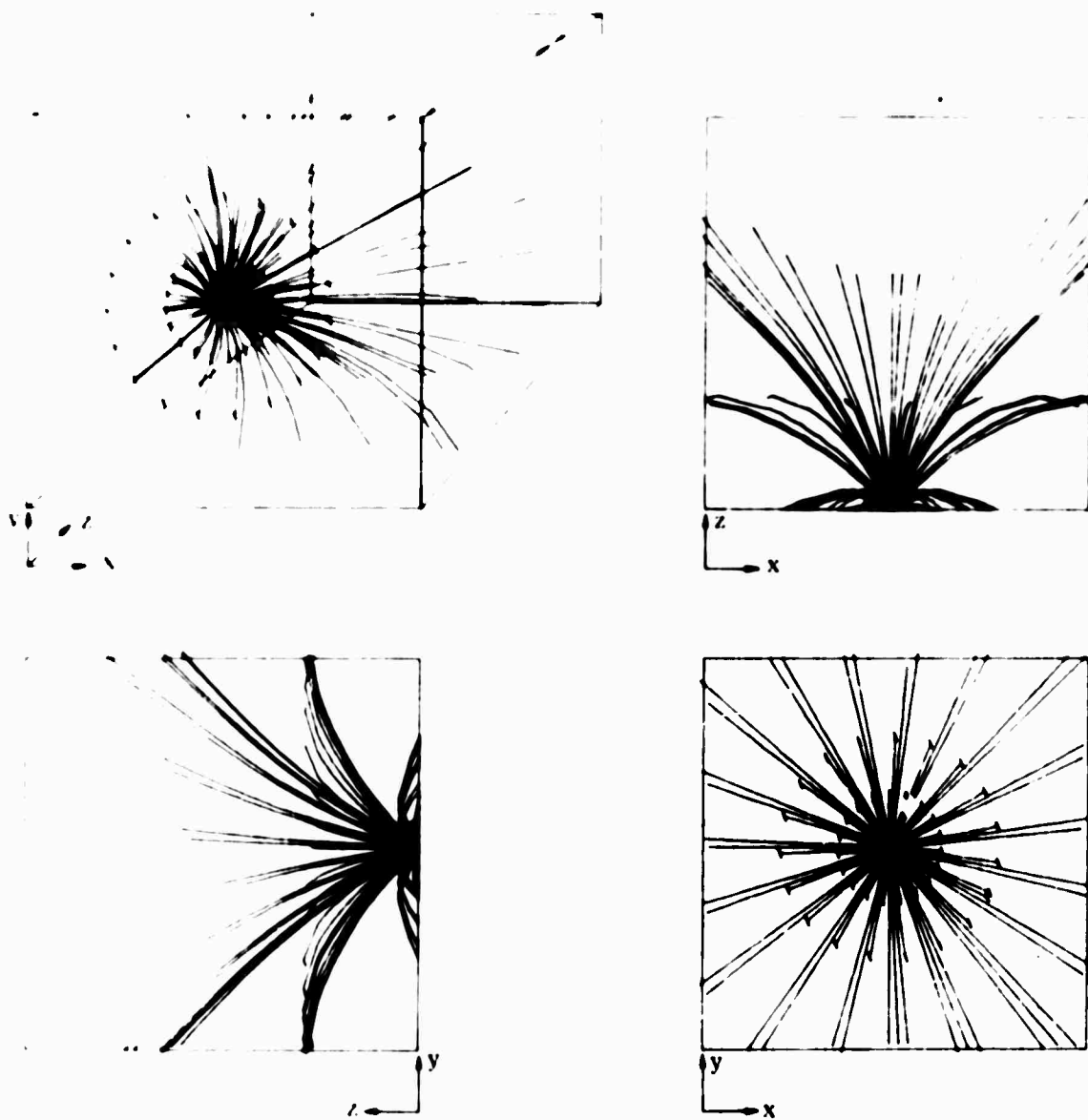
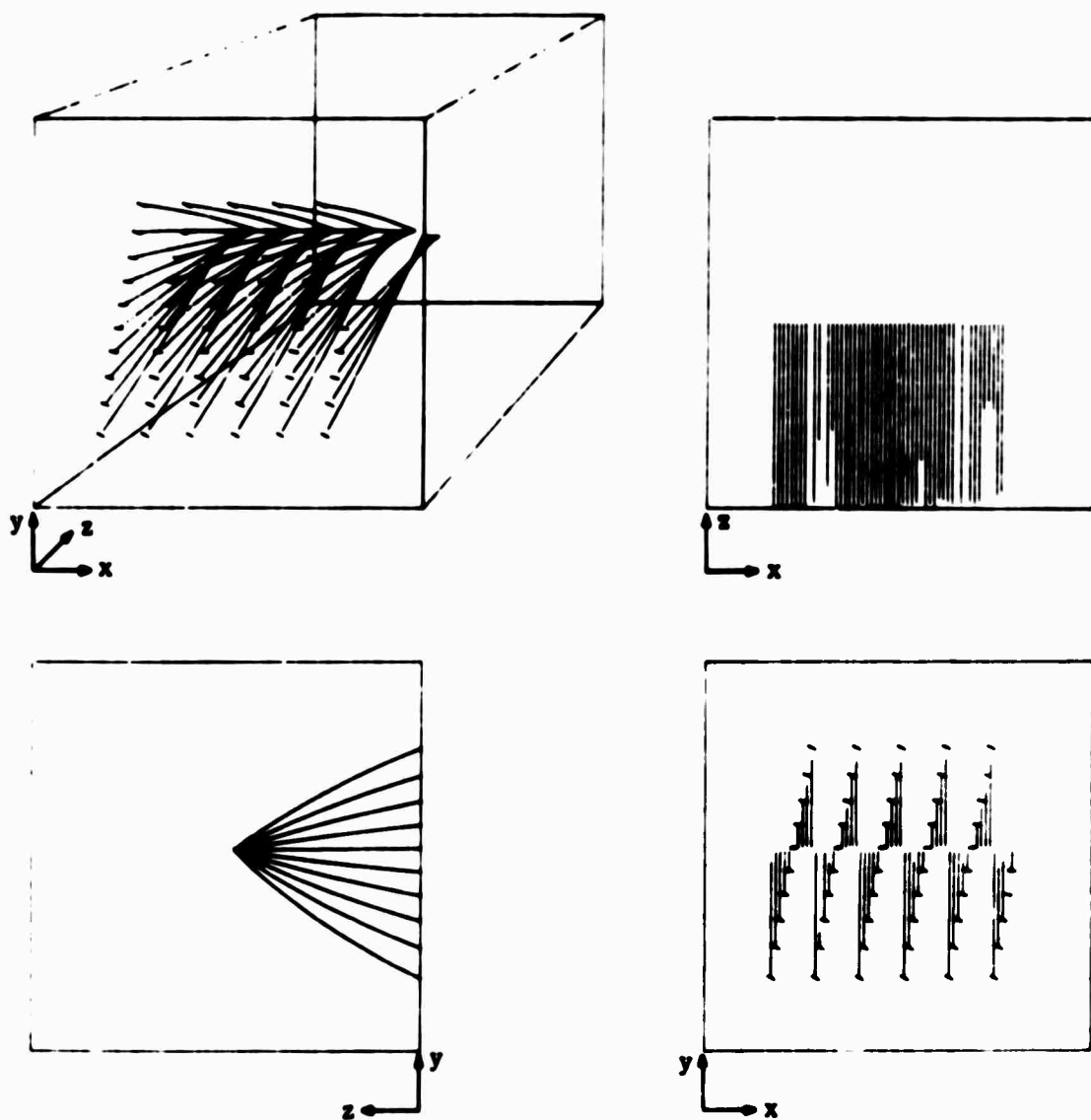


FIGURE 8. THREE DIMENSIONAL RAY TRACING IN A REGION DEFINED BY 30 x 30 x 30 VELOCITY SAMPLES. Constant velocity in planes parallel to the x, y plane, increasing velocity in z-direction for 15 sample points from the x, y plane. Four cones of rays originating from point in the x, y plane. Rays emerging at the x, y plane shown by slash marks with orientation of angle of emergence. Upper left: one-point perspective; remaining views: labelled orthographic projections.



**FIGURE 9. LINE SOURCE AT DEPTH FOR THREE-DIMENSIONAL REPRESENTATION AS SHOWN IN FIGURE 8. Plotting defects in upper right (x, z) projection; all lines should extend to x-axis.**

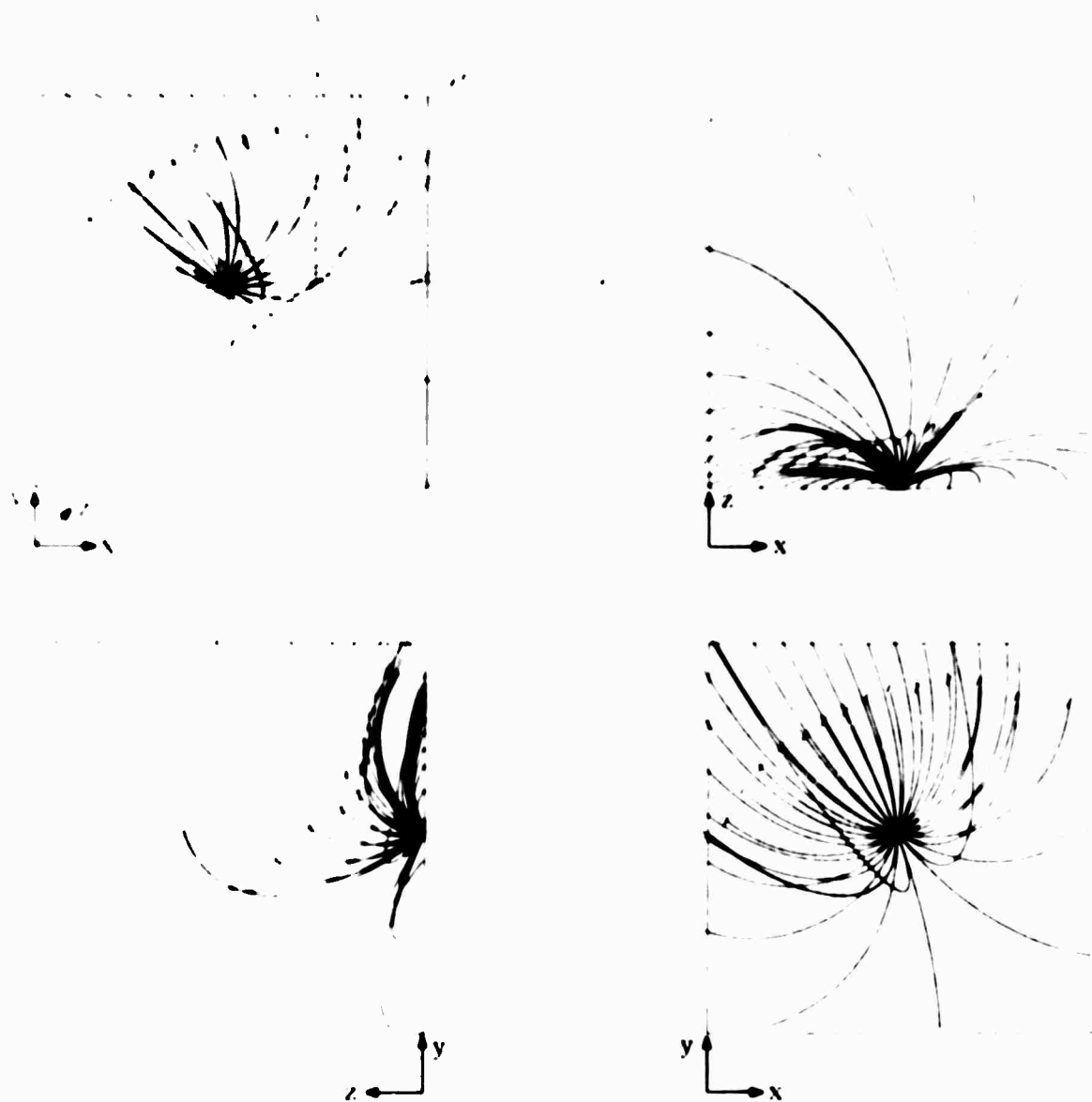
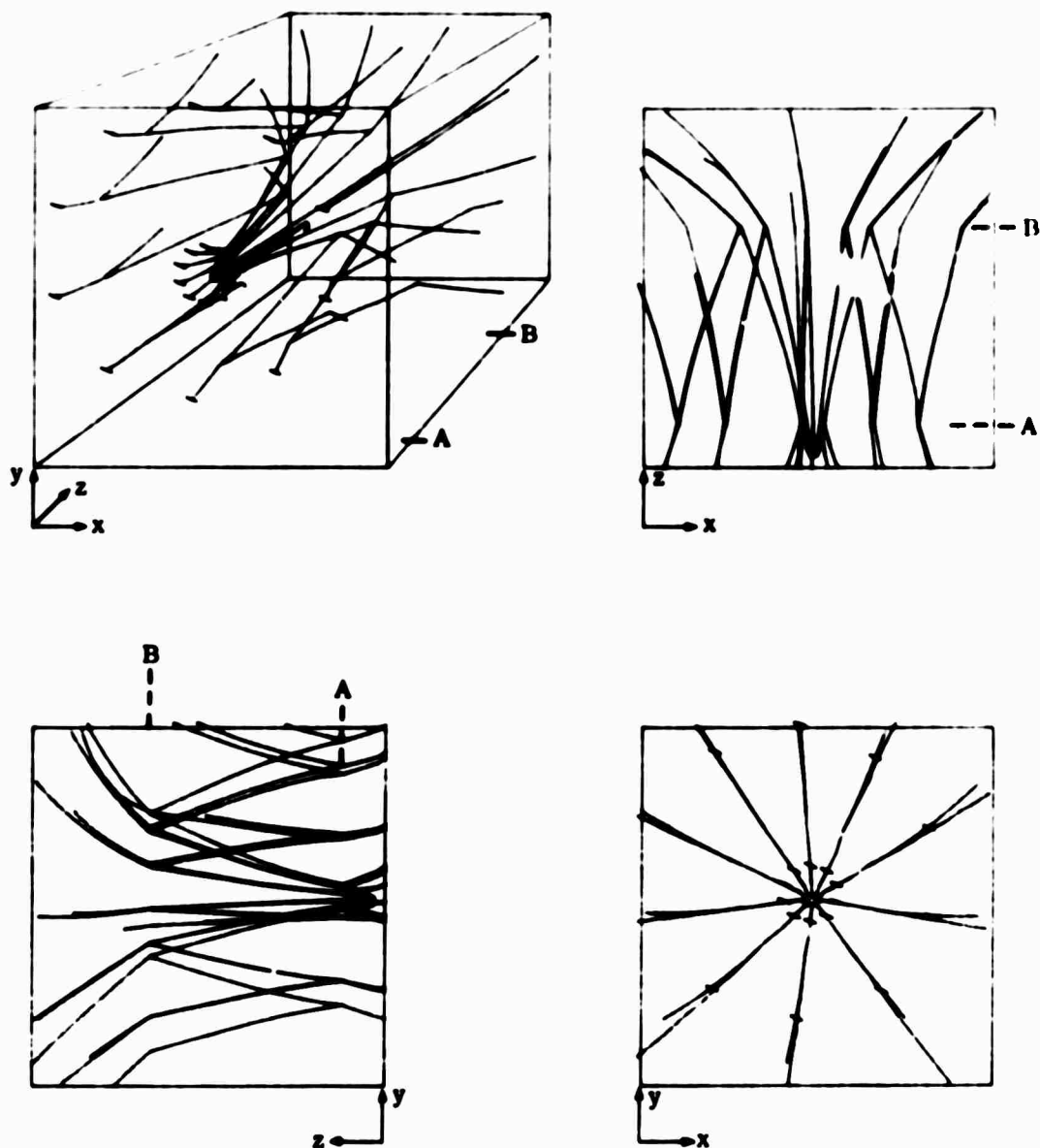


FIGURE 10. THREE-DIMENSIONAL RAY TRACING WITH VELOCITY DISTRIBUTION DEFINED BY CONTINUOUS MATHEMATICAL FUNCTION. Velocity =  $4.0 + 0.15x + 0.3y + 0.6z$ , where volume is defined as in Figure 8.





**FIGURE 11. THREE-DIMENSIONAL RAY TRACING WITH VELOCITY FUNCTIONS SPECIFIED FOR DIFFERENT REGIONS.** Sampled values for intermediate layer between A and B. Velocity =  $4.0 + 0.15x + 0.3y + 0.6z$  for layers above A and below B. Volume is defined as in Figure 8.

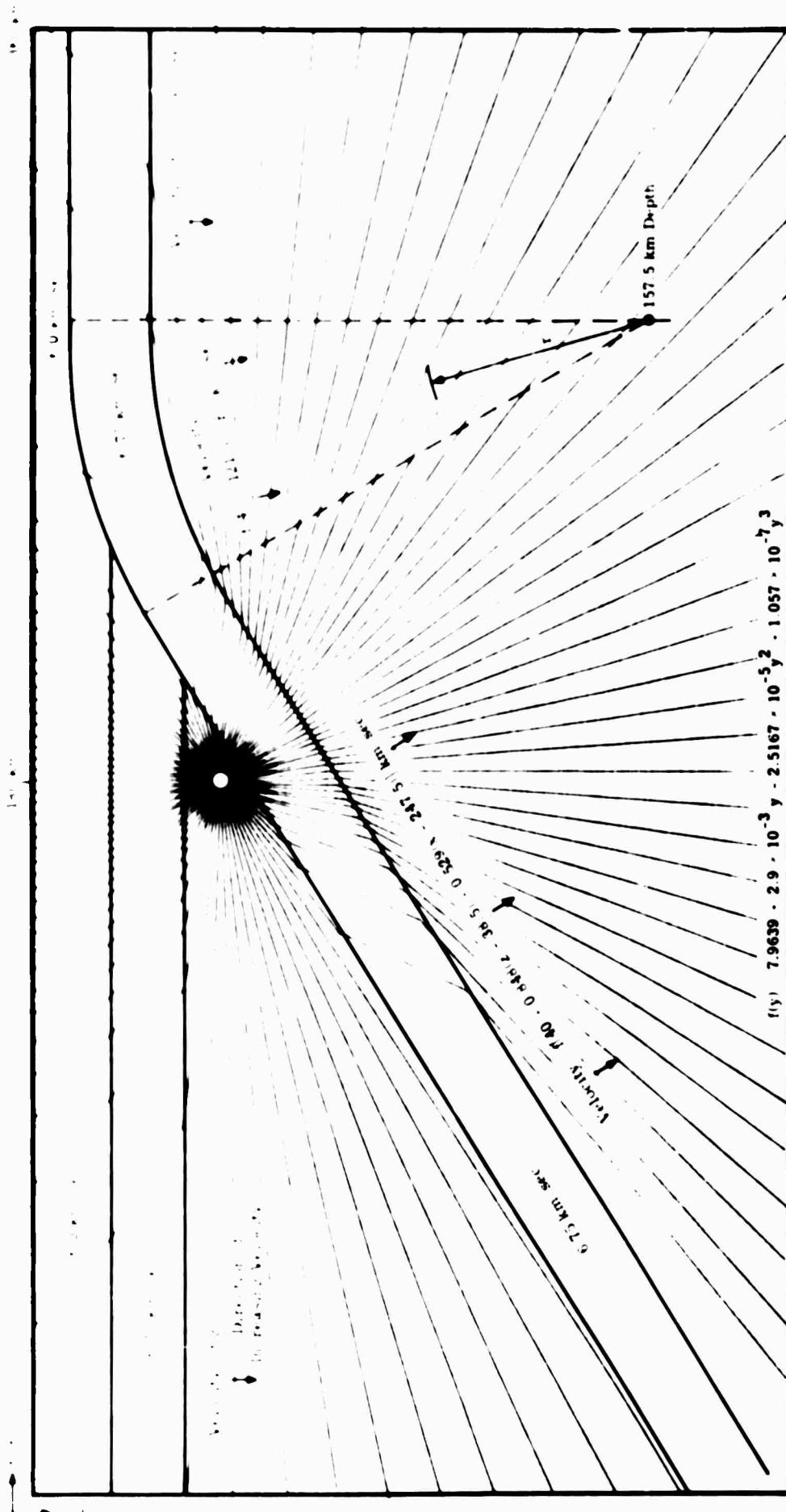


FIGURE 12. RAY PATHS FROM EARTHQUAKE ABOVE UNDERTHRUSTING LITHOSPHERE AT CONTINENTAL PLATE BOUNDARY. Depth of focus 50 km. Velocity distribution for Figure 12-19 based upon Isacks, Oliver, and Sykes (1968). Travel times for this plot are shown in Figure 16.

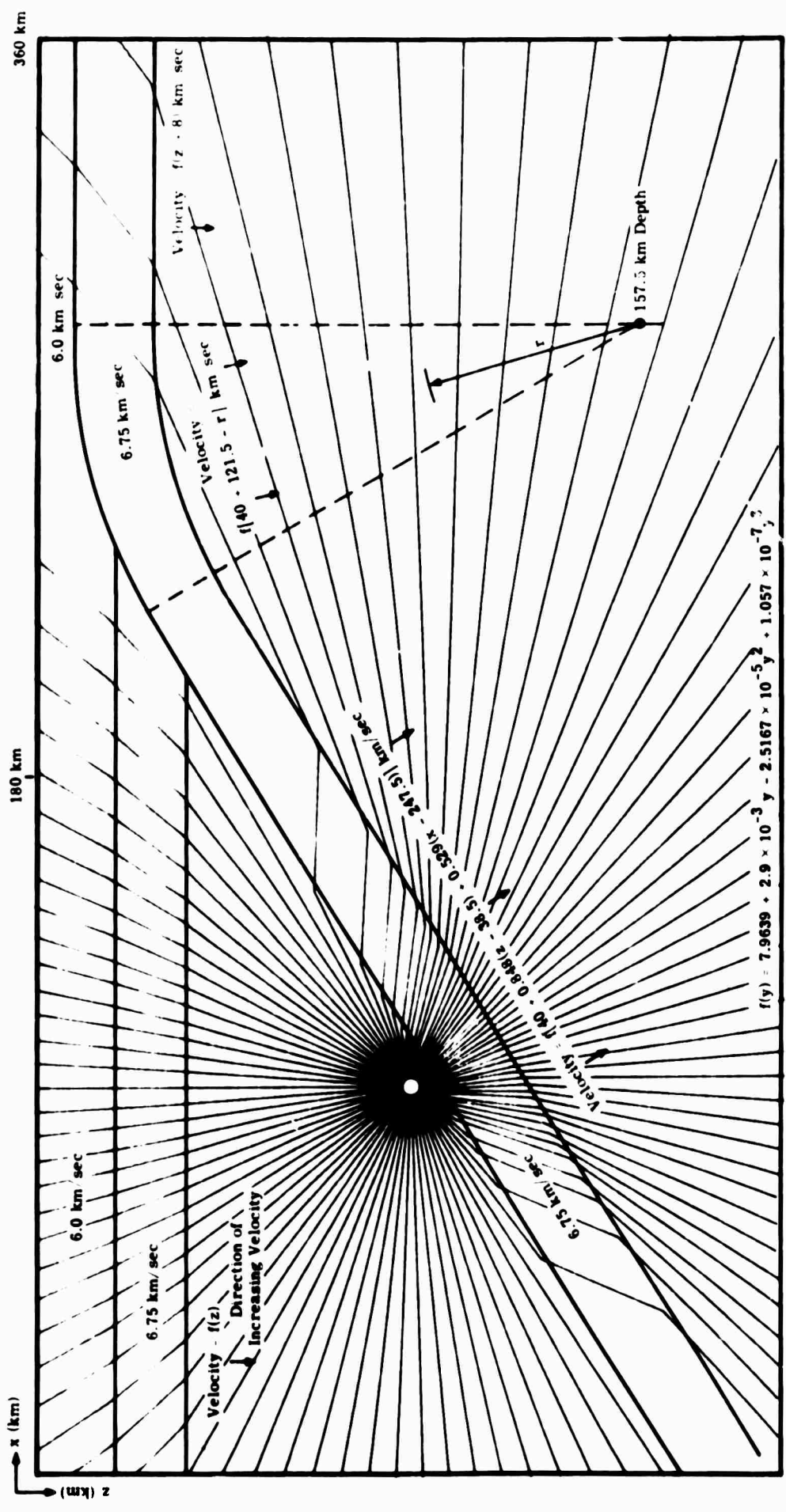


FIGURE 13. RAY PATHS FROM EARTHQUAKE ABOVE UNDERTHrusting LITHOSPHERE AT CONTINENTAL PLATE BOUNDARY. Depth of focus: 100 km. Travel times for this plot are shown in Figure 17.

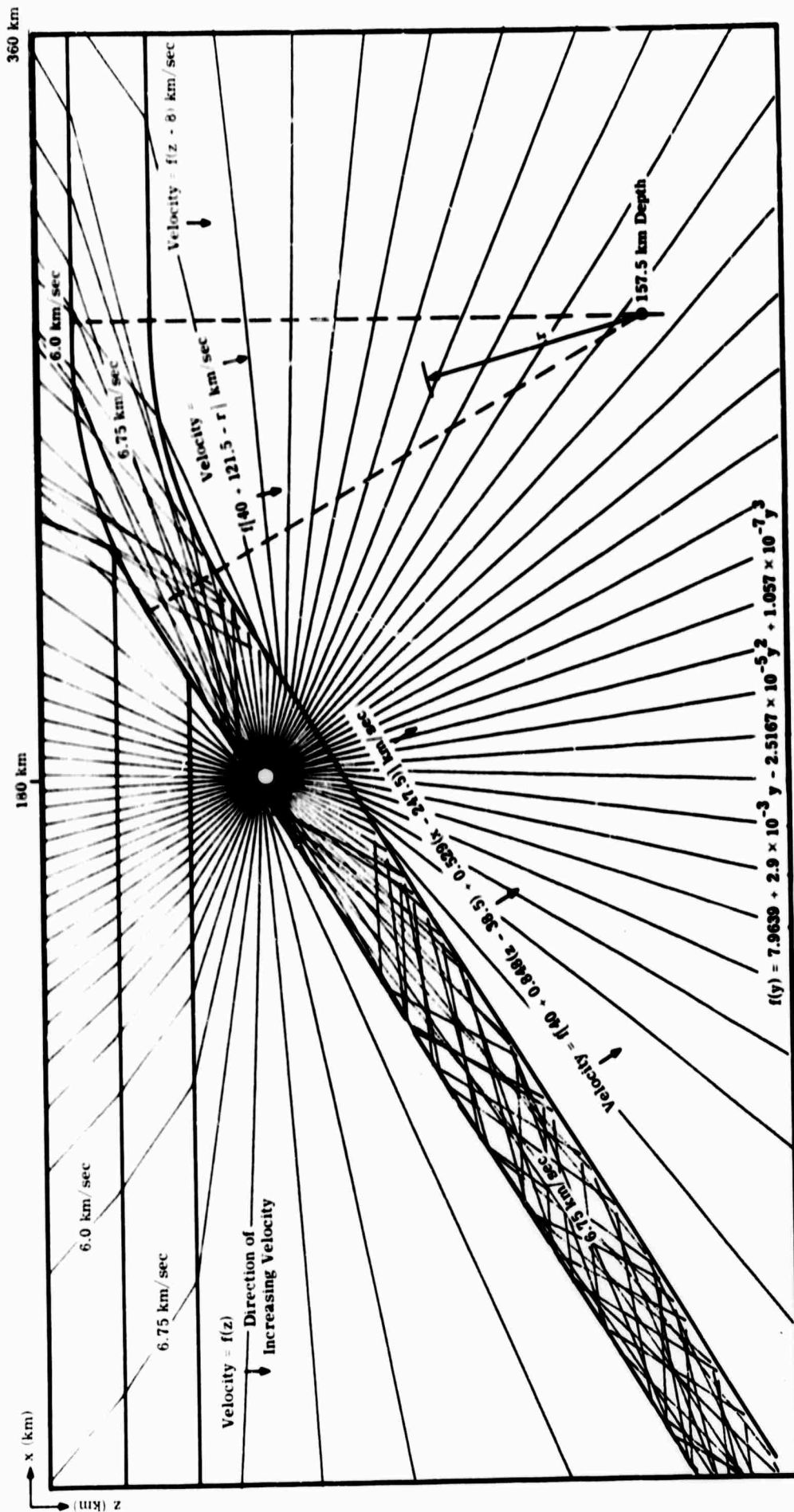


FIGURE 14. RAY PATHS FROM EARTHQUAKE WITHIN UNDERTHRUSTING LITHOSPHERE AT CONTINENTAL PLATE BOUNDARY. Depth of focus: 60 km. Travel times for this plot are shown in Figure 18.

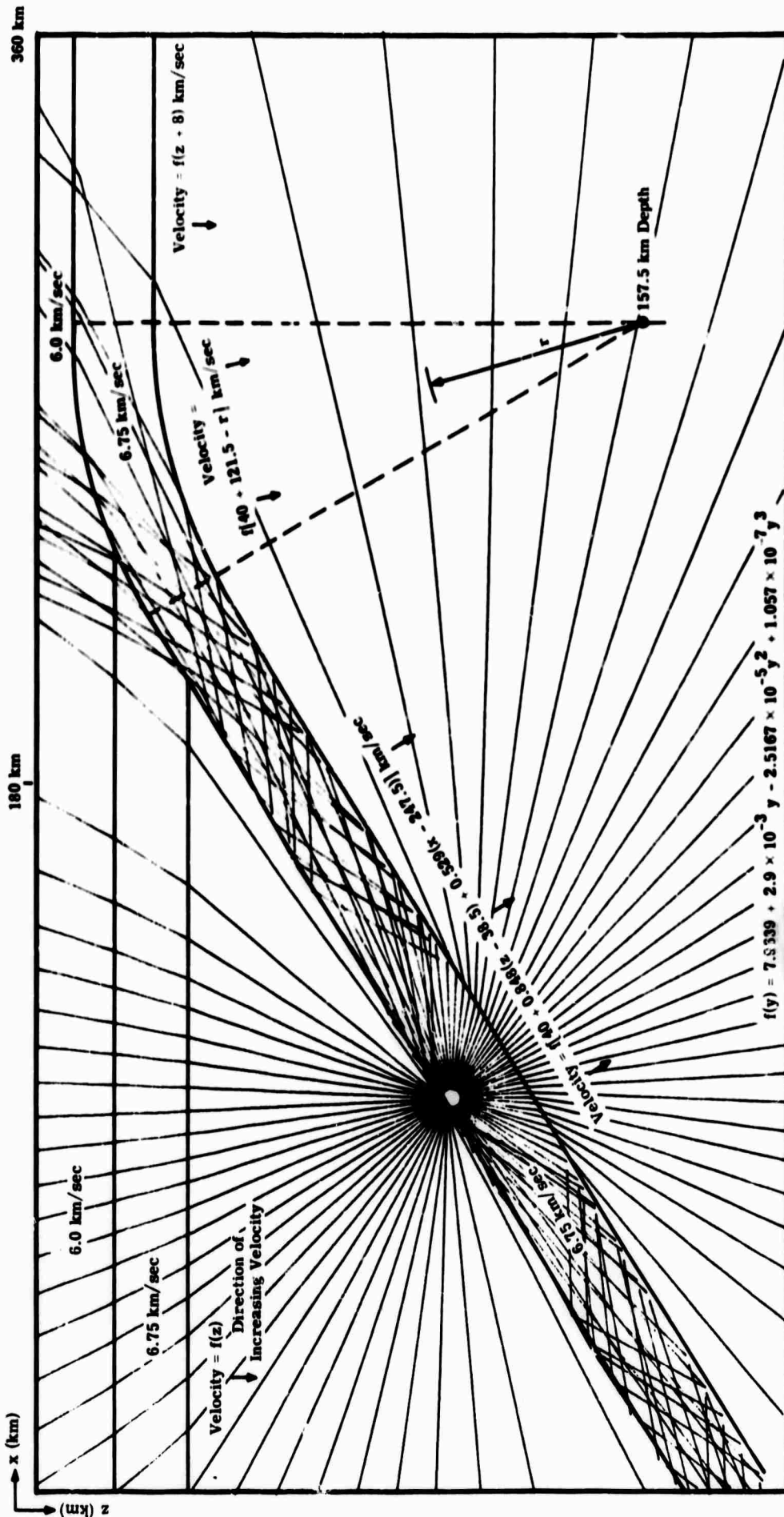


FIGURE 15. RAY PATHS FROM EARTHQUAKE WITHIN UNDERTHRUSTING LITHOSPHERE AT CONTINENTAL PLATE BOUNDARY. Depth of focus: 110 km. Travel times for this plot are shown in Figure 19.

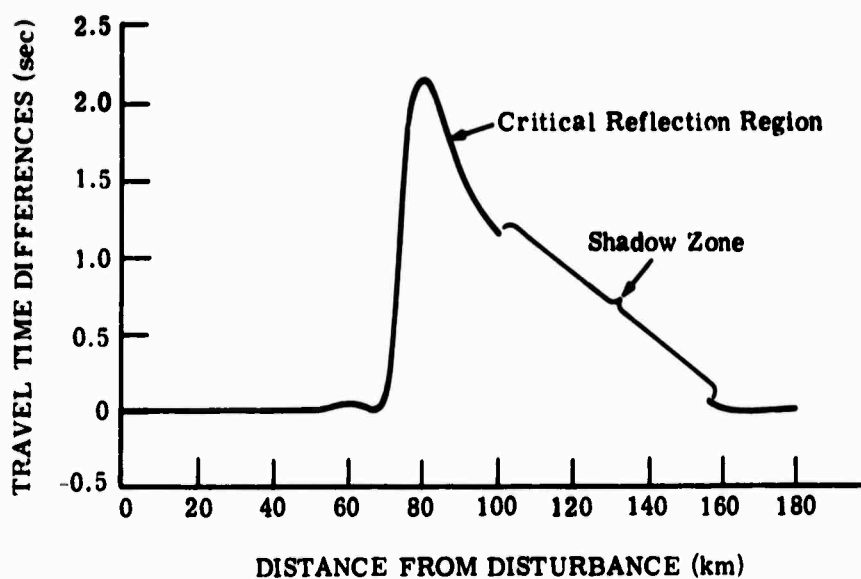
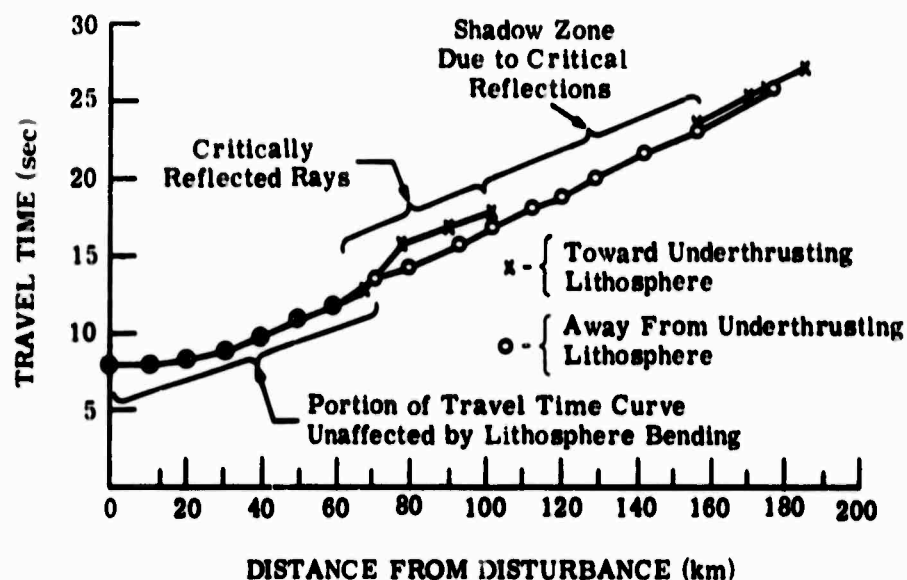


FIGURE 16. EARTHQUAKE ABOVE UNDERTHRUSTING LITHOSPHERE AT CONTINENTAL PLATE BOUNDARY. Depth of focus: 50 km. Above: Travel times toward and away from underthrusting lithosphere. Below: Differences between travel times toward and away from underthrusting lithosphere. See Figure 12 for ray paths and velocity distribution.

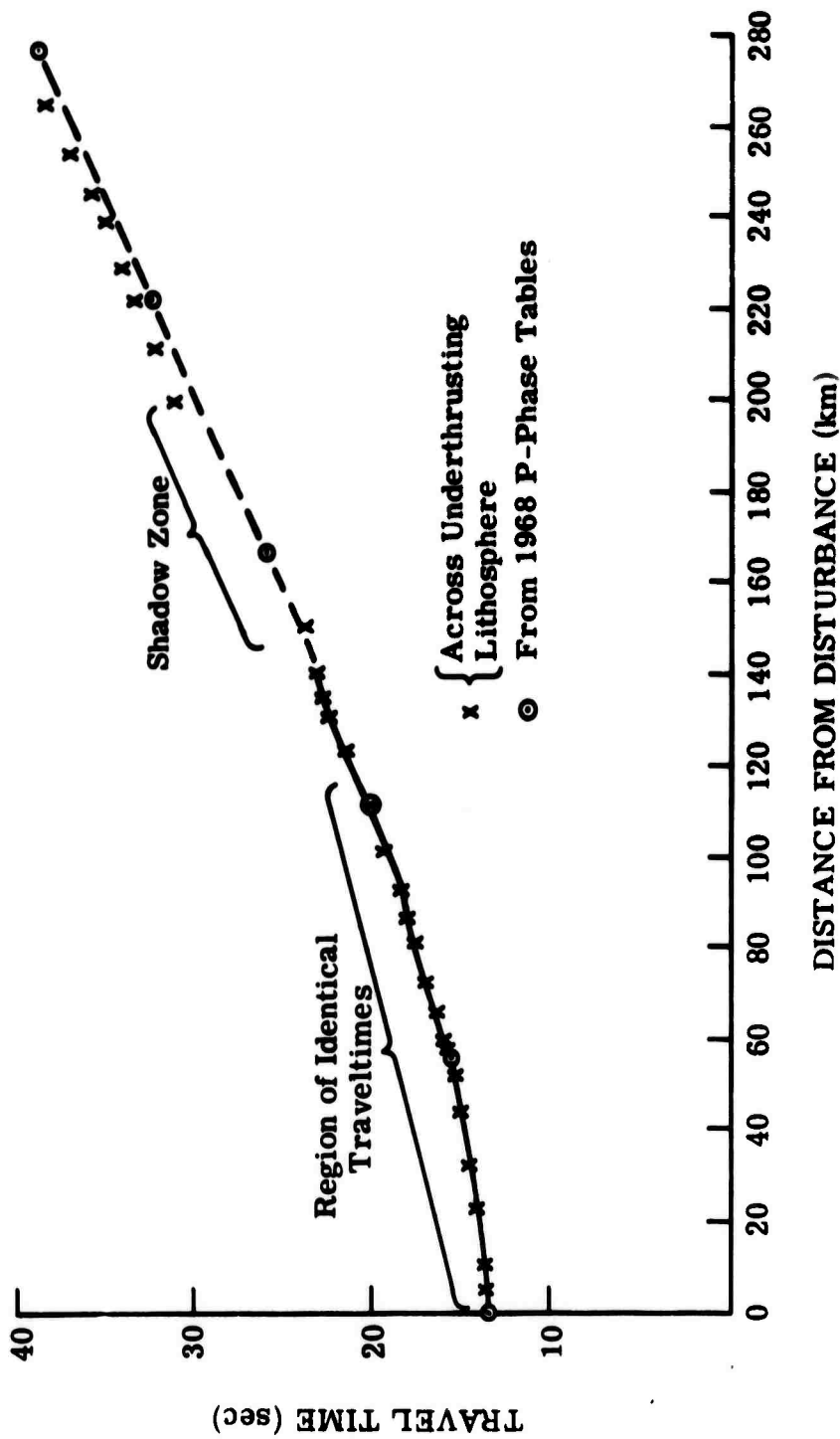
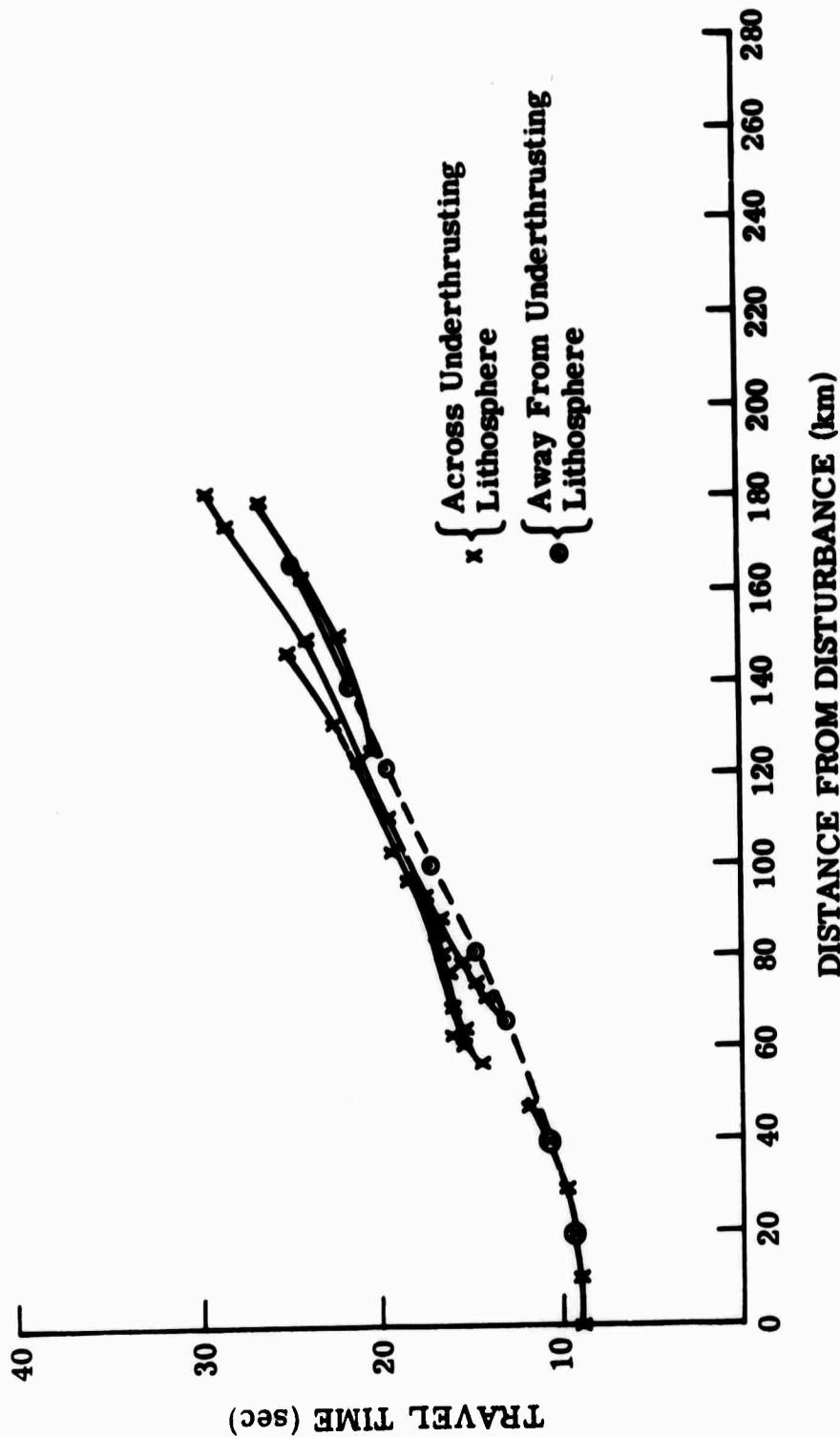


FIGURE 17. EARTHQUAKE ABOVE UNDERTHRUSTING LITHOSPHERE AT CONTINENTAL PLATE BOUNDARY. Depth of focus: 100 km. Travel times from 1968 P-phase tables shown for comparison. See Figure 13 for ray paths and velocity distribution.



**FIGURE 18. EARTHQUAKE WITHIN UNDERTHRUSTING LITHOSPHERE AT CONTINENTAL PLATE BOUNDARY** Depth of focus: 60 km. Travel times across and away from underthrusting lithosphere. Separate arrival times beyond 65 km caused by trapped critical reflections in the low velocity layer. See Figure 14 for ray paths and velocity distribution.



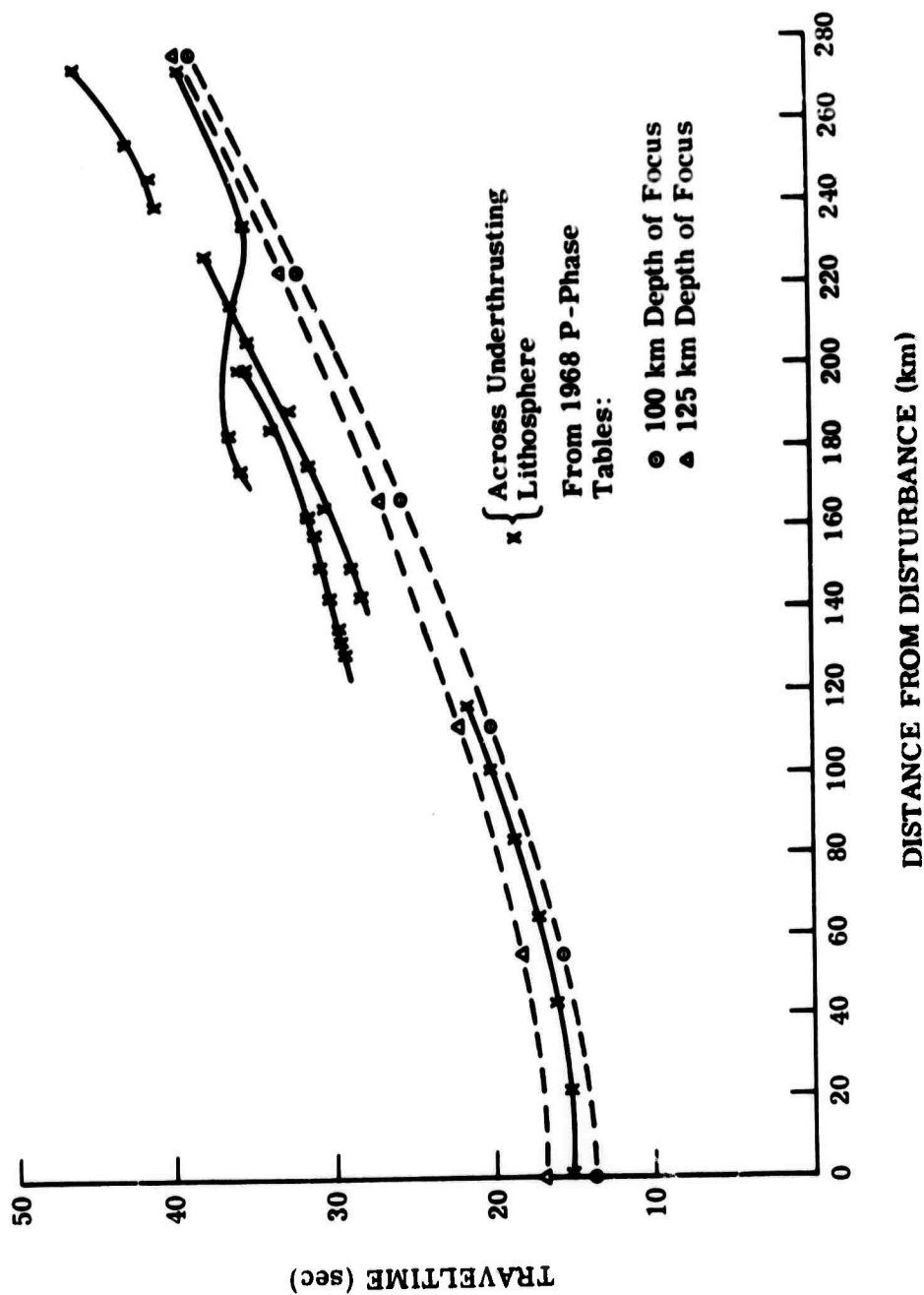


FIGURE 19. EARTHQUAKE WITHIN UNDERTHRUSTING LITHOSPHERE AT CONTINENTAL PLATE BOUNDARY. Depth of focus: 110 km. Travel times across underthrusting lithosphere. Travel times for 100 km and 125 km depth of focus from 1968 P-phase tables shown for comparison. Different arrival times beyond 135 km caused by trapped critical reflections in the low velocity layer. See Figure 15 for ray paths and velocity distribution.

**APPENDIX**  
**Listings of Computer Programs**

C	PROGRAM FOR A FLAT EARTH CROSS-SECTION MODEL	A	1
C	WHERE THE VELOCITY DISTRIBUTION IS SET UP AND RAYS ARE PROPAGATED	A	2
C	THROUGH THE MODEL	A	3
C	TRAVEL TIMES, DISTANCES, APPROXIMATE AMPLITUDES ARE COMPUTED.	A	4
C	NAMLIST PARAMETERS ALPHABETICALLY LISTED	A	5
C		A	6
C	A ARRAY OF SAMPLED VELOCITY VALUES	A	7
C	ANGLE MINIMUM ANGLE AT WHICH PRECISE INTERFACE LOCATION IS USED	A	8
C	B ARRAY CONTAINING SAMPLED SLOPE VALUES	A	9
C	BEGIN INITIAL ANGLE OF RAY	A	10
C	DEIN INCREMENTATION ANGLE OF INCIDENT RAYS	A	11
C	DEC EXPONENTIAL INCREMENT BY ATTENUATION	A	12
C	DEIH HORIZONTAL INCREMENTATION OF INCIDENT RAYS	A	13
C	DEIV VERTICAL INCREMENTATION OF INCIDENT RAYS	A	14
C	DIFRAC DISTANCE IN KM BETWEEN SAMPLE POINTS	A	15
C	G RAY SEGMENT LENGTH	A	16
C	IGCIE MAXIMUM NUMBER OF RAY INCREMENTATIONS	A	17
C	IEXACT SWITCH TO INCLUDE PRECISE INTERFACE LOCATIONS	A	18
C	IMOVIE SWITCH TO MULTIPLY G BY VELOCITY TO GIVE APPEARANCE OF RAYS	A	19
C	PROPAGATING PROPORTIONAL TO VELOCITY WHEN MAKING A COMPUTER MOVE	A	20
C	INAME SWITCH TO INCLUDE NAMLIST INPUT OF VELOCITY AND SLOPE DATA	A	21
C	IPLANE SWITCH TO INCLUDE CALCULATIONS FOR INCIDENT PLANE WAVE	A	22
C	IPIOT SWITCH TO INCLUDE CALCOMP PLOTTING	A	23
C	IPORSH LIMIT OF NUMBER OF HORIZONTAL SAMPLE POINTS	A	24
C	IPORVSH LIMIT OF VERTICAL NUMBER OF VERTICAL SAMPLE POINTS	A	25
C	IPRINT SWITCH TO INCLUDE DIAGNOSTIC WRITINGS	A	26
C	MATH SWITCH TO INCLUDE CONTINUOUS MATHEMATICAL FUNCTION	A	27
C	NMULT NUMBER OF MULTIPLE REFLECTIONS ALLOWED	A	28
C	NOR NUMBER OF INITIAL ANGLE INCREMENTS	A	29
C	NOH NUMBER OF INITIAL HORIZONTAL INCREMENTS	A	30
C	NOIN TOTAL NUMBER OF INITIAL RAYS	A	31
C	NOV NUMBER OF INITIAL VERTICAL INCREMENTS	A	32
C	NOULINE NUMBER OF CALCOMP LINES NECESSARY TO OUTLINE STRUCTURE	A	33
C	ORIGH INITIAL HORIZONTAL POSITION OF RAY	A	34
C	ORIGV INITIAL VERTICAL POSITION OF RAY	A	35
C	PNM INITIAL AMPLITUDE VALUE	A	36
C	REFVEL REFERENCE VELOCITY TO MAKE MOVIE	A	37
C	SCA PRINT SCALING FACTOR	A	38
C	TEST SMALL VALUE TO TEST REPEATED EMERGE ANGLE DIFFERENCES	A	39
C	VELDIF VELOCITY DIFFERENCE NECESSARY TO CAUSE REFLECTION	A	40
C	X ARRAY CONTAINING HORIZONTAL POSITIONS FOR PLOTTING	A	41
C	Y ARRAY CONTAINING VERTICAL POSITIONS FOR PLOTTING	A	42
C			
C	SYMBOL TABLE	A	43
C	AMPL AMPLITUDE	A	44
C	ANGLE1 INCIDENT ANGLE OF RAY	A	45
C	ANGLE2 EMERGING ANGLE OF RAY	A	46
C	ANT ARRAY FOR AMPLITUDES AFTER REFLECTIONS	A	47
C	AT ARRAY FOR TRAVEL TIMES	A	48
C	CTI ARRAY FOR VALUES OF ANGLES TO BE RETURNED TO AFTER REFLECT	A	49
C	COMBEG SUBROUTINE TO INCREMENT INITIAL ANGLE OF INCIDENCE	A	50
C	COMHOP SUBROUTINE TO INCREMENT INITIAL HORIZONTAL POSITION	A	51
C	COMVER SUBROUTINE TO INCREMENT INITIAL VERTICAL POSITION	A	52
C	DETA DISTANCE FROM SOURCE TO EMERGENCE OF RAY	A	53
C	DKM DISTANCE FROM EDGE OF FIELD TO EMERGENCE OF RAY	A	54
C	EEF SINE OF EMERGING ANGLE (ABOVE 1.00 IF CRITICAL ANGLE)	A	55
C	GINRAD SUBROUTINE TO BRING RAY END PRECISELY TO INTERFACE	A	56
C	GG VERTICAL INCREMENT FOR PROBING ANGLE	A	57
C	GGG VERTICAL INCREMENT	A	58
C	HH HORIZONTAL INCREMENT FOR EMERGING ANGLE	A	59

C	HHH	HORIZONTAL INCREMENT	A 60
C	ICRIT	SWITCH TO INDICATE CRITICAL REFLECTION	A 61
C	III	INTEGER VALUE OF DIP	A 62
C	INT	SWITCH TO INDICATE RETURN FROM REFLECTED RAY	A 63
C	IM	HORIZONTAL PROBED INDEX POSITION	A 64
C	INAM1	SWITCH TO INDICATE USE OF SECOND NAMELIST	A 65
C	INT	ARRAY FOR VELOCITY VALUES AFTER REFLECTION	A 66
C	INTERAC	SWITCH TO INDICATE INTERFACE	A 67
C	INUM	NUMBER OF TIMES THROUGH INNER LOOP	A 68
C	IS	VERTICAL PROBED INDEX POSITION	A 69
C	ISFC	TRAVEL TIME IN INTEGER NUMBER OF MINUTES	A 70
C	ISURF	SWITCH TO INDICATE EMERGENCE TO SURFACE	A 71
C	IW	SWITCH TO INDICATE REFLECTION	A 72
C	I7	INDEX FOR NUMBER OF RAY REFLECTION	A 73
C	JJJ	INTEGER VALUE OF P.I.	A 74
C	NDIOT	NUMBER OF PLOTTING INCREMENTS	A 75
C	ON	ARRAY FOR DISTANCES RAYS HAVE TRAVELLED	A 76
C	PI	ARRAY FOR VALUES OF HORIZONTAL POSITION	A 77
C	PIP	HORIZONTAL POSITION OF RAY SEGMENT TO DETERMINE VELOCITY	A 78
C	PJPRSH	HORIZONTAL "PROBED" POSITION	A 79
C	PJ	VERTICAL POSITION OF RAY SEGMENT TO DETERMINE VELOCITY	A 80
C	P1	CONSTANT: 3.14159	A 81
C	P1TEST	PROBED HORIZONTAL POSITION FOR COMPUTING VELOCITY	A 82
C	P1T1	CONSTANT: 1.5708	A 83
C	PJ	ARRAY FOR VALUES OF VERTICAL POSITION	A 84
C	PJPRSH	VERTICAL PROBED POSITION	A 85
C	P1TEST	PROBED VERTICAL POSITION FOR COMPUTING VELOCITY	A 86
C	PLANT1	SUBROUTINE FOR INCIDENT TRAVEL TIME FOR PLANE WAVE	A 87
C	PLV	CUBIC FUNCTION TO COMPUTE VELOCITY	A 88
C	PRGH	ORIGINAL ORIGIN	A 89
C	SEC	TRAVEL TIME IN SECONDS ABOVE INTEGER MINUTES	A 90
C	SINDET	SUBROUTINE TO COMPUTE EMERGING ANGLE FOR ANY GIVEN ANGLE	A 91
C	AND SLOPE		A 92
C	SLOP	INTERMEDIATE (SAVED) VALUE OF SLOPE	A 93
C	SPEED	PROBED VALUE OF VELOCITY	A 94
C	TMIN	TRAVEL TIME IN MINUTES	A 95
C	TRENCH	SUBROUTINE TO COMPUTE VELOCITIES FOR UNDERTHRUSTING LITHOSP	A 96
C	TSPEED	TENTATIVE VALUE OF VELOCITY	A 97
C	VEI	VELOCITY	A 98
C		DIMENSION PI(10), PJ(10), CJ(10), ON(10), AT(10), ANT(10), INT(10	A 99
C		1)	A 100
C		DIMENSION A(121,75), R(121,75), SLPRAT(121,75)	A 101
C		***PLOTTING INSTRUCTIONS***	A 102
C		DIMENSION X(1000), Y(1000)	A 103
C		***	A 104
C		DATA P1T,ICRIT,P1T1,INUM,ISURF/3.1415927,0,1.5708,0,0/	A 105
C		NAMELIST /NAM1/ NDIN,DELN,REFIN,NMILT,ORIGV,ORIGH,G,IPORSH,JPORSH,	A 106
C		INTERAC,VELDIE,THWTE,DEC,INAM1,NOR,NOV,NOH,DELV,DELM,TEST,MATH,ICV	A 107
C		2CLE,REFVEL,IMOVIE,TEXACT,PNM,ANTE,X,Y,NILINF,SCA,IPLANE,IPLNT/NAM2	A 108
C		3/A,R,SLPRAT	A 109
C		READ (4,NAM1)	A 110
C		PRGH=ORIGH	A 111
C		IF (IPLNT.EQ.0) GO TO 1	A 112
C		CALL PLOTDS (0.,SCA,0.,SCA,4.,3.)	A 113
1		IF (INAM1.EQ.1) GO TO 2	A 114
C		READ (6,34) ((A(I,1),I=1,IPORSH),J=1,JPORSH)	A 115
C		READ (6,34) ((R(I,1),I=1,IPORSH),J=1,JPORSH)	A 116
2		READ (4,NAM2)	A 117
C		WRITE (7,37)	A 118

	WRITE (7,36)	A 119
C	***PRINTING INSTRUCTION***	A 120
	IF ((PRINT,EO,0) GO TO 3	A 121
	CALL PLTIME (Y(1),Y(1),NDTIME,1,0,0,1)	A 122
3	CONTINUE	A 123
C	***	A 124
	DO 42 I=1,NDIM	A 125
	NPLT=0	A 126
	WRITE (7,35) BEGIN,DRIGH,DR(GV	A 127
	ANGLE2=REF(1)	A 128
	DO 4 I=1,10	A 129
	AT(I)=0.	A 130
4	DN(I)=0.	A 131
	IF ((PLANE,EO,1) CALL PLANTT (BEGIN,DRIGH,AT(1),DN(1),RIGH,DIFRAC,	A 132
	REFVEL)	A 133
	IMV=0	A 134
	I7=1	A 135
	ANT(I7)=1.	A 136
	PI(I7)=DRIGH	A 137
	PJ(I7)=DRIGV	A 138
	I=PI(I7)+.5001	A 139
	J=PJ(I7)+.5001	A 140
	VF(=A(1,1)	A 141
	INTERAC=0	A 142
	INT=0	A 143
5	IF (I7,IF,A) GO TO 31	A 144
	NPLT=NPLT+1	A 145
	INIME=INIM+1	A 146
	IF (INIM,GE,10000) CALL SYSTEM	A 147
	ANGLE1=ANGLE2	A 148
C		A 149
C		A 150
	IF (ANGLE1,GT,7.) GO TO 14	A 151
	IF (IMOVIF,EO,1) G=AT(1,1)/REFVEL	A 152
C	***PRINTING INSTRUCTION***	A 153
	IF ((PRINT,EO,0) GO TO 6	A 154
	IF (NPLT,NF,1) GO TO 7	A 155
	Y(NPLT)=PJ(I7)	A 156
	V(NPLT)=PI(I7)	A 157
	NPLT=NPLT+1	A 158
6	CONTINUE	A 159
C	***	A 160
7	HMH=G*SIN(ANGLE1)/2.	A 161
	GGG=G*COS(ANGLE1)/2.	A 162
	PIP=PI(I7)+HMH	A 163
	PII=PJ(I7)+GGG	A 164
	PI(I7)=PIP+HMH	A 165
	PJ(I7)=PII+GGG	A 166
	AT(I7)=AT(I7)+DIFRAC*G/VF.	A 167
	DN(I7)=DN(I7)+DIFRAC*G	A 168
C	***PRINTING INSTRUCTION***	A 169
	IF ((PRINT,EO,0) GO TO 8	A 170
	IF (IVFL,EO,1,AND,NPLT,GE,4) NPLT=NPLT-1	A 171
	X(NPLT)=PI(I7)	A 172
	Y(NPLT)=PJ(I7)	A 173
8	CONTINUE	A 174
C	***	A 175
	IF (P.I(I7),GE,.5) GO TO 11	A 176
9	ISURE=1	A 177
	IF (IFXACT,EO,1) CALL GINMAD (ANGLE1,SLNP,PI(I7),PJ(I7),IM,IS,AT(1	A 178

	17),ON(17),DIFRAC,VFL,ISURF,ANGLE,SLPRAT(1,J))	A 179
	ISURF=0	A 180
	DISTA=(PI(17)-ORIGH)*DIFRAC	A 181
	DKM=(PI(17)-1)*DIFRAC	A 182
	AMPL=PRIM*ANT(17)/IN(17)*EXP(DEC*ON(17))	A 183
	TMIN=AT(17)/60.	A 184
	ISFC=TMIN	A 185
	SEC=60.*(TMIN-ISFC)	A 186
	WRITE (7,35) DISTA,DKM,TMIN,SEC,AT(17),AMPL	A 187
	IF (IWRITE,FO,1) WRITE (7,35) PJ(17),PI(17),ANGLE1	A 188
C	****PRINTING INSTRUCTION****	A 189
	IF (PRINT,FO,0) GO TO 10	A 190
	X(NPI T)=PJ(17)	A 191
	Y(NPI T)=PI(17)	A 192
	NPI T=NPI T-1	A 193
	CALL PLINE (X(2),Y(2),NPI T,1,0,0,1)	A 194
	NPI T=0	A 195
10	CONTINUE	A 196
C	****	A 197
	GO TO 14	A 198
11	IF (PJ(17).GT..5.AND,PJ(17).GT..5.AND,PJ(17).LT.JPORSH-.5.AND,PJ(17).LT.JPORSH-.5) GO TO 15	A 199
C	****PRINTING INSTRUCTION ****	A 200
	IF (PRINT,FO,0) GO TO 12	A 201
	NPI T=NPI T-1	A 202
	CALL PLINE (X(2),Y(2),NPI T,1,0,0,1)	A 203
	NPI T=0	A 204
12	CONTINUE	A 205
C	****	A 206
13	CONTINUE	A 207
	WRITE (7,38) PI(17),PJ(17),ANGLE1,ON(17),AT(17)	A 208
C	PI(17)=PI(17)+.5-ORIGH	A 209
C	CALL WORD(PI,PJ,ON,ANT,AT,ANGLE2,12,X,Y,L1	A 210
14	IF (17,FO,1) GO TO 31	A 211
	17=0	A 212
	ANT(17-1)=(1-ANT(17))*ANT(17-1)	A 213
	17=17-1	A 214
	1=PTP+.5	A 215
	J=PI,1+.5	A 216
	ANGLE2=C1,1(17)	A 217
	GO TO 5	A 218
15	1=PI(17)+.5	A 219
	J=PJ(17)+.5	A 220
C		A 221
	PJPORR=PJP+HRR	A 222
	PJPORR=PJ,1+GGG	A 223
	1M=PJPORR+.5	A 224
	IS=PJPORR+.5	A 225
	IF (IWRITE,FO,0) GO TO 16	A 226
	WRITE (1,35) PJ(17),PI(17),VFL,SLOP,ANGLE1	A 227
16	IF (INTRAC,FO,1) GO TO 18	A 228
	IF (MATH,FO,1) GO TO 17	A 229
	IF (IS,1,1) GO TO 9	A 230
	IF (1M.GT.JPORSH.OR,IS.GT.JPORSH.OR,1M.LT.1) GO TO 13	A 231
	11=PJP+.5	A 232
	J,J=PJ,1+.5	A 233
	VFL=A(111,J,J)+GG*(PI,J-J,J)*(A(111,J,J)-A(111,J,J))	A 234
	GO TO 18	A 235
17	CALL TRENCH (PIP,PI,J,VFL,SLOP,DIFRAC)	A 236
	IF (11INT,FO,1) VFL=INT(17)	A 237
		A 238

18	IVFI=0	A 239
	IF (INTFAC.EQ.1) SINPF=SINP	A 240
	INTFAC=0	A 241
	INTI=0	A 242
	IF (IVW.NE.1) GO TO 19	A 243
	IVW=0	A 244
	GO TO 5	A 245
19	TSPEED=VEI	A 246
	ICRIT=0	A 247
	DO 24 I,J=1,10	A 248
	HH=G*SIN(ANGLE2)	A 249
	GG=G*COS(ANGLE2)	A 250
	PITEST=PI(I7)+HH/2.	A 251
	PJTEST=P(I7)+GG/2.	A 252
	IF (PITEST.LT.1.) GO TO 9	A 253
	IF (MATH.EQ.1) GO TO 20	A 254
	III=PITEST+.5	A 255
	JJJ=PJTEST+.5	A 256
	SPEED=A(III,JJJ)+GG*(PITEST-JJJ)*(A(III,JJJ-1)-A(III,JJJ))	A 257
	SINP=S(I,J)	A 258
	IF (SPEED.EQ.VFI.AND.I,J.L.EQ.1) GO TO 22	A 259
	IF (ANGLE1.GT.PITT+.5585.AND.ANGLE1.LT.3.*PITT+.5585) SLOP=B(IM,IS	A 260
	1)	A 261
	GO TO 21	A 262
20	CALL TRENCH (PITEST,PJTEST,SPEED,SLP,DIFRAC)	A 263
	IF (SPEED.EQ.VFI.AND.I,J.L.EQ.1) GO TO 22	A 264
21	IVW=0	A 265
	SINP=S(I,J)	A 266
	GO TO 23	A 267
22	IVFI=1	A 268
	GO TO 5	A 269
23	CONTINUE	A 270
	IF (ANGLE1.GT.PITT+.5585.AND.ANGLE1.LT.3.*PITT+.5585.AND.ABS(VEL-S	A 271
	PEED).GT..7) SINP=SINPF	A 272
	IF (ABS(SPEED-TSPEED).LT.TEST) GO TO 25	A 273
	TSPEED=SPEED	A 274
	CALL SINDET (ANGLE1,ANGLE2,VFI,SPEED,SLOP,ICRIT,FFF)	A 275
24	CONTINUE	A 276
25	CONTINUE	A 277
	IF (IWRITE.EQ.1) WRITE (1,33) VEL,SPEED,ANGLE2,ANGLE1,SLOP,PJTEST	A 278
	IF (ABS(SPEED-VFI).GE.VELDIF.AND.IZ.LE.NMULT.AND.IVW.LT.1.OR.ICRIT	A 279
	1.EQ.1) GO TO 26	A 280
	VFI=SPEED	A 281
	INTFAC=1	A 282
	IVW=0	A 283
	GO TO 5	A 284
26	IF (IWRITE.EQ.1) WRITE (1,33) PI(I7),PJ(I7),IM,IS	A 285
	IF (IFXACT.LT.2) GO TO 27	A 286
	CALL GINMAN (ANGLE1,SLOP,PI(I7),PJ(I7),IM,IS,AT(IZ),ON(IZ),DIFRAC,	A 287
	IVFI,ISIRF,ANTF,SLPRAT(I,J))	A 288
27	CONTINUE	A 289
	IF (IWRITE.EQ.1) WRITE (1,33) PI(I7),PJ(I7),IM,IS	A 290
C	***PLOTING INSTRUCTION***	A 291
	IF (IPILOT.EQ.0) GO TO 28	A 292
	X(NPLOT)=P,I(I7)	A 293
	Y(NPLOT)=P,I(I7)	A 294
	NPLOT=NPLOT+1	A 295
	CALL PLINE (X(2),Y(2),NPLOT,1,0,0,1)	A 296
	NPLOT=0	A 297
28	CONTINUE	A 298

C	***	***	A 299
	IF (ICRIT+IVW,GE,2) GO TO 5		A 300
	IF (ICRIT,FO,1) GO TO 30		A 301
	IVW=1		A 302
	I7=I7+1		A 303
	NN(I7)=NN(I7-1)		A 304
	AT(I7)=AT(I7-1)		A 305
	PI(I7)=PI(I7-1)		A 306
	PJ(I7)=PJ(I7-1)		A 307
	ANT(I7)=ANT(I7-1)*(SPEED-VEL)/(SPEED+VEL)		A 308
	VEL=SPEED		A 309
	CL(I7-1)=ANGLE2		A 310
	INT(I7-1)=SPEED		A 311
	IF (I7-NMHT) 30,29,29		A 312
29	I7=I7-1		A 313
	INT=1		A 314
	GO TO 5		A 315
30	ANGLE2=PI-ANGLE1+2.*SLDP		A 316
	IF (ANGLE2,GE,2.*PI) ANGLE2=ANGLE2-2.*PI		A 317
	IF (ANGLE2,LT,0.) ANGLE2=ANGLE2+2.*PI		A 318
	IVW=1		A 319
	GO TO 5		A 320
31	CONTINUE		A 321
	CALL COMBEG (BEGIN,DELN,NMHT,IR)		A 322
	CALL COMVER (ORIGV,DELV,NOV,IV)		A 323
	CALL COMHOR (ORIGH,DEHH,NMHT,IH)		A 324
32	CONTINUE		A 325
C	***PLOTTING INSTRUCTION***		A 326
	CALL PLTEND		A 327
C			A 328
C			A 329
33	FORMAT ('0',2F4,2,2I4)		A 330
34	FORMAT ('0F4,2)		A 331
35	FORMAT ('16F10,2)		A 332
36	FORMAT ('DISTANCE KILOMETERSTT(MIN)TT(SEC)', 'TOTAL(SEC)AMPLITUDE')		A 333
37	FORMAT ('0INITIAL ANGLE,INITIALDISTANCE,INITIALDEPTH')		A 334
38	FORMAT ('0NON-SURFACE',5F7,3)		A 335
	END		A 336
C			
	SUBROUTINE GINMAD (ANGLE1,R,PI,PJ,IM,IS,AT,NN,H,A,ISURF,ADIF,SLPRA	H	1
	IT)	H	2
	DATA PIF2,PIF,PIF32/1.57079,3.1459,4.71239/	H	3
	ANDIF1=ABS(ANGLE1-R-PIF2)	H	4
	ANDIF2=ABS(ANGLE1-R-PIF32)	H	5
	IF (ANDIF1,LT,ADIF,OR,ANDIF2,LT,ADIF) RETURN	H	6
	IF (ISURF,EO,0) GO TO 1	H	7
	DV=1.-PJ	H	8
	ANG=ABS(COS(PIF-ANGLE1))	H	9
	IF (ANG,LT,.02) ANG=.02	H	10
	GIN=DV/ANG	H	11
	GO TO 7	H	12
1	V=SLPRAT/100.	H	13
	IM=SLPRAT	H	14
	H=SLPRAT-IM	H	15
	IF (V,LT,.01) V=.5	H	16
	IF (H,LT,.01) H=.5	H	17
	DV=IS-PJ-1.+V	H	18
	DH=IM-PI-1.+H	H	19
	IF (ANGLE1,GT,PIF2,AND,ANGLE1,LT,PIF32) DV=DV+1.	H	20
	IF (ANGLE1,GT,PIF) DH=DH+1.	H	21



	IF (ARS(DH),LT,.001) DH=.001	A	22
	DVH=DV/DH	A	23
	H=SQRT(DV*DV+DH*DH)	A	24
	GAMMA=ATAN(DVH)	A	25
	IF (DH*DV.GT,0.) GO TO 2	A	26
	DELT=ARS(GAMMA)-R	A	27
	GO TO 3	A	28
2	CONTINUE	A	29
	DELT=ARS(GAMMA)+R	A	30
3	CONTINUE	A	31
	GIN=ARS(H*SIN(DELT)/SIN(ANGLE1))	A	32
	RR=R	A	33
	IF (R.GT,1.5) RR=1.5	A	34
	IF (R.LT,-1.5) RR=-1.5	A	35
	IF (ANGLE1.LT,PI/2) GO TO 4	A	36
	IF (ANGLE1.GE,PI/2.AND,ANGLE1.LT,PI) GO TO 5	A	37
	IF (ANGLE1.GE,PI.AND,ANGLE1.LT,PI/2) GO TO 4	A	38
	IF (DV.LT,-DH*TAN(RR)) GIN=-GIN	A	39
	IF (RR.GT,ANGLE1-PI/2) GIN=-GIN	A	40
	GO TO 7	A	41
4	CONTINUE	A	42
	IF (DV.GT,-DH*TAN(RR)) GIN=-GIN	A	43
	IF (RR.LT,0..AND,ARS(RR).GT,PI/2-ANGLE1) GIN=-GIN	A	44
	GO TO 7	A	45
5	CONTINUE	A	46
	IF (DV.GT,-DH*TAN(RR)) GIN=-GIN	A	47
	IF (RR.GT,ANGLE1-PI/2) GIN=-GIN	A	48
	GO TO 7	A	49
6	CONTINUE	A	50
	IF (DV.LT,-DH*TAN(RR)) GIN=-GIN	A	51
	IF (RR.LT,0..AND,ARS(RR).GT,PI/2-ANGLE1) GIN=-GIN	A	52
7	CONTINUE	A	53
	P1=GIN*SIN(ANGLE1)+P1	A	54
	P1=GIN*CONST(ANGLE1)+P1	A	55
	AT=AT+D*GIN/A	A	56
	DN=DN+D*GIN	A	57
	RETURN	A	58
	END	A	59
C.	SUBROUTINE TRENCH (PI,P1,VFL,SLOPE,DIFRAC)	C	1
1	IF (PI,GE,3.2) GO TO 2	C	2
	VFL=A.	C	3
	SLOPE=0.	C	4
	GO TO 12	C	5
2	IF (PI,LT,40.2) GO TO 4	C	6
	IF (PI,GE,7.2) GO TO 3	C	7
	VFL=A.75	C	8
	SLOPE=0.	C	9
	GO TO 12	C	10
3	DEPTH=40.+(PI-7.2)*DIFRAC	C	11
	VFL=POLY(DEPTH)	C	12
	SLOPE=0.	C	13
	GO TO 12	C	14
4	IF (PI,GE,5.) GO TO 5	C	15
	VFL=A.	C	16
	SLOPE=0.	C	17
	GO TO 6	C	18
5	VFL=A.75	C	19
	SLOPE=0.	C	20
6	GRADE1=.84R*(PI-3.4)+.529*(PI-50.5)	C	21

	IF (GRADE).GT.0.1 GO TO 8	C 22
	IF (PI).GT.4.1 GO TO 7	C 23
	GO TO 12	C 24
7	DEPTH=40.+(PI-4.1)*DIFRAC	C 25
	VFI=DN(V(DEPTH)	C 26
	SLNPF=0.	C 27
	GO TO 12	C 28
8	IF (1.7724*(PIP-45.7).GT.PI-6.81 GO TO 10	C 29
	IF (GRADE).GT.4.1 GO TO 9	C 30
	VFI=6.75	C 31
	SLNPF=.5585	C 32
	GO TO 12	C 33
9	DEPTH=40.+(.468*(PI-8.7)+.529*(PIP-50.5))*DIFRAC	C 34
	VFI=DN(V(DEPTH)	C 35
	SLNPF=.5585	C 36
	GO TO 12	C 37
10	DENUM=40.2-PIP	C 38
	IF (DENUM.LT..001) DENUM=.001	C 39
	SLNPF=1.5708-ATAN((32.5-PI.1)/DENUM)	C 40
	RAN=CORU((32.5-PI.1)**2.+DENUM**2.)	C 41
	IF (RAN.GT.24.3) GO TO 12	C 42
	IF (RAN.GT.25.3) GO TO 11	C 43
	DEPTH=40.+(25.3-RAN)*DIFRAC	C 44
	VFI=DN(V(DEPTH)	C 45
	GO TO 12	C 46
11	VFI=6.75	C 47
	SLNPF=0.	C 48
12	RETURN	C 49
	END	C 50*
C	FUNCTION DN(V(X)	D 1
	DN(V)=7.0434+.2904E-07*X-.25167E-14*X**2+.1057E-06*X**3	D 2
	RETURN	D 3
	END	D 40
C	SUBROUTINE SINDEF (CI1,CI2,CI3,CI4,CI5,CI6,CI7)	E 1
	ICRIT=0	E 2
	DATA PI/3.1415927	E 3
	DATA DPF/1.5757463/	E 4
	AA=AMC/AT1	E 5
	GM=0.	E 6
	MC=1.	E 7
	CC=CI1-M1.1	E 8
	IF (CC.EQ.0..OR.CC.EQ.PI.MC.CC.EQ.2.*PI) GO TO 5	E 9
	IF (CI1.GE.0..AND.CI1.LE.PI) GO TO 1	E 10
	IF (CC.LT.3.*PI) GO TO 3	E 11
	GM=2.*PI	E 12
	GO TO 3	F 13
1	IF (CC.GT.PI) GO TO 2	F 14
	GO TO 3	F 15
2	GM=PI	F 16
	MC=-1.	F 17
3	FFF=AA*SIN(CC)	F 18
	IF (ABS(FFF).GE.1.) GO TO 4	F 19
	ARC=MC*ARC[N(FFF)	F 20
	PI=ARC*MC/1.6GM	F 21
	IF (CI1.GT.2.*PI) CI1=CI1-2.*PI	F 22
	IF (CI1.LT.0.) CI1=CI1+2.*PI	F 23
	GO TO 4	E 24
4	ICRIT=1	F 25

	GO TO A	F	26
5	PT=CTH	F	27
6	RETURN	F	28
	END	F	29
C			
	SUBROUTINE COMPER (R,DR,N,IR)	F	1
	IF (IR,GT,N) RETURN	F	2
	IR=IR+1	F	3
	R=R+DR	F	4
	RETURN	F	5
	END	F	6
C			
	SUBROUTINE COMVER (V,DV,N,IV)	C	1
	IF (IV,GT,N) RETURN	C	2
	IV=IV+1	C	3
	V=V+DV	C	4
	RETURN	C	5
	END	C	6
C			
	SUBROUTINE COMHOR (H,DH,N,TH)	H	1
	IF (TH,GT,N) RETURN	H	2
	TH=TH+1	H	3
	H=H+DH	H	4
	RETURN	H	5
	END	H	6
C			
	SUBROUTINE PLANIT (R,DR,IC,AT,ON,R,DI,OFF)	I	1
	IN=TR-ON/IC/STN/RTN/DT	I	2
	AT=ON/IFF	I	3
	RETURN	I	4
	END	I	5
954 LINES PRINTED			

C	PROGRAM FOR A SPHERICAL EARTH CROSS-SECTION	A	1
C	MODEL OF VELOCITY DISTRIBUTION IS SET UP AND RAYS ARE PROPAGATED	A	2
C	THROUGH THE MODEL	A	3
C	TRAVEL TIMES, DISTANCES IN DELTA DEGREES AND KILOMETERS, AND	A	4
C	APPROXIMATE AMPLITUDES ARE COMPUTED.	A	5
C			
C	NAMELIST PARAMETERS ALPHABETICALLY LISTED	A	6
C	CIRC1 SIZE OF CIRCLE TO BE PLOTTED FOR EARTH'S CIRCUMFERENCE		
C	CIRC2 SIZE OF CIRCLE TO BE PLOTTED FOR CORE-MANTLE BOUNDARY	A	8
C	CIRC3 SIZE OF CIRCLE TO BE PLOTTED FOR INNER CORE	A	9
C	CMAJ MAXIMUM RADIAL ANGLE TO WHICH CIRCLES ARE PLOTTED	A	10
C	CMIN MINIMUM RADIAL ANGLE TO WHICH CIRCLES ARE PLOTTED	A	11
C	DECFAC EXPONENTIAL DECREMENT BY ATTENUATION	A	12
C	DECKM KILOMETERS PER DEGREE OF EARTH'S ARC	A	13
C	EDGE SMALL DISTANCE TO WHICH INTERFACE SHOULD BE APPROACHED	A	14
C	FACDAT FACTOR TO MULTIPLY DATA TO CHANGE VELOCITY INPUT	A	15
C	HORMAX MAXIMUM HORIZONTAL POSITION	A	16
C	HORMIN MINIMUM HORIZONTAL POSITION	A	17
C	IAAP SWITCH TO INCLUDE APPARENT VELOCITY	A	18
C	ICIRC SWITCH TO INDICATE PLOTTING OF CIRCLES	A	19
C	ICVCF MAXIMUM NUMBER OF RAY INCREMENTATIONS	A	20
C	IDAT SWITCH TO CHANGE PORTION OF DATA BY FACTOR FACDAT	A	21
C	IDIFUS 50% REFLECTION OF AMPLITUDE (DIFFUSION COEFFICIENT)	A	22
C	IDINT SWITCH TO INCLUDE CALCOMP PLOTTING	A	23
C	IPP SWITCH TO TRACE MULTIPLE P-RAYS (PP, PPP, ETC.)	A	24
C	ISAMP NUMBER OF SAMPLE POINTS TO CENTER OF EARTH	A	25
C	ISWTF SWITCH TO INCLUDE DIAGNOSTIC WRITEDITS	A	26
C	MAYDAT MAXIMUM NUMBER IN DATA LIST TO BE CHANGED BY FACDAT	A	27
C	MAYDEL MAXIMUM DELTA AT WHICH OUTPUT IS WISHED	A	28
C	MAYDIS MAXIMUM DISTANCE TO WHICH OUTPUT IS WISHED	A	29
C	MINDAT MINIMUM NUMBER IN DATA LIST TO BE CHANGED BY FACDAT	A	30
C	MINDEL MINIMUM DELTA AT WHICH OUTPUT IS WISHED	A	31
C	MINDIS MINIMUM DISTANCE TO WHICH OUTPUT IS WISHED	A	32
C	NUMREF NUMBER OF MULTIPLE REFLECTIONS ALLOWED	A	33
C	PRM INITIAL AMPLITUDE VALUE	A	34
C	REFCT LOCATION OF INTERFACE BETWEEN SAMPLE POINTS	A	35
C	ITMHNH NUMBER OF HORIZONTAL SAMPLE POINTS USED	A	36
C	ITMNEF NUMBER OF TIMES INTERFACE OR SURFACE SHOULD BE APPROACHED	A	37
C	ITMVER NUMBER OF VERTICAL SAMPLE POINTS USED	A	38
C	SAMPEN NUMBER OF KILOMETERS BETWEEN SAMPLE POINTS	A	39
C	SEGLEN RAY SEGMENT LENGTH	A	40
C	SHRE MINIMUM HORIZONTAL POSITION ALLOWED	A	41
C	ISAMP FLATTING POINT REPRESENTED DISTANCE TO CENTER OF EARTH	A	42
C	VEHDE VELOCITY DIFFERENCE NECESSARY TO CAUSE REFLECTION.	A	43
C	VERMAX MAXIMUM VERTICAL POSITION	A	44
C	VERMIN MINIMUM VERTICAL POSITION	A	45
C		A	46
C		A	47
C	SYMBOL TABLE		
C	AMPL AMPLITUDE	A	48
C	ANGLE1 INCIDENT ANGLE OF RAY	A	49
C	ANGLE2 EMERGING ANGLE OF RAY	A	50
C	ANT ARRAY FOR AMPLITUDES AFTER REFLECTIONS	A	51
C	AT ARRAY FOR TRAVEL TIMES	A	52
C	APPVEI APPARENT VELOCITY (DISTANCE IN KM DIVIDED BY TRAVEL TIME)	A	53
C	ARG VERTICAL POSITION DIVIDED BY HORIZONTAL POSITION	A	54
C	ARRN SURFACING TO PRECISELY END RAY AT SURFACE	A	55
C	CTI ARRAY FOR VALUES OF ANGLES TO BE RETURNED TO AFTER REFLECTI	A	56
C	D RADIAL VELOCITY DISTRIBUTION OF A SPHERICAL EARTH	A	57
C	DEPTH MAXIMUM DEPTH REACHED BY RAY (6371 KM-RADIUS)	A	58
C	DWM DISTANCE IN KM	A	59

C	DISTA	DELTA IN DEGREES	A	60
C	ENDEF	SUMMATION OF SMALL INCREMENTS WHEN APPROACHING INTERFACE	A	61
C	EFF	SINE OF EMERGING ANGLE (ABOVE 1.00 IF CRITICAL ANGLE)	A	62
C	HORINC	HORIZONTAL INCREMENTATION OF RAY SEGMENT	A	63
C	HOR7KM	HORIZONTAL POSITION IN KILOMETERS	A	64
C	ICRIT	SWITCH TO INDICATE CRITICAL REFLECTION	A	65
C	IINTER	SWITCH FOR HAVING REACHED INTERFACE	A	66
C	IMERGE	SWITCH FOR HAVING EMERGED AT SURFACE WITH RAY	A	67
C	INIM	NUMBER OF TIMES THROUGH INNER LOOP	A	68
C	ISFC	TRAVEL TIME IN INTEGER NUMBER OF MINUTES	A	69
C	IREF	SWITCH TO INDICATE REFLECTION AT INTERFACE	A	70
C	IUV	SWITCH FOR REACHING REFLECTION (CRITICAL OR NON-CRITICAL)	A	71
C	IUMR	COUNT FOR NUMBER OF SEQUENTIAL CRITICAL REFLECTIONS	A	72
C	I7	INDEX FOR NUMBER OF RAY REFLECTION	A	73
C	ICRIT	SWITCH FOR HAVING REACHED CRITICAL ANGLE	A	74
C	KDEPR	INTEGER VALUE OF DEPTH OF DEPRN VALUE	A	75
C	KVFI	VERTICAL POSITION IN INTEGER NUMBER OF SAMPLE POINTS	A	76
C	KVFI1	VERTICAL POSITION IN NEAREST INTEGER NUMBER OF SAMPLES	A	77
C	I	SWITCH TO READ DATA ON FIRST CALL WHEN USED AS SUBROUTINE	A	78
C	MIN7D	TOTAL NUMBER OF REFLECTIONS	A	79
C	NPINT	NUMBER OF PLOTTING INCREMENTS	A	80
C	ON	ARRAY FOR DISTANCES RAYS HAVE TRAVELLED	A	81
C	PI	ARRAY FOR VALUES OF HORIZONTAL POSITION	A	82
C	PI1	HORIZONTAL POSITION IN SAMPLE POINTS FROM REFERENCE	A	83
C	PI7	CONSTANT: 3.14159	A	84
C	PI11	DEPRN VALUE OF HORIZONTAL POSITION FROM REFERENCE	A	85
C	PI12	HORIZONTAL POSITION IN SAMPLE POINTS FROM REFERENCE	A	86
C	PIPRN	DEPRN VALUE OF HORIZONTAL POSITION	A	87
C	PIREF	HORIZONTAL POSITION FOR DETERMINATION OF VELOCITY	A	88
C	P1	ARRAY FOR VALUES OF VERTICAL POSITION	A	89
C	P1.1	VERTICAL POSITION IN SAMPLE POINTS FROM CENTER OF EARTH	A	90
C	P1.11	DEPRN VALUE OF VERTICAL POSITION FROM CENTER OF EARTH	A	91
C	P1.12	VERTICAL POSITION IN SAMPLE POINTS FROM CENTER OF EARTH	A	92
C	P1PRN	DEPRN VALUE OF VERTICAL POSITION	A	93
C	P1REF	VERTICAL POSITION FOR DETERMINATION OF VELOCITY	A	94
C	RAN1	DISTANCE FROM CENTER OF EARTH IN SAMPLE POINTS	A	95
C	RAN2	DISTANCE FROM CENTER OF EARTH	A	96
C	RAN11	DISTANCE FROM CENTER OF EARTH IN SAMPLE POINTS	A	97
C	RAN15	MINIMUM RADIUS REACHED BY RAY IN KILOMETERS	A	98
C	RPOINT	SUBROUTINE TO PRECISELY REFLECT RAY FROM INTERFACE	A	99
C	SFC	TRAVEL TIME IN SECONDS ABOVE INTEGER MINUTES	A	100
C	SINDET	SUBROUTINE TO COMPUTE EMERGING ANGLE FOR ANY GIVEN ANGLE AND SLOPE	A	101
C	SINDE	SLOPE	A	102
C	SLOPER	SAVED VALUE OF SLOPE	A	103
C	DEPRN	DEPTH OF DEPRN LOCATION	A	104
C	TMIN	TRAVEL TIME IN MINUTES	A	105
C	VFI	VERTICAL DISTANCE FROM CENTER OF EARTH IN SAMPLE POINTS	A	106
C	VEL01	VELOCITY	A	107
C	VEL01R	VELOCITY SAVED PRIOR REFLECTION	A	108
C	VEL02	VELOCITY	A	109
C	VEL03	INTERMEDIATE DEPTH IN SAMPLE POINTS	A	110
C	VEL04	VELOCITY	A	111
C	VEL05	ARRAY TO HOLD PREVIOUS VELOCITY VALUES AFTER REFLECTIONS	A	112
C	VERINC	VERTICAL INCREMENTATION OF RAY SEGMENT	A	113
C	VERTKM	DEPTH IN KILOMETERS	A	114
C			A	115
	SUBROUTINE MORID (PI,PJ,ON,ANT,AT,ANGLE2,IZ,X,Y,L)		A	117
	DIMENSION PI(10), PJ(10), CJ(10), ON(10), ANT(10), AT(10), D(1000)		A	118
	II, VEL0V(10)		A	119

	DIMENSION X(1000), Y(1000)	A 120
	DATA PIT,PIT2,ICRT,INIM,IV,IV,IM/3,14159,1.5708,0,0,0,0,0/	A 121
	IF (1,RT,1) GO TO 4	A 122
	NAMPTST /DATAIN/ SEGMEN,TSAMP,LIMVER,LIMHOR,SAMPKM,VFLDIF,DFCLIG,	A 123
	INIMH,ICVCLF,EDGE,SURE,TSAMP,DNM,IMINC,IMRTE,PHEC,SCA,CIRC,C	A 124
	2RC2,CIRC3,HORMIN,HORMAX,VERMIN,VERMAX,HEGKM,INAT,IPLOT,IPP,MINDAT,	A 125
	3MAXDAT,FACDAT,TOFUS,LAAP,ICIRC,MINDEF,MAXDEF,CMIN,CMAX,MINDKM,MAX	A 126
	4HVM	A 127
	READ (A,DATAIN)	A 128
	READ (A,27) (D11,1=1,LIMVER)	A 129
	IF (INAT,0,0) GO TO 2	A 130
	DO 1 J=MINDAT,MAXDAT	A 131
	D11=D11+FACDAT	A 132
1	CONTINUE	A 133
2	CONTINUE	A 134
	WRITE (7,24)	A 135
C	*****PRINTING INSTRUCTION*****	A 136
	IF (IPLOT,0,0) GO TO 4	A 137
	CALL PITRES TO,SCA,0,SCA,4,4,1	A 138
	IF (ICIRC,0,0) GO TO 3	A 139
	CALL PCIRC1 (TSAMP,1,CMIN,CMAX,CIRC1,CIRC1,0,1)	A 140
	CALL PCIRC1 (TSAMP,1,CMIN,CMAX,CIRC3,CIRC3,0,1)	A 141
	CALL PCIRC1 (TSAMP,1,CMIN,CMAX,CIRC2,CIRC2,0,1)	A 142
3	CONTINUE	A 143
4	CONTINUE	A 144
	VERTRM=(D11/71-1,1=SAMPKM	A 145
	HORTRM=(D11/71-1,1=SAMPKM	A 146
	NDIT=0	A 147
	MINTID=0	A 148
	KVFL=D11/71	A 149
	IF (KVFL,GT,LIMVER-1) KVFL=2,0=SAMPKM-1-KVFL	A 150
	KVFL=D11/71+.5	A 151
	VFL=TSAMP-D11/71	A 152
	VFL=D11-KVFL+.5*SEGMEN*(D(KVFL+1)-D(KVFL))*ANS(SIN(ANGLE2))	A 153
	VFL=D11-KVFL	A 154
	DANDIC=TSAMP-D11/71	A 155
	HORINC=SEGMEN*(N(ANGLE2)	A 156
	VERINC=SEGMEN*(N(ANGLE2)	A 157
	ICRT=0	A 158
	INTHOR=0	A 159
	IMERCK=0	A 160
	IVM=0	A 161
	IVM=0	A 162
	EDGE=0,	A 163
5	CONTINUE	A 164
C	*****PRINTING INSTRUCTION*****	A 165
	IF (IPLOT,0,0) GO TO 7	A 166
	NDIT=NDIT+1	A 167
	IF (NDIT,NE,1) GO TO 6	A 168
	VINDIT=D11/71	A 169
	VINDIT=D11/71	A 170
	NDIT=NDIT+1	A 171
A	CONTINUE	A 172
7	CONTINUE	A 173
C	*****	A 174
	INIM=INIM+1	A 175
	IF (INIM,GE,ICVCLF) RETURN	A 176
	ANGLE=ANGLE2	A 177
	DIFF=D11/71+.5*HORINC	A 178
	D,DIFF=D11/71+.5*VERINC	A 179

	P1(17)=P1(17)+HNRINC	A 180
	PJ(17)=P1(17)+VERINC	A 181
	IF (P1(17).LT.HNRMIN.OR.P1(17).GT.HNRMAX.OR.PJ(17).LT.VERMIN.OR.PJ(17).GT.VERMAX) GO TO 25	A 182
C	*****PLOTTING INSTRUCTIONS*****	A 183
	IF (IPLOT.EQ.0) GO TO 8	A 184
	X(NPLOT)=P1(17)	A 185
	Y(NPLOT)=PJ(17)	A 186
A	CONTINUE	A 187
C	*****	A 188
	IF (IWRITE.GE.1) WRITE (7,28) P1(17),PJ(17),VELN1,ANGLE1	A 189
	IF (P1(17).LT.SURE) RETURN	A 190
	P11=P1REF-1.	A 191
	PJ1=TSAMP-PJREF	A 192
	RAN1=SQRT(P11*P11+PJ1*PJ1)	A 193
	IF (RAN1.GT.RAN1) RAN1=RAN1	A 194
	VEL=TSAMP-RAN1	A 195
	KVEL=VEL	A 196
	KVEL1=VEL+.5	A 197
	P112=ARCS(P1(17)-1.)	A 198
	PJ12=TSAMP-PJ(17)	A 199
	IF (P112.LT..0001) P112=.0001	A 200
	IF (P11.LT.0.) P112=-P112	A 201
	ARG=PJ12/P112	A 202
	IF (ARG.GE.0.) GO TO 9	A 203
	SLOPE=ATAN(ARG)+P112	A 204
	GO TO 10	A 205
9	CONTINUE	A 206
	SLOPE=ATAN(ARG)-P112	A 207
10	CONTINUE	A 208
	IF (IVFLN.EQ.0) GO TO 11	A 209
	VELN1=VELN2	A 210
	IF (IVW.EQ.1) VELN1=VELN1R	A 211
	IVW=0	A 212
11	IF (VELN3.LT..05) GO TO 12	A 213
	VELN4=VELN3	A 214
	AT(12)=AT(12)+SEGMENT*SAMPKM/VELN4	A 215
12	HW(12)=HW(12)+SEGMENT*SAMPKM	A 216
	IF (RAN1.GT.TSAMP-1.) GO TO 23	A 217
13	RAN3=RAN1	A 218
	ICRIT=0	A 219
	IF (IVFLN.EQ.0) VELN1=VELN2	A 220
	IVFLN=0	A 221
	NN 14 11=1,4	A 222
	PIPRN=P1(12)+HNRINC/2.	A 223
	PJPRN=PJ(12)+VERINC/2.	A 224
	P11=P1PRN-1.	A 225
	PJ1=TSAMP-PJPRN	A 226
	RAN2=SQRT(P11*P11+PJ1*PJ1)	A 227
	IF (RAN2.GT.TSAMP-1.) GO TO 23	A 228
	IF (ABS(RAN3-RAN2).LT..003) GO TO 15	A 229
	RAN3=RAN2	A 230
	SPEED=TSAMP-RAN2	A 231
	KSPEED=SPEED	A 232
	VELN2=0(KSPEED)+(SPEED-KSPEED)*(0(KSPEED+1)-0(KSPEED))	A 233
	IF (ABS(VELN1-VELN2).LT..005) GO TO 5	A 234
	CALL SINDET (ANGLE1,ANGLE2,VELN1,VELN2,SLOPE,ICRIT,FFF)	A 235
	ICRIT=ICRIT+ICRIT	A 236
	IF (ICRIT.GE.3) GO TO 25	A 237
	IF (ICRIT.EQ.1) GO TO 14	A 238

	HDR INC=SEGMEN* $\sin(\text{ANGLE2})$	A 240
	VDR INC=SEGMEN* $\cos(\text{ANGLE2})$	A 241
14	CONTINUE	A 242
15	CONTINUE	A 243
	IF (IVWR.GT.0) IVWR=IVWR-1	A 244
	KVEL2=SPEED+.5	A 245
	VELD2=VELD1	A 246
	IF (INTER.EQ.1) GO TO 21	A 247
	IF (IWRITE.GE.6) WRITE (7,30) VELD1,VELD2,SLOPE,IZ	A 248
	IF (IVWR.NE.0) GO TO 17	A 249
16	IF (SPEED.GT.VEL.AND.ABS(D(KVEL1)-D(KVEL1+1)).GT.VELDIF) GO TO 19	A 250
	IF (VEL.GT.SPEED.AND.ABS(D(KVEL1)-D(KVEL1-1)).GT.VELDIF) GO TO 19	A 251
17	CONTINUE	A 252
	IF (ICRIT.EQ.0) GO TO 18	A 253
	SLOPER=SLOPE	A 254
	GO TO 22	A 255
18	CONTINUE	A 256
	GO TO 5	A 257
19	CONTINUE	A 258
	VELD3=VELD1	A 259
	CALL RPOINT (ANGLE1,SLOPE,PI(IZ),PJ(IZ),TSAMP,EDGE,VEL,ON(IZ),AT(IZ),SAMPKM,VELD3,PIT,PIT2,ARG,SPEED,LIMINC,RADAR,PREC1,EDGES,KVEL1)	A 260
C	*****PLOTTING INSTRUCTION*****	A 261
	IF (IPLOT.EQ.0) GO TO 20	A 262
	X(MPT)=PJ(IZ)	A 263
	Y(MPT)=PI(IZ)	A 264
	CALL PLINE (X(1),Y(1),NPLT,1,0,0,1)	A 265
	NPLT=0	A 266
20	CONTINUE	A 267
C	*****	A 268
	IF (IWRITE.GE.5) WRITE (7,30) PI(IZ),ANGLE1,SLOPE	A 269
	SLOPER=SLOPE	A 270
	IF (ICRIT.EQ.1) GO TO 22	A 271
	INTER=1	A 272
	VELD2=VELD1	A 273
	VELD3=VELD1	A 274
	GO TO 13	A 275
21	INTER=0	A 276
	IVFIDC=1	A 277
	IF (IZ.EQ.NUMHIT) GO TO 5	A 278
	IZ=IZ+1	A 279
	IF (IZ.GT.NUMHIT) RETURN	A 280
	ON(IZ)=(ON(IZ-1))	A 281
	AT(IZ)=AT(IZ-1)	A 282
	PJ(IZ)=PJ(IZ-1)	A 283
	PJ(IZ)=PJ(IZ-1)	A 284
	ICRIT=0	A 285
	ANT(IZ)=ANT(IZ-1)*((D(KVEL1)-D(KVEL2))/(D(KVEL1)+D(KVEL2)))	A 286
	IF (IDIFUS.EQ.1) ANT(IZ)=.5*ANT(IZ-1)	A 287
	VELDVC(IZ-1)=VELD2	A 288
	CIJ(IZ-1)=ANGLE2	A 289
	IF (RADIUS.GT.RADAR) RADIUS=RADAR	A 290
	IVWR=3	A 291
22	CONTINUE	A 292
	IMERGE=0	A 293
	MULTIP=MULTIP+1	A 294
	VELD3R=VELD1	A 295
	ANGLE2=PIT-ANGLE1+2.*SLOPER	A 296
	IF (IWRITE.GE.4) WRITE (7,30) ANGLE1,SLOPER,ANGLE2	A 297
	IVFIDC=1	A 298
		A 299



	IF (ANGLE2.GT.2.*PI) ANGLE2=ANGLE2-2.*PI	A 300
	IF (ANGLE2.LT.0.) ANGLE2=ANGLE2+2.*PI	A 301
	HORINC=(SEGMEN+EDGES)*SIN(ANGLE2)	A 302
	VERINC=(SEGMEN+EDGES)*COS(ANGLE2)	A 303
	AT(I2)=AT(I2)+SAMPKM*EDGES/VEL04	A 304
	ON(I2)=ON(I2)+EDGES*SAMPKM	A 305
	VEL03=VEL04	A 306
	EDGES=0.	A 307
	IVW=1	A 308
	IVWR=3	A 309
	GO TO 5	A 310
23	CONTINUE	A 311
	IF (IWRITE.GE.3) WRITE (7,28) AT(I2),ON(I2),VEL01,SAMPM,ANGLE1,PI(I	A 312
	I2),P,I(I2)	A 313
	CALL ADDR (PI(I2),P,I(I2),ANGLE1,ISAMP,EDGE,ON(I2),AT(I2),SAMPKM,D(	A 314
	IKVEL),DISTA)	A 315
	IF (PI(I2).LT.1.) DISTA=DISTA+180.	A 316
	DKM=DEGKM*DISTA	A 317
	APPVEL=DKM/AT(I2)	A 318
	AMPL=(PNM*ANT(I2)/ON(I2))*EXP(DECLOG*ON(I2))	A 319
	TMIN=AT(I2)/60.	A 320
	ISFC=TMIN	A 321
	SEC=60.*(TMIN-ISFC)	A 322
	IF (IWRITE.GE.2) WRITE (7,28) AT(I2),ON(I2)	A 323
	RADIUS=SAMPKM*RADIUS	A 324
	DEPTH=SAMPKM*(ISAMP-1)-RADIUS	A 325
	IF (DKM.LE.MINDKM.OR.DKM.GE.MAXDKM) GO TO 24	A 326
	WRITE (7,28) DISTA,DKM,TMIN,SEC,AT(I2),RADIUS,DEPTH,AMPL,MULTIP	A 327
	IF (IAAP.EQ.1) WRITE (7,31) APPVEL	A 328
24	CONTINUE	A 329
	IVLOC=1	A 330
	IMERGE=1	A 331
	SLDPER=SLDPE	A 332
C	*****PLOTTING INSTRUCTION*****	A 333
25	IF (IPLNT.EQ.0) GO TO 26	A 334
	X(NPLT)=P,I(I2)	A 335
	Y(NPLT)=PI(I2)	A 336
	CALL PLINE (X(1),Y(1),NPLY,1,0,0,1)	A 337
	NPLT=0	A 338
26	CONTINUE	A 339
C	*****	A 340
	IF (IMERGE.EQ.1) GO TO 22	A 341
	IF (IPP.EQ.1.AND.IMERGE.EQ.1) GO TO 22	A 342
	MULTIP=MULTIP-1	A 343
	IF (I2.EQ.1) RETURN	A 344
	I7=I2-1	A 345
	JCRIT=0	A 346
	ANGLE2=CIJ(I2)	A 347
	VEL03=VELOCITY(I2)	A 348
	VEL02=VEL03	A 349
	HORINC=SEGMEN*SIN(ANGLE2)	A 350
	VERINC=SEGMEN*COS(ANGLE2)	A 351
	IVLOC=1	A 352
	GO TO 5	A 353
C		A 354
27	FORMAT (10F4.2)	A 355
28	FORMAT ('',F6.2,F10.2,F7.2,F6.2,FA.2,2F9.2,FA.2,I6)	A 356
29	FORMAT ('INITIAL ANGLE,DEPTH, & DISTANCE'/'DELTA', 'KMMINSECTOTSECRAD	A 357
	IIISDEPTHAMPL', 'MULTIPLES')	A 358
30	FORMAT ('',3F6.2,3I3)	A 359

31	FORMAT ('APPARENTVELOCITY=',F5.2)	A	360
	END	A	361*
C			
	SIARRDITINE RORD (PIR,PJR,ANGLE1,TSAMP,EDGE,ON,AT,DIFRAC,A,DISTA)	R	1
	RAMP=(SAMP-1.)	R	2
	SAMP=TSAMP	R	3
	DO 1=1,30	R	4
	H=1.	R	5
	PINC.I=EDGE*SIN(ANGLE1)	R	6
	PINC.J=EDGE*COS(ANGLE1)	R	7
	PRR=SAMP-PJR	R	8
	PIT=PIR-1.	R	9
	RADI=SQRT(PRR*PRR+PIT*PIT)	R	10
	IF (RADI.LT.RAMP) GO TO 1	R	11
	PINC.I=-PINC.I	R	12
	PINC.J=-PINC.J	R	13
	H=-1.	R	14
1	PIR=PIR+PINC.I	R	15
	PJR=PJR+PINC.J	R	16
	AT=AT+DIFRAC*H*EDGE/A	R	17
	ON=ON+DIFRAC*EDGE*H	R	18
	IF (RADI.GT.RAMP-EDGE.AND.RADI.LT.RAMP+EDGE) GO TO 3	R	19
2	CONTINUE	R	20
3	IF (ABS(PIR-1.).LT..0001) PIR=1.01	R	21
	ARG=(SAMP-PJR)/(PIR-1.)	R	22
	THETA=ATAN(ARG)	R	23
	DISTA=(1.5708-ARS(THETA))*57.2958	R	24
	IF (THETA.LT.0.) DISTA=(1.5708+ARS(THETA))*57.2958	R	25
	RETURN	R	26
	END	R	27*
C			
	SIARRDITINE RPOINT (ANGLE1,SLP,PIR,PJR,TSAMP,EDGE,VEL,ON,AT,SAMPKM,	C	1
	1VFL01,PIT,PIT2,ARG,SPEED,LIMINC,RADI,PREC1,EDGES,K1)	C	2
	NF=0.	C	3
	PIT=PIR-1.	C	4
	PRR=TSAMP-PJR	C	5
	RADI=SQRT(PRR*PRR+PIT*PIT)	C	6
C	*****CHECK TO SEE IF RAY IS INWARD OR OUTWARD*****	C	7
	KVFL=K1	C	8
	IF (SPEED.LT.VFL) KVFL=K1-1	C	9
	RADTES=TSAMP-KVFL-PREC1	C	10
	IF (SPEED.LE.VFL) GO TO 1	C	11
	IF (RADTES.LT.RADI) GO TO 2	C	12
	GO TO 3	C	13
1	CONTINUE	C	14
	IF (RADI.LT.RADTES) GO TO 2	C	15
	GO TO 3	C	16
2	CONTINUE	C	17
	H=1.	C	18
	GO TO 4	C	19
3	H=-1.	C	20
4	CONTINUE	C	21
C	*****SET HORIZONTAL & VERTICAL INCREMENTS OF RAY*****	C	22
	PINC.I=EDGE*SIN(ANGLE1)	C	23
	PINC.J=EDGE*COS(ANGLE1)	C	24
	DO 5 I=1,LIMINC	C	25
	PRR=TSAMP-PJR	C	26
	PIT=PIR-1.	C	27
	RADI=SQRT(PRR*PRR+PIT*PIT)	C	28
C	*****TEST FOR CLOSENESS TO RADIUS OF REFLECTION	C	29

	IF (ABS(RADTES-RADI).LT..6*EDGE) GO TO 6	C	30
	NE=NE+1.	C	31
C	*****INCREMENT & FIND TRAVELTIME & DISTANCE*****	C	32
	PTR=PTR+H*PINC.I	C	33
	PJR=PJR+H*PINC.I	C	34
	AT=AT+H*SAMPKM*EDGE/VFLO1	C	35
	DN=DN+H*SAMPKM*EDGE	C	36
5	CONTINUE	C	37
6	CONTINUE	C	38
	PIII=ABS(PII)	C	39
	IF (PIII.LT..0001) PIII=.0001	C	40
	IF (PII.LT.0.) PIII=-PIII	C	41
	ARG=PII/PIII	C	42
	IF (ARG.GE.0.) GO TO 7	C	43
	SLP=ATAN(ARG)+PI/2	C	44
	GO TO 8	C	45
7	CONTINUE	C	46
	SLP=ATAN(ARG)-PI/2	C	47
8	CONTINUE	C	48
	EDGES=NE*EDGE*H	C	49
	RETURN	C	50
	END	C	51*

C	PROGRAM FOR THREE-DIMENSIONAL MODEL OF EARTH SECTION	A	1
C	MODEL OF VELOCITY DISTRIBUTION IS SET UP AND RAYS ARE PROPAGATED	A	2
C	THROUGH THE MODEL	A	3
C	TRAVEL TIMES, DISTANCE IN KILOMETERS, AND	A	4
C	APPROXIMATE AMPLITUDES ARE COMPUTED	A	5
C	SYMBOL TABLE	A	6
C	A ARRAY OF SAMPLED VELOCITY VALUES	A	7
C	ARREF PROREF VELOCITY VALUE	A	8
C	ANIF MINIMUM ANGLE AT WHICH PRECISE INTERFACE LOCATION IS USED	A	9
C	AEFI INCIDENT VELOCITY	A	10
C	ALPHA ANGLE FROM ROTATED Z-AXIS	A	11
C	AMPL AMPLITUDE	A	12
C	ANGLE2 EMERGING ANGLE IN X-Y PLANE	A	13
C	AMT ARRAY FOR AMPLITUDES AFTER REFLECTIONS	A	14
C	AT ARRAY FOR TRAVEL TIMES	A	15
C	R ARRAY CONTAINING SAMPLED SLOPE VALUES	A	16
C	RASF DISTANCE ALONG SURFACE IN KM	A	17
C	RD ARRAY FOR DIPS	A	18
C	RDARG COSINE OF MATHEMATICALLY DETERMINED INCLINATION	A	19
C	RDREF SLOPE	A	20
C	REGIN INITIAL ANGLE OF RAY	A	21
C	REGIND INITIALIZATION FOR INCLINATION	A	22
C	RMA DIP	A	23
C	RMV INTERMEDIATE VALUE FOR ROTATION	A	24
C	CLJ ARRAY FOR VALUES OF ANGLES TO BE RETURNED TO AFTER REFLECT	A	25
C	CLJ ARRAY FOR SAVING REFRACTED INCLINATION AFTER REFLECTION	A	26
C	CLINE1 INCLINATION	A	27
C	CLINE2 EMERGING ANGLE FROM Z-AXIS	A	28
C	CLINE3 INCLINATION IN DEGREES	A	29
C	COMBEG SUBROUTINE TO INCREMENT INITIAL ANGLE OF INCIDENCE	A	30
C	COMDEP SUBROUTINE FOR INITIALIZING Z-VALUES	A	31
C	COMMON SUBROUTINE TO INCREMENT INITIAL HORIZONTAL POSITION	A	32
C	COMVER SUBROUTINE TO INCREMENT INITIAL VERTICAL POSITION	A	33
C	CONST CONSTANT FOR MATH FUNCTION	A	34
C	CPI RE-ROTATED X-POSITION	A	35
C	CREF COSINE OF INCLINATION	A	36
C	CX PROJECTION ON ROTATED X AXIS	A	37
C	CY PROJECTION ON Y-AXIS IN ROTATED COORDINATES	A	38
C	CZ PROJECTION ON Z-AXIS IN ROTATED COORDINATES	A	39
C	DDO INCREMENTATION IN Z-DIRECTION	A	40
C	DEID INITIALIZATION INCREMENT FOR Z VALUE	A	41
C	DEIN INCREMENTATION ANGLE OF INCIDENT RAYS	A	42
C	DEIV INITIALIZATION INCREMENT IN Y	A	43
C	DIFRAC DISTANCE IN KM BETWEEN SAMPLE POINTS	A	44
C	DISTA DISTANCE IN KM FROM ORIGIN	A	45
C	DKM DISTANCE IN KILOMETERS	A	46
C	DV DISTANCE TO INTERFACE OR SURFACE	A	47
C	EACD FACTOR WITH Z IN MATH FUNCTION	A	48
C	EACH X FACTOR FOR MATH FUNCTION	A	49
C	EACV FACTOR FOR Y-VALUE IN MATH FUNCTION	A	50
C	EEF SINE OF EMERGING ANGLE(AROUND 1.00 IF CRITICAL ANGLE)	A	51
C	G RAY SEGMENT LENGTH	A	52
C	GGG INCREMENTATION IN ROTATED Y-DIRECTION	A	53
C	GIM INCREMENT TO INTERFACE OR SURFACE	A	54
C	GRAD GRADIENT	A	55
C	HHH Y INCREMENT	A	56
C	WDERS PLOTTING VARIABLE FOR PERSPECTIVE	A	57
C	IR COUNTER FOR SUBROUTINE CALLS	A	58
C	IRD COUNT FOR INITIALIZATION INCREMENTS IN Z	A	59
C	ICRIT SWITCH TO INDICATE CRITICAL REFLECTION	A	60

C	ICRYT	SWITCH FOR CRITICAL REFLECTIONS	A	61
C	ICVIF	MAXIMUM NUMBER OF RAY INCREMENTATIONS	A	62
C	ID	INTEGER VALUE OF TID	A	63
C	IDK	SWITCH USED IN PLOTTING	A	64
C	IFEXCT	SWITCH TO INCLUDE PRECISE INTERFACE LOCATIONS	A	65
C	IGIN	SWITCH FOR ROTATION LOOP	A	66
C	IH	COUNTER FOR HORIZONTAL INITIALIZATION INCREMENTS	A	67
C	IM	INTEGER VALUE OF DRIVEN P1 VALUE	A	68
C	IMATH	ARRAY FOR INDICATING MATH FUNCTION AFTER REFLECTION	A	69
C	IMI	SWITCH FOR RE-ROTATION LOOP	A	70
C	IPLANE	SWITCH FOR PLANE WAVE INITIALIZATIONS	A	71
C	IPLOT	SWITCH TO INCLUDE CALCOMP PLOTTING	A	72
C	IRREF	SWITCH FOR REFLECTIONS	A	73
C	IS	DRIVEN V VALUE	A	74
C	ISFC	TRAVEL TIME IN INTEGER NUMBER OF MINUTES	A	75
C	ITIME	SWITCH TO INDICATE EMERGENCE TO SURFACE	A	76
C	IMATH	ARRAY FOR RETAINING MATH FUNCTION AFTER REFLECTION	A	77
C	INIM	NUMBER OF TIMES THROUGH INNER LOOP	A	78
C	IV	COUNTER FOR INITIALIZATIONS OF Z	A	79
C	IUP1	SWITCH FOR PLOTTING INSTRUCTION	A	80
C	IUI	SWITCH FOR REFLECTION	A	81
C	IUI1	SWITCH FOR ENTERING LOOP	A	82
C	IUIX	SWITCH FOR REFLECTION	A	83
C	IUIY	SWITCH FOR REFLECTION	A	84
C	IUIZ	SWITCH FOR REACHING REFLECTION (CRITICAL OR NON-CRITICAL)	A	85
C	IWRITE	SWITCH TO INCLUDE DIAGNOSTIC WRITINGS	A	86
C	I2	INDEX FOR NUMBER OF RAY REFLECTION	A	87
C	JMATH	SWITCH FOR MATH FUNCTION	A	88
C	JDPKSH	LIMIT OF VERTICAL NUMBER OF VERTICAL SAMPLE POINTS	A	89
C	KMATH	SWITCH FOR USING MATH FUNCTION	A	90
C	KDPRSH	LIMIT OF V-VALUES	A	91
C	LMATH	SWITCH FOR MATHEMATICAL FUNCTION	A	92
C	MATH	SWITCH FOR MATH FUNCTION	A	93
C	M17	MAXIMUM LIMIT FOR MATH FUNCTION IN Z	A	94
C	M1X	MAXIMUM X-VALUE FOR MATH FUNCTION	A	95
C	M1V	MAXIMUM V-VALUE FOR MATH FUNCTION	A	96
C	M1X	MINIMUM LIMIT FOR MATH FUNCTION IN X	A	97
C	M1V	MINIMUM V-VALUE FOR MATH FUNCTION	A	98
C	M1Z	MINIMUM Z VALUE FOR MATH FUNCTION	A	99
C	NMATH	SWITCH FOR MATH FUNCTION	A	100
C	NNULT	NUMBER OF MULTIPLE REFLECTIONS ALLOWED	A	101
C	NNR	NUMBER OF INITIALIZED ANGLES	A	102
C	NNI	NUMBER OF Z INITIALIZATION INCREMENTS	A	103
C	NNH	INITIALIZATION INCREMENT FOR X VALUE	A	104
C	NNIM	TOTAL NUMBER OF INITIAL RAYS	A	105
C	NNV	NUMBER OF V-VALUE INITIALIZATION INCREMENTS	A	106
C	NNPT	COUNTER FOR PLOTTING	A	107
C	NNLINF	NUMBER OF CALCOMP LINES NECESSARY TO OUTLINE STRUCTURE	A	108
C	NNSYM1	SYMMETRY FOR PLOTTING	A	109
C	NNSYM2	SYMMETRY FOR PLOTTING	A	110
C	ORZ	PROJECTION ON Z AXIS	A	111
C	OR	ARRAY FOR DISTANCES RAYS HAVE TRAVELLED	A	112
C	ORIGD	INITIAL DEPTH OF RAY SOURCE	A	113
C	ORIGH	INITIAL HORIZONTAL POSITION OF RAY	A	114
C	ORIGV	INITIAL V-VALUE	A	115
C	ORIGD	SIN ALGORITHM DETERMINING POSITION IN SPHERICAL COORDINATES	A	116
C	ORIGK	OID IN ANGLE FROM Z-AXIS	A	117
C	ORIGLE	PLOTTING VARIABLE FOR PERSPECTIVE	A	118
C	OR	ARRAY FOR X-VALUES	A	119
C	OR	CONSTANT: 3.14159	A	120

C	P1T	CONSTANT: 1.5708	A 121
C	P1	ARRAY FOR V-VALUES	A 122
C	P2	ARRAY FOR Z-VALUES	A 123
C	P3	INITIAL AMPLITUDE VALUE	A 124
C	P4	DEFAULT INMMV VARIABLE OF ZERO FOR SLOPE IN SINDET	A 125
C	P5	REFERENCE VELOCITY	A 126
C	P6	DIRECTION OF POINT 7 POSITION IN ROTATED COORDINATES	A 127
C	P7	ORIGINAL ORIGIN	A 128
C	P8	POINTED X-VALUE IN ROTATED COORDINATES	A 129
C	P9	RE-ROTATED Y-POSITION	A 130
C	P10	INTERMEDIATE VALUE FOR RE-ROTATING COORDINATES	A 131
C	P11	SINDE OF P1	A 132
C	P12	PIST SCALING FACTOR	A 133
C	P13	TRAVEL TIME IN SECONDS ABOVE INTEGER MINUTES	A 134
C	P14	R.O. IN	A 135
C	P15	ROTATING POINT IN	A 136
C	P16	ROTATING POINT VALUE OF IS	A 137
C	P17	SIN NUMBER	A 138
C	P18	ANGLE IN X-Y PLANE IN ROTATED COORDINATES	A 139
C	P19	RE-ROTATED POINTED Z-VALUE	A 140
C	P20	POINTED X POSITION	A 141
C	P21	POINTED Y-VALUE	A 142
C	P22	TRAVEL TIME IN MINUTES	A 143
C	P23	ARRAY CONTAINING HORIZONTAL POSITIONS FOR PLOTTING	A 144
C	P24	ARRAY FOR PLOTTING	A 145
C	P25	ARRAY FOR PLOTTING	A 146
C	P26	ARRAY FOR PLOTTING	A 147
C	P27	ROTATED VALUE OF P1(12)	A 148
C	P28	ROTATED Y POSITION	A 149
C	P29	ROTATED Z VALUE	A 150
C	P30	X DIRECTION IN ROTATED COORDINATE SYSTEM	A 151
C	P31	POINTED VALUE IN ROTATED COORDINATES	A 152
C	P32	POINTED X-VALUE AFTER ROTATION	A 153
C	P33	POINTED Y-VALUE IN ROTATED COORDINATES	A 154
C	P34	INTERMEDIATE VALUE IN ROTATING COORDINATES	A 155
C	P35	INTERMEDIATE VALUE FOR ROTATION	A 156
C	P36	INTERMEDIATE VALUE FOR RE-ROTATION	A 157
C	P37	INTERMEDIATE VALUE FOR ROTATING COORDINATES	A 158
C	P38	ARRAY CONTAINING VERTICAL POSITIONS FOR PLOTTING	A 159
C	P39	ARRAY FOR PLOTTING	A 160
C	P40	ARRAY FOR PLOTTING	A 161
C	P41	ARRAY FOR PLOTTING	A 162
C	P42	ROTATED Y-VALUE	A 163
C	P43	ROTATED Z-VALUE	A 164
C	P44	Z DIRECTION OF RAY SEGMENT IN RE-ROTATED COORDINATES	A 165
C	P45	ROTATED Z POSITION	A 166
C	P46	SAVED EMERGING POSITION FOR TESTING	A 167
C	P47	EMERGING POSITION FOR TESTING	A 168
C	P48	COMPUTED VALUE OF MATH FUNCTION	A 169
C	P49	VELOCITY VALUE	A 170
C	P50	VELOCITY VALUE	A 171
C	P51	PLOTTING VARIABLE FOR PERSPECTIVE	A 172
C			A 173
C		DIMENSION P1(10), P2(10), C1(10), P3(10), AN(10), AT(10), CKJ(10)	A 174
C		11, P4(10), 1MATH(10)	A 175
C		DIMENSION A(30,30,30), B(30,30,30), AD(30,30,30), SLPRAT(30,30,30)	A 176
C		***PLOTTING INSTRUCTIONS***	A 177
C		DIMENSION X(200), Y(200), XORTH(200), YORTH(200), XORTH2(200), Y	A 178
C		ORTH2(200), YORTH2(200), YORTH3(200)	A 179
C		***	A 180



	K=PK(17)+.500)	A 241
	IF (WAYH.WF.1) GO TO 4	A 242
	RMA=PI/2.-ATAN(FACH/FACV)	A 243
	RNARC=FACH/CONY(FACH*FACH+FACV*FACV+FACH*FACH)	A 244
	RDRFF=ARCOS(RNARC)	A 245
	GO TO A	A 246
5	CONTINUE	A 247
	RMA=PI/2.-H1(.1,K)	A 248
	RDRFF=H1(.1,K)	A 249
A	CONTINUE	A 250
	CRM=COS(RMA)	A 251
	CRM=SIN(RMA)	A 252
	CREF=COS(RDRFF)	A 253
	CREF=SIN(RDRFF)	A 254
	XP1=P1(12)+CRM*P1(12)SRM	A 255
	XP1=P1(12)+CRM*P1(12)SRM	A 256
	XP1=XP1+CREF*PK(17)SRFF	A 257
	XPK=PK(17)+CREF*XP1+SRFF	A 258
	C7=COS(C1*INE2)	A 259
	NY=ARC(SIN(C1*INE2))	A 260
	CX=NR7+OSIN(ANGLE2)	A 261
	CY=NR7+CONS(ANGLE2)	A 262
	XX=CX+CRM+CXSRM	A 263
	YREF=CX+CRM-CXSRM	A 264
	YREF=XX+CREF-C7+SRFF	A 265
	YREF=C7+CREF+XX+SRFF	A 266
	IF (ARS(YREF),(F,.005) YREF=.005	A 267
	THEYA=ATAN(YREF/YREF)	A 268
	IF (YREF,LT,0.) THEYA=PI+THEYA	A 269
	IF (XREF,LT,0.,AND,YREF,GE,0.) THEYA=2.+PI+THEYA	A 270
	ALPHA=ARCOS(YREF)	A 271
	RNARC=CONY(FACH*FACH+FACH*FACH+FACV*FACV)	A 272
7	IF (17,(F,0) GO TO 4B	A 273
	NPLT=NPLT+1	A 274
	INIM=INIM+1	A 275
	IF (INIM,GE,1000) CALL SYSTEM	A 276
	ALPHA=ALPHA1	A 277
	ANGLE1=ANGLE2	A 278
	C1INE1=C1INE2	A 279
C	***** INSTRUCTION *****	A 280
	IF (1PNT,FO,0) GO TO A	A 281
	IF (1NFC,FO,0,AND,NPLT,GT,1) GO TO 4	A 282
	X(NPLT)=P1(12)-(PK(12)-1)*(VPRS+P1(12))/PERSLE	A 283
	VINDY1=P1(12)+(PK(12)-1)*(VPRS+P1(12))/PERSLE	A 284
	XNTH1(1)=P1(12)+50.	A 285
	VNTH1(1)=P1(12)+50.	A 286
	VNTH2(1)=31.-PK(12)	A 287
	VNTH2(1)=P1(12)+50.	A 288
	VNTH3(1)=P1(12)+50.	A 289
	VNTH3(1)=31.-PK(12)	A 290
	NPLT=NPLT+1	A 291
7	*****	A 292
B	CONTINUE	A 293
Q	NR1=CONY(ARC(SIN(ALPHA)))	A 294
	MMH=NR1*CONY(SIN(THEYA))	A 295
	ARR=NR1*CONY(SIN(THEYA))	A 296
	NNN=CONY(ARC(SIN(ALPHA)))	A 297
	IF (1REFL,FO,1,AND,IVINI,FO,1) GO TO 15	A 298
	IF (1VII,FO,1) GO TO 24	A 299
	XP1=XP1+MMH	A 300



	VP,1=XP,1+GGG	A 301
	XPK=XPK+NNN	A 302
10	CONTINUE	A 303
	VXP=XPT+CRFF+XPK+SRFF	A 304
	PK(12)=-XP+SRFF+XPK+CRFF	A 305
	P(12)=XXP+CRM-XP+CRM	A 306
	P,1(12)=VXP+CRM+XP,1+CRM	A 307
	IF (IGD,FO,1) GO TO 41	A 308
	IF (MATH,NE,1) GO TO 11	A 309
	VMATH=CONST+FACTH*(P(12)-1)+FACV*(P,1(12)-1)+FACD*(PK(12)-1)	A 310
	GO TO 12	A 311
11	CONTINUE	A 312
	VMATH=A(1,1,K)	A 313
12	CONTINUE	A 314
	AT(12)=AT(12)+H)FRACOG/VMATH	A 315
	ON(12)=ON(12)+H)TERACOG	A 316
	IF (PIHT,FO,0) GO TO 13	A 317
C	***PLACING INSTRUCTIONS***	A 318
	10)C=1	A 319
	IF (IVF,FO,1,ANN,NPLT,GF,1) NPLT=NPLT+1	A 320
	V(NPLT)=P,1(12)-(PK(12)-1)*(VPRS+PJ(12))/PERSLE	A 321
	V(NPLT)=P(12)+(PK(12)-1)*(HPRS-P(12))/PERSLE	A 322
	XNTH1(NPLT)=P,1(12)+50	A 323
	VNTH1(NPLT)=P(12)+50	A 324
	XNTH2(NPLT)=31.-PK(12)	A 325
	VNTH2(NPLT)=P(12)+50	A 326
	XNTH3(NPLT)=P,1(12)+50	A 327
	VNTH3(NPLT)=31.-PK(12)	A 328
C	***	A 329
13	CONTINUE	A 330
	IF (WRITE,GF,2) WRITE (7,5R) ALPHA,THETA,ICRYT,12,MATH	A 331
	IF (PK(12),GF,1,1) GO TO 19	A 332
14	ISURF=1	A 333
15	CONTINUE	A 334
	XXR=MMH+CRFF+NNN+SRFF	A 335
	ZPK=-MMH+SRFF+NNN+CRFF	A 336
	ZP1=XXR+CRM+GGG+CRM	A 337
	ZP,1=XXR+CRM+GGG+CRM	A 338
	IF (ARS(ZP,1),LF,0,005) ZP,1=,005	A 339
	ANGLE1=ATAN(ZP1/ZP,1)	A 340
	IF (ZP,1,LT,0,1) ANGLE1=PI+ANGLE1	A 341
	IF (ZP,1,GT,0,1,ANN,ZP,1,GE,0,1) ANGLE1=2*PI+ANGLE1	A 342
	CLINE2=ARCS(ZPK)	A 343
	IF (IVU,FO,1) GO TO 27	A 344
	IF (IVIH,FO,1) GO TO 46	A 345
	IF (IM,FO,1) GO TO 24	A 346
	IF (IRFF,FO,1) GO TO 4	A 347
	IF (MATH,NE,1) GO TO 16	A 348
	VMATH3=CONST+FACTH*(P(12)-1)+FACV*(P,1(12)-1)	A 349
	GO TO 17	A 350
16	CONTINUE	A 351
	VMATH3=A(1,1,K)	A 352
17	CONTINUE	A 353
	DV=1.-PK(12)	A 354
	IF (IFACT,FO,1) CALL GINMAD (P(12),P,1(12),PK(12),DV,AT(12),ON(12	A 355
	1),HIFRAC,VMATH3,CLINE2,ANGLE1,ANGLE1	A 356
	ISURF=0	A 357
	PAGE=SQRT(P(12)+P(12)+P,1(12)+P,1(12)+HIFRAC	A 358
	DISTA=SQRT((P(12)-ORIGH)*(P(12)-ORIGH)+(P,1(12)-ORIGV)*(P,1(12)-OR	A 359
	IGV)+HIFRAC	A 360

	DEMO=ASC=1,772011FMAF	A 361
	AMPI=(PNUM-ANT(17)/PA(17))/EVD(PFC=ON(17))	A 362
	TMIN=AT(17)/40.	A 363
	ISFC=TMIN	A 364
	SEF=40.01TMIN-1SEF	A 365
	WRITE(17,56) (1)STA,PKM,YMIN,SEF,AT(17),AMPI	A 366
	IF 11PINT,FO,0) GO TO 18	A 367
C	DOOPI=TYTNG TACTYHIF YINWOO	A 368
	YINDI TI=D,1171-(PK1171)-1.101VPERKSD,11711/PERKLE	A 369
	VINDI TI=D,1171-(PK1171)-1.101WPERKSD,11711/PERKLE	A 370
	YORTW1INDI TI=D,1171-40.	A 371
	VORTW1INDI TI=D,1171-40.	A 372
	YORTW2INDI TI=31,-PK1171	A 373
	VORTW2INDI TI=D,1171-40.	A 374
	YORTW3INDI TI=D,1171-40.	A 375
	VORTW3INDI TI=31,-PK1171	A 376
	C1 INEM=57,24580CLINE1	A 377
	CALL PLINE (X(11),Y(11),NPLT,1,0,0,1)	A 378
	CALL PCYMR (XINDI TI),YINDI TI,1,MISYM2,CLINEM,-1,1)	A 379
	CALL PLINE (YORTW1(1),YORTW1(1),NPLT,1,0,0,1)	A 380
	CALL PCYMR (YORTW1(NPLT),YORTW1(NPLT),1,MISYM2,CLINEM,-1,1)	A 381
	CALL PLINE (YORTW2(1),YORTW2(1),NPLT,1,0,0,1)	A 382
	CALL PLINE (YORTW3(1),YORTW3(1),NPLT,1,0,0,1)	A 383
	NPLT=0	A 384
C	DOO	A 385
18	CONTINUE	A 386
	GO TO 22	A 387
19	IF 11P(17),CY,0.5,AND,PJ(17),CY,0.5,AND,PJ(17),LY,JPORSH=0.5,AND,PT(1	A 388
	17),LT,JPORSH=0.5,AND,PK(17),LT,KPORSH=0.5) GO TO 23	A 389
20	IF 11PINT,FO,0) GO TO 21	A 390
	CALL PLINE (X(11),Y(11),NPLT,1,0,0,1)	A 391
	CALL PLINE (YORTW1(1),YORTW1(1),NPLT,1,0,0,1)	A 392
	CALL PLINE (YORTW2(1),YORTW2(1),NPLT,1,0,0,1)	A 393
	CALL PLINE (YORTW3(1),YORTW3(1),NPLT,1,0,0,1)	A 394
	NPLT=0	A 395
21	CONTINUE	A 396
22	IF 117,FO,1) GO TO 40	A 397
	IVW=0	A 398
	ANT(17-1)=1-ANT(17)+ANT(17-1)	A 399
	17=17-1	A 400
	ANG1F2=0.11171	A 401
	CLTNE2=PK,1171	A 402
	MATH=1MATH(17)	A 403
	1MATH=MAYH	A 404
	IF 1MATH,FO,1) IVX=3	A 405
	IF 1MATH,FO,0) IVX=4	A 406
	GO TO 4	A 407
23	1=0,1171-0.5	A 408
	1=0,1171-0.5	A 409
	K=PK(17)-0.5	A 410
24	CONTINUE	A 411
	V11=0,010MMH	A 412
	V11=0,010GGG	A 413
	V11=0,010K01111	A 414
C		A 415
	V11=0,010K01111	A 416
	T11=0,010K01111	A 417
	T11=0,010K01111	A 418
	T11=0,010K01111	A 419
	1M=0,010	A 420

	IS=TIS+.5	A 421
	IN=IIN+.5	A 422
	DV=SI PRAT(I,J,K)/100.	A 423
	IF (DV,LT,.01) DV=.5	A 424
	IF (ALPHA,LT,PITT) SLID=ID-DV	A 425
	IF (ALPHA,GE,PITT) SLID=ID+1.-DV	A 426
	SI IM=IM	A 427
	SLIS=IS	A 428
	RRIM=SI IM*(CHM+SI IS*SRM	A 429
	WIS=SI IS*(CHM-SI IM*SRM	A 430
	RIM=RRIM*CRFF-SLID*SRFF	A 431
	RID=SI ID*CRFF+RIM*SRFF	A 432
	DV=RID-XPX	A 433
	IF (IVII,EO,1) GO TO 20	A 434
C.	TEST TO SEE IF RAY END IS IN SAMPLED REGION. SET SWITCHES	A 435
C.	IN CORRESPOND TO THE REGION. IF NECESSARY, RECOMPUTE	A 436
C.	ROTATION OF COORDINATES AND RESULTING DIRECTIONS...	A 437
	IF (IM,GE,MISX,AND,IM,LT,MILX,AND,IS,GE,MISY,AND,IS,LT,MILY,AND,IN	A 438
	1,GE,MISZ,AND,IN,LT,MILZ) GO TO 26	A 439
	IVX=IVX+1	A 440
	IVXX=0	A 441
	IF (MATH,EO,1,AND,IVX,GE,3) GO TO 29	A 442
	MATH=1	A 443
	IMATH(IZ)=1.	A 444
	IF (IVX,EO,2) KMATH=1	A 445
	LMATH=1	A 446
	IF (IVX,EO,1) GO TO 29	A 447
	IMI=1	A 448
	GO TO 15	A 449
25	CONTINUE	A 450
	IM1=0	A 451
	IVXX=0	A 452
	CRM=COS(RMA)	A 453
	SRM=SIN(RMA)	A 454
	CRFF=COS(RDRFF)	A 455
	SRFF=SIN(RDRFF)	A 456
	GO TO 28	A 457
26	CONTINUE	A 458
	IVXX=IVXX+1	A 459
	IF (IVXX,EO,2) LMATH=0	A 460
	KMATH=0	A 461
	IVX=0	A 462
	IF (MATH,EO,0) GO TO 29	A 463
	MATH=0	A 464
	IMATH(IZ)=0	A 465
	IVII=1	A 466
	GO TO 15	A 467
27	CONTINUE	A 468
	DRJ,IK=PI-T-H(I,J,K)	A 469
	CRM=COS(DRJ,IK)	A 470
	SRM=SIN(DRJ,IK)	A 471
	CRFF=COS(RD(I,J,K))	A 472
	SRFF=SIN(RD(I,J,K))	A 473
28	CONTINUE	A 474
	XXPI=PI(IZ)*CRM+PI(IZ)*SRM	A 475
	XP,IP,II(IZ)*CRM-PI(IZ)*SRM	A 476
	YPI=XXPI*CRFF-IPK(IZ)*SRFF	A 477
	XPX=PK(IZ)*CRFF+XXPI*SRFF	A 478
	C7=COS(C) INF2)	A 479
	DR7=ARC(SIN(C) INF2)	A 480

	CX=OH7*SIN(ANG1E1)	A 481
	CY=OH7*COS(ANG1E1)	A 482
	XX=CX*CRM+CY*CRM	A 483
	YREF=CX*CRM-CY*CRM	A 484
	YREF=XX*CRM-C7*SRFF	A 485
	ZREF=C7*CRM+XX*SRFF	A 486
	IF (ARS(YREF),IF,.005) YREF=.005	A 487
	THETA=ATAN(YREF/YREF)	A 488
	IF (YREF.LT.0.) THETA=PIT+THETA	A 489
	IF (XREF.LT.0.,AND,YREF.GE.0.) THETA=2.*PIT+THETA	A 490
	ALPHA1=ARCS(ZREF)	A 491
	ALPHA=ALPHA1	A 492
	IF (IWI.FO.1) GO TO 9	A 493
29	CONTINUE	A 494
	IWI=0	A 495
	IF (MATH.NE.1) GO TO 30	A 496
	VMATH2=CONST+FACH*TIM+FACV*TIS+FACD*TID	A 497
	GO TO 31	A 498
30	CONTINUE	A 499
	VMATH2=A(IM,IS,ID)	A 500
31	CONTINUE	A 501
	IF (ID.LT.1) GO TO 14	A 502
	IF (IM.GT.IPORSH,OR,IS.GT.IPORSH,OR,IM.LT.1,OR,IS.LT.1,OR,ID.GT.KP	A 503
	IPORSH) GO TO 20	A 504
	IF (IWRITE.FO.0) GO TO 32	A 505
	WRITE (7,51) PJ(IZ),PT(IZ),PK(IZ),VMATH1	A 506
		A 507
32	IF (ARS(VMATH2-VMATH1).GT,.0001) GO TO 33	A 508
	IWEI=1	A 509
	IWE=0	A 510
	GO TO 7	A 511
33	IWEI=0	A 512
	IF (IWE.NE.1) GO TO 34	A 513
	IWE=0	A 514
	GO TO 7	A 515
34	CONTINUE	A 516
	AFFI=VMATH1	A 517
	GRAD=G*SQRT(FACH*FACH+FACH*FACH+FACV*FACV)	A 518
	ALPHA2=ALPHA	A 519
	LOOP TO DETERMINE EMERGING VELOCITY AND ANGLE****	A 520
	DO 38 III=1,10	A 521
	IF (MATH.FO.1,AND,IMATH.FO.MATH) GO TO 35	A 522
	ARFF=VMATH1+(VMATH2-VMATH1)*ARS(COS(ALPHA1))	A 523
	GO TO 36	A 524
35	CONTINUE	A 525
	ARFF=VMATH1+GRAD*COS(ALPHA1)	A 526
36	CONTINUE	A 527
	CALL SINDET (ALPHA,ALPHA1,AFFI,ARFF,REFFA1,(CRYT,FFF)	A 528
	IF (ALPHA1.GT.PIT,AND,ALPHA1.LT.2.*PIT) THETA=THETA+PIT	A 529
	IF (ALPHA1.GT.PIT) ALPHA1=2.*PIT-ALPHA1	A 530
	IF (IWRITE.GE.3) WRITE (7,54) AFFI,ARFF,ALPHA1,THETA	A 531
	ZTEST=PK(IZ)+G*COS(ALPHA1)	A 532
	IF (III.FO.1) GO TO 37	A 533
	IF (ARS(ZTEST-ZTE),IF,.01) GO TO 39	A 534
37	CONTINUE	A 535
	ZTE=ZTEST	A 536
38	CONTINUE	A 537
	END OF EMERGING ANGLE AND VELOCITY DETERMINATION LOOP****	A 538
39	CONTINUE	A 539
	IMATH=MATH	A 540

	ALPHA=ALPHA1	A 541
	IF (ABS(VMATH1-ARFF).GE.VELDIF.AND.IZ.LE.NMULT.AND.IVW.I.T.1) GO TO	A 542
1	40	A 543
	IF (ICRYT.FO.1) GO TO 43	A 544
	IVW=0	A 545
	IRFFI=0	A 546
	GO TO 7	A 547
40	CONTINUE	A 548
	IF (IWRITE.GE.4) WRITE (7,57) XPI,XPJ,XPK,MATH,KMATH,LMATH	A 549
	IF (IFXACT.FO.1) CALL CINMAD (XPI,XPJ,XPK,DV,AT(IZ),ON(IZ),DIFRAC,	A 550
	1ARFF1,ALPHA2,THETA,ADIF)	A 551
	IF (IPLDT.FO.0) GO TO 42	A 552
	IGIN=1	A 553
	GO TO 10	A 554
41	CONTINUE	A 555
	IGIN=0	A 556
C	***PLOTTING INSTRUCTION***	A 557
	X(NPLT)=P.I(IZ)-(PK(IZ)-1.)*(VPERF+PJ(IZ))/PERSLF	A 558
	Y(NPLT)=P.I(IZ)+(PK(IZ)-1.)*(HPERF-PJ(IZ))/PERSLF	A 559
	XNORTH1(NPLT)=P.I(IZ)+50.	A 560
	YNORTH1(NPLT)=P.I(IZ)+50.	A 561
	XNORTH2(NPLT)=41.-PK(IZ)	A 562
	YNORTH2(NPLT)=P.I(IZ)+50.	A 563
	XNORTH3(NPLT)=P.I(IZ)+50.	A 564
	YNORTH3(NPLT)=31.-PK(IZ)	A 565
	CALL PLINE (X(1),Y(1),NPLT,1,0,0,1)	A 566
	CALL PLINE (XNORTH1(1),YNORTH1(1),NPLT,1,0,0,1)	A 567
	CALL PLINE (XNORTH2(1),YNORTH2(1),NPLT,1,0,0,1)	A 568
	CALL PLINE (XNORTH3(1),YNORTH3(1),NPLT,1,0,0,1)	A 569
	NPLT=0	A 570
C	***	A 571
42	CONTINUE	A 572
	IF (IWRITE.GE.4) WRITE (7,56) GIN,THETA,ALPHA2,XPI,XPJ,XPK	A 573
43	IF (ICRYT+IVW.GE.2) GO TO 7	A 574
	IF (ICRYT.FO.1) GO TO 45	A 575
	IVW=1	A 576
	IZ=IZ+1	A 577
	ON(IZ)=ON(IZ-1)	A 578
	AT(IZ)=AT(IZ-1)	A 579
	PI(IZ)=PI(IZ-1)	A 580
	PJ(IZ)=PJ(IZ-1)	A 581
	PK(IZ)=PK(IZ-1)	A 582
	ANT(IZ)=ANT(IZ-1)*(VMATH2-VMATH1)/(VMATH2+VMATH1)	A 583
	IVIII=1	A 584
	GO TO 9	A 585
44	CONTINUE	A 586
	IVIII=0	A 587
	CT.I(IZ-1)=ANG1.F1	A 588
	CK.I(IZ-1)=CLINE2	A 589
	VMATH(IZ-1)=MATH	A 590
45	IF (IZ.LE.NMULT) GO TO 46	A 591
	GO TO 22	A 592
46	CONTINUE	A 593
	IF (ICRYT.FO.1.OR.ABS(ARFF-ARFF1).GE.VELDIF) ALPHA1=PII-ALPHA2	A 594
	DO 47 I=1,2	A 595
	IF (ALPHA1.LT.0.) ALPHA1=-ALPHA1	A 596
	IF (ALPHA1.GT.PI) ALPHA1=2.*PI-ALPHA1	A 597
	ALPHA=ALPHA1	A 598
47	CONTINUE	A 599
	VMATH(IZ)=MATH	A 600

	IF (MATH.FO.1.AND.KMATH.FO.0) MATH=0	A 601
	IF (1/MATH(17),FO.0.AND.1/MATH.FO.1) MATH=1	A 602
	1/MATH(17)=MATH	A 603
	IF (ABS(AFF1-ARF),DE,VF10(F) VW=1	A 604
	IF (MATH.FO.0) GO TO 7	A 605
	1/RF1=1	A 606
	GO TO 9	A 607
48	CONTINUE	A 608
	CALL COMBEC (REGIN,DEIN,NOR,IR)	A 609
	CALL COMDEP (REGIN,DEIN,NOR,IR)	A 610
	CALL COMVER (ORIGV,DEIV,NOR,IV)	A 611
	CALL COMHOR (ORIGH,DEIH,NOR,IH)	A 612
49	CONTINUE	A 613
		A 614
	***PRINTING INSTRUCTION***	A 615
	CALL PLEND	A 616
		A 617
50	FORMAT (1D6,2)	A 618
51	FORMAT (11,6F8,2)	A 619
52	FORMAT ('DISTANCE KILOMETERSTT(MN)TT(SFC)', 'TOTAL (SEC)AMPLITUDE') A 620	
53	FORMAT ('INITIAL ANGLE,INITIALDISTANCE,INITIALDEPTH') A 621	
54	FORMAT (11,6F8,2)	A 622
55	FORMAT ('UNCONDITIONAL WRIEOUTSASFOLLOWS:11WRITE=1:PI,PJ,PK,VMATH A 623	
	1111WRITE=2:ADD:ALPHA,THETA,ICRYT,IZ,MATH11WRITE=3:ADD:AFF1,ARF A 624	
	2F,ALPHA1,THETA111WRITE=4:ADDTWO LINES:11.XPI,XPJ,XPK', 'MATH,KMAT A 625	
	3H,1/MATH11AND2,GIN,THETA,ALPHA2,XPI,XPJ11WRITE=1,12) A 626	
56	FORMAT (11,6F10,2)	A 627
57	FORMAT (11,3F10,2,312)	A 628
58	FORMAT (11,2F5,2,312)	A 629
	END	A 630*
	SUBROUTINE GINMAD (PI,PJ,PK,DV,AT,ON,D,A,CLINE2,ANGLE1,ADIF)	R 1
	IF (ABS(CLINE2-1.57),LT,ADIF) RETURN	R 2
	CLICOS=COS(CLINE2)	R 3
	IF (ABS(CLINE2-PIE2),LT,.01) CLICOS=.01	R 4
	GIN=DV/CLICOS	R 5
	ORI=D=GIN*SIN(CLINE2)	R 6
	PI=PI+ORI/D*SIN(ANGLE1)	R 7
	PJ=PJ+ORI/D*COS(ANGLE1)	R 8
	PK=PK+GIN*COS(CLINE2)	R 9
	IF (A,1,1.) A=6.	R 10
	AT=AT+D*GIN/A	R 11
	ON=ON+D*GIN	R 12
	RETURN	R 13
	END	R 14*

644 LINES PRINTED

DOCUMENT CONTROL DATA - R & D

(Security classification of title, body of abstract and indexing annotation must be entered when the overall report is classified)

1. ORIGINATING ACTIVITY (Corporate author) Willow Run Laboratories of the Institute of Science and Technology, The University of Michigan, Ann Arbor, Michigan		2a. REPORT SECURITY CLASSIFICATION UNCLASSIFIED	
		2b. GROUP	
3. REPORT TITLE  DIGITAL SIMULATION OF SEISMIC RAYS			
4. DESCRIPTIVE NOTES (Type of report and inclusive dates)  Scientific.....Final. Part 2			
5. AUTHOR(S) (First name, middle initial, last name)  P. L. Jackson			
6. REPORT DATE  August 1970		7a. TOTAL NO. OF PAGES  xii + 85	7b. NO. OF REFS  23
8a. CONTRACT OR GRANT NO.  AF 49(638)-1759		9a. ORIGINATOR'S REPORT NUMBER(S)  8071-33-F <sub>1</sub>	
b. PROJECT NO.  8652			
c.  62701D		9b. OTHER REPORT NO(S) (Any other numbers that may be assigned this report)  AFOSR-70-2391TR	
d.			
10. DISTRIBUTION STATEMENT  1. This document has been approved for public release and sale; its distribution is unlimited.			
11. SUPPLEMENTARY NOTES  TECH, OTHER		12. SPONSORING MILITARY ACTIVITY  AF Office of Scientific Research (SRPG) 1400 Wilson Boulevard Arlington, VA 22209	
13. ABSTRACT  Simulation of seismic rays for a spherical earth and a flat earth has been achieved in highly complex models. Travel times and approximate amplitudes of seismic waves can be found for both two- and three-dimensional models of portions of the earth. In seismology and other disciplines ray construction customarily has been applied to simplified geometries. It has been necessary to assume that the seismic wave velocity distribution of the earth was relatively uniform and symmetric.  Recently, however, the earth has been found to be more complex and non-uniform than formerly assumed. A need has thus arisen in seismology to test highly heterogeneous models of seismic velocity distribution. At the same time the development of the modern digital computer has provided a means of performing the necessary ray constructions and numerical calculations.  The problem of complicated seismic velocity distributions was therefore investigated in terms of the most appropriate use of the digital computer. For this investigation a velocity field was set up, and the propagation computations made for short segments of rays within this field. Total travel times are found by adding the travel times of connected ray segments. Essentially, the nature of propagation was duplicated on the computer, in that, at the location of each segment along the path of propagation, the initial condition and effect of the surroundings determine the succeeding direction of the following segment.  Both visual and numerical results have shown that this simulation method can be usefully applied to investigation of seismic velocity distributions of portions of the earth of any size or complexity.			
14. KEY WORDS  Seismology                      Seismic Rays                      Seismic Velocity Digital Simulation              Seismic Travel Times              Distributions			